

DNP: Practical aspects and applications in biomolecular applications

Joanna R. Long
DNP Workshop
August 27, 2025

NATIONAL
MAGLAB DNP User Program

600 MHz MAS DNP

- 90 – 300K range
- 3.2 mm/1.3 mm probes
- Triple resonance NMR
- >100x ¹³C Enhancement
- User facility 2016

Applications:

Biosolids

Materials

Dissolution DNP

- 1 K, 5 T polarizer
- Interfaced with 7, 11.1, 14.1 T MRI/NMR systems
- >10⁴x ¹³C Enhancement
- User facility 2014

Applications:

Mechanistic studies

In vivo metabolic flux

600 MHz Overhauser DNP

- 293-373K range
- Organic/CO₂ solvent
- High resolution NMR
- Goal: 10-20x ¹H
- Development project

Applications:

Metabolomics

Natural products

NMR division

Rob Schurko (Tim Cross)
Fred Mentink-Vigier
Lucio Frydman
Zhehong Gan
Faith Scott
Sungsool Wi

AMRIS division

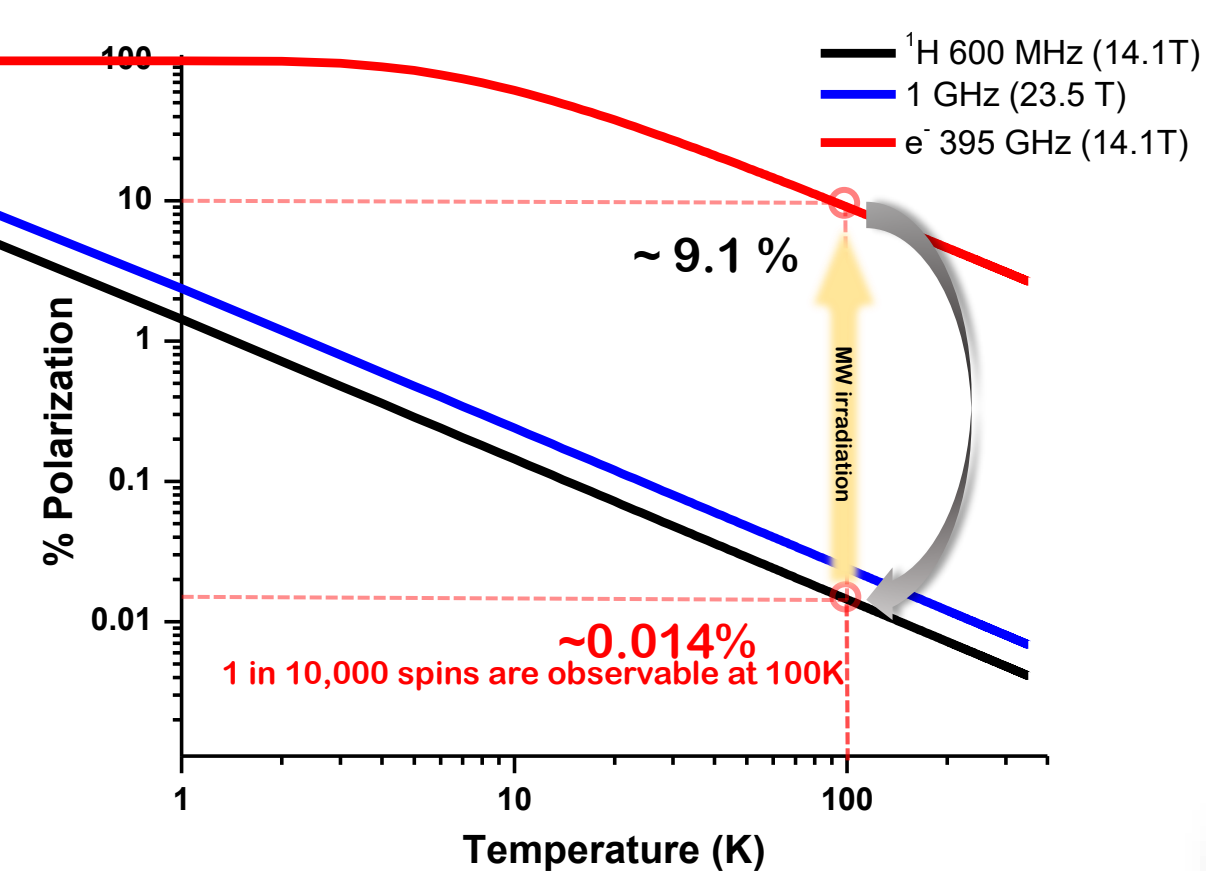
Joanna Long
Matt Merritt
James Collins
Luiza Caldas-Nogueira
Nhi Tran
Adam Smith

EMR division

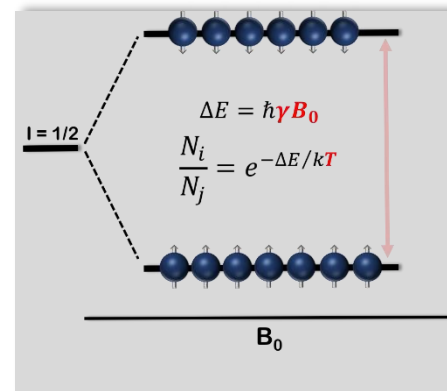
Steve Hill
Thierry Dubroca
Hans van Tol
Bianca Trociewitz
Gail Fanucci

The promise.....

Population difference between energy states ~ "polarization"



$$\text{Polarization} \propto \frac{N_i}{N_j} = e^{-\Delta E/kT}$$



Only 1 in ~8 million ^1H spins are NMR observable at RT!

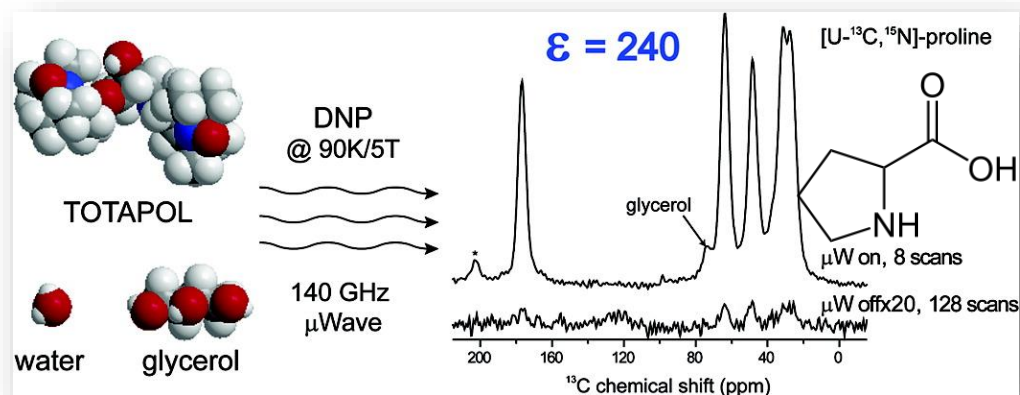
$$\epsilon_{\text{Theoretical max}} = \frac{\gamma_e}{\gamma_H} \sim 660$$

$$\text{Time savings} \propto \epsilon^2$$

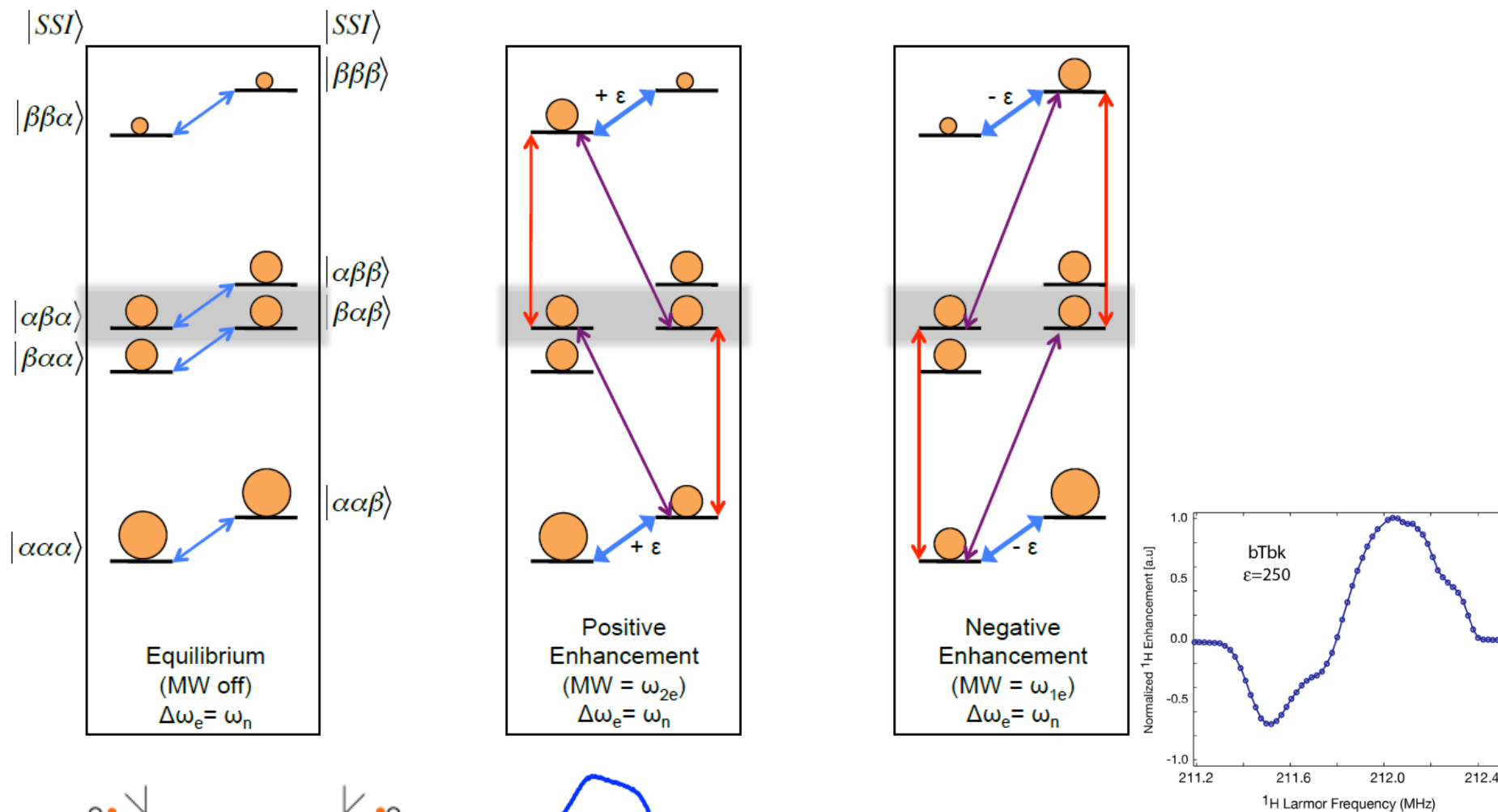
$$\epsilon = 240$$

1 week signal averaging reduced to ~11 sec !

1 year signal averaging reduced to ~9 min!!!



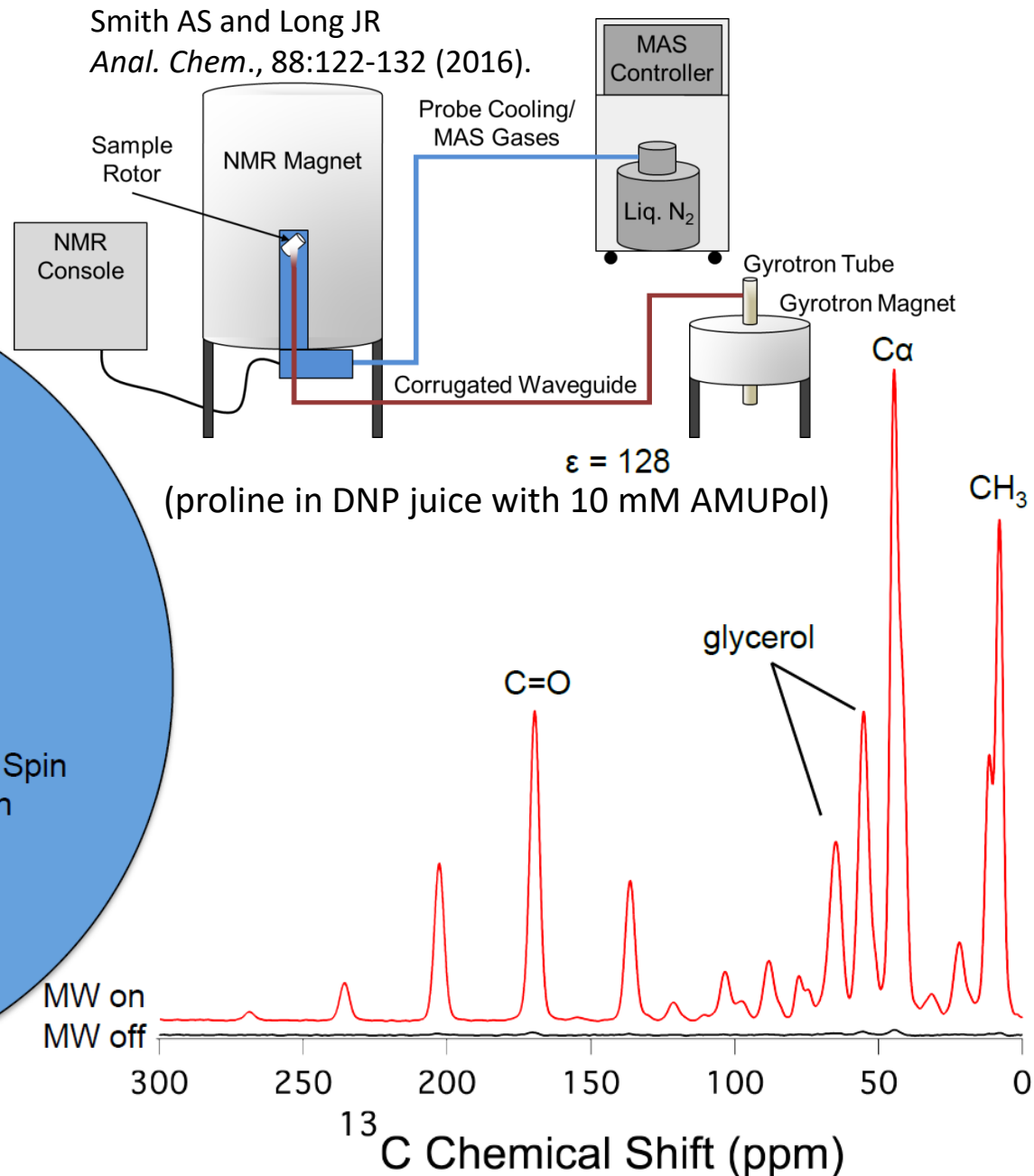
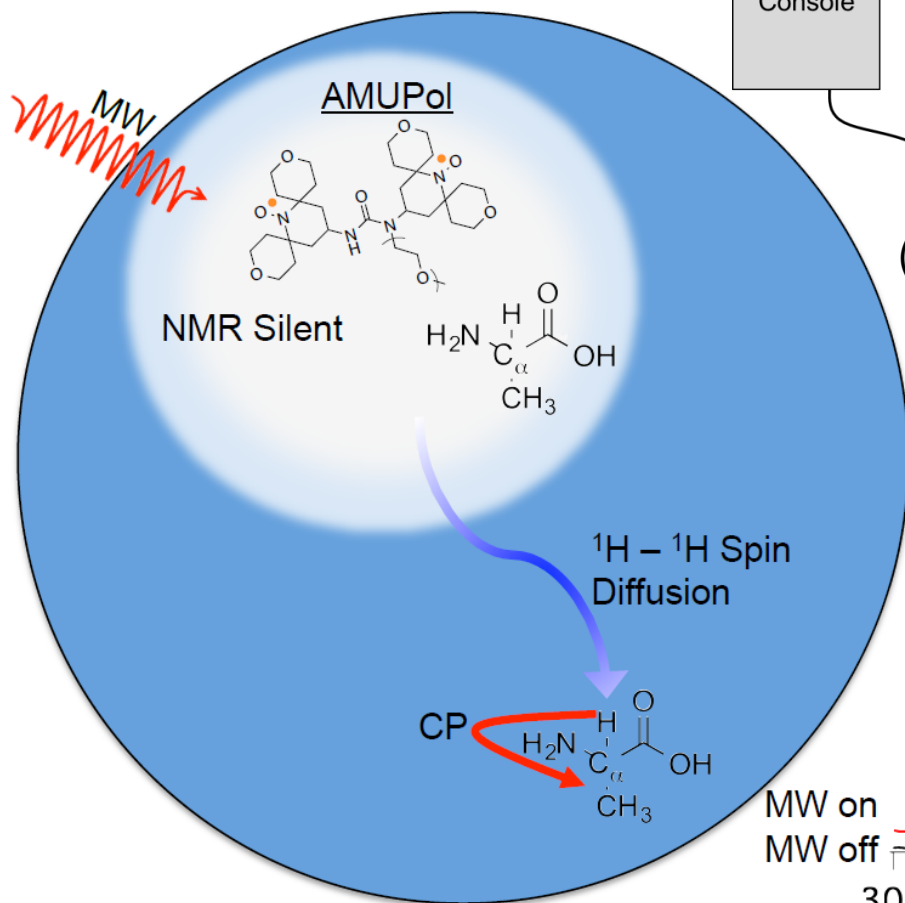
DNP: the cross effect at ~100 K



Smith AS and Long JR
Anal. Chem., 88:122-132 (2016).

MAS DNP on a model system at 600 MHz

$\epsilon = 128$ leads to a time savings of ≈ 16384
10-12 days \rightarrow 1 minute



Biomolecular DNP MAS ssNMR

| Biosystem | ϵ | Temp. (K) | Radical (mM) | B_0 (^1H freq.) |
|-----------------------|------------|-----------|--------------|-----------------------------|
| GNNQQNY | 20 | 100 | TOTAPOL | 400 MHz |
| TTR105-115 | 12 | 100 | TOTAPOL | 400 MHz |
| PI3-SH3 | 30 | 100 | TOTAPOL | 400 MHz |
| A β 1-40 | 20 | 96 | TOTAPOL | 400 MHz |
| Peptidoglycan | 8.8 | 100 | TOTAPOL | 400 MHz |
| h Φ 17W | 18 | 100 | bTbKa | 400 MHz |
| M218-60 | 2.5 | 100 | TOTAPOL | 600 MHz |
| Arabidopsis cell wall | 27 | 100 | TOTAPOL | 600 MHz |
| Whole cells | 10 | 100 | TOTAPOL | 400 MHz |
| Cell envelopes | 26 | 100 | TOTAPOL | 400 MHz |
| Ribosome | 25 | 100 | TOTAPOL | 400 MHz |
| Cell wall | 20 | 100 | TOTAPOL | 400 MHz |
| nAChR-bound NTII | 26 | 100 | TOTAPOL | 400 MHz |
| bR | 75 | 83 | AMUPol | 380 MHz |

Using DNP to capture biomolecular structure and dynamics at atomic resolution

Insights / Understanding

Optimal experiments

Trapping biological states

DNP to enhance sensitivity

Isotopically enriched samples

Solid-State NMR

High Field Magnets



Simulations incorporating multimodal data

Resolution, SNR, processing, quantitation

Physiologic conditions, sample freezing

MW source, biradicals, DNP probe

Synthesis / heterologous expression

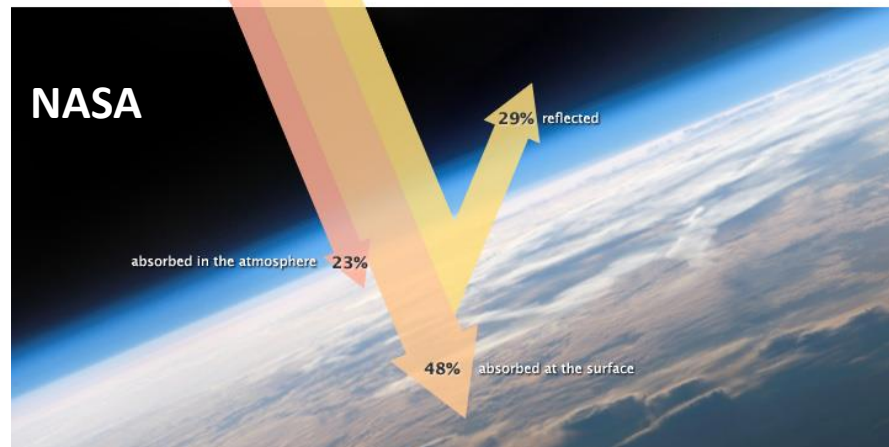
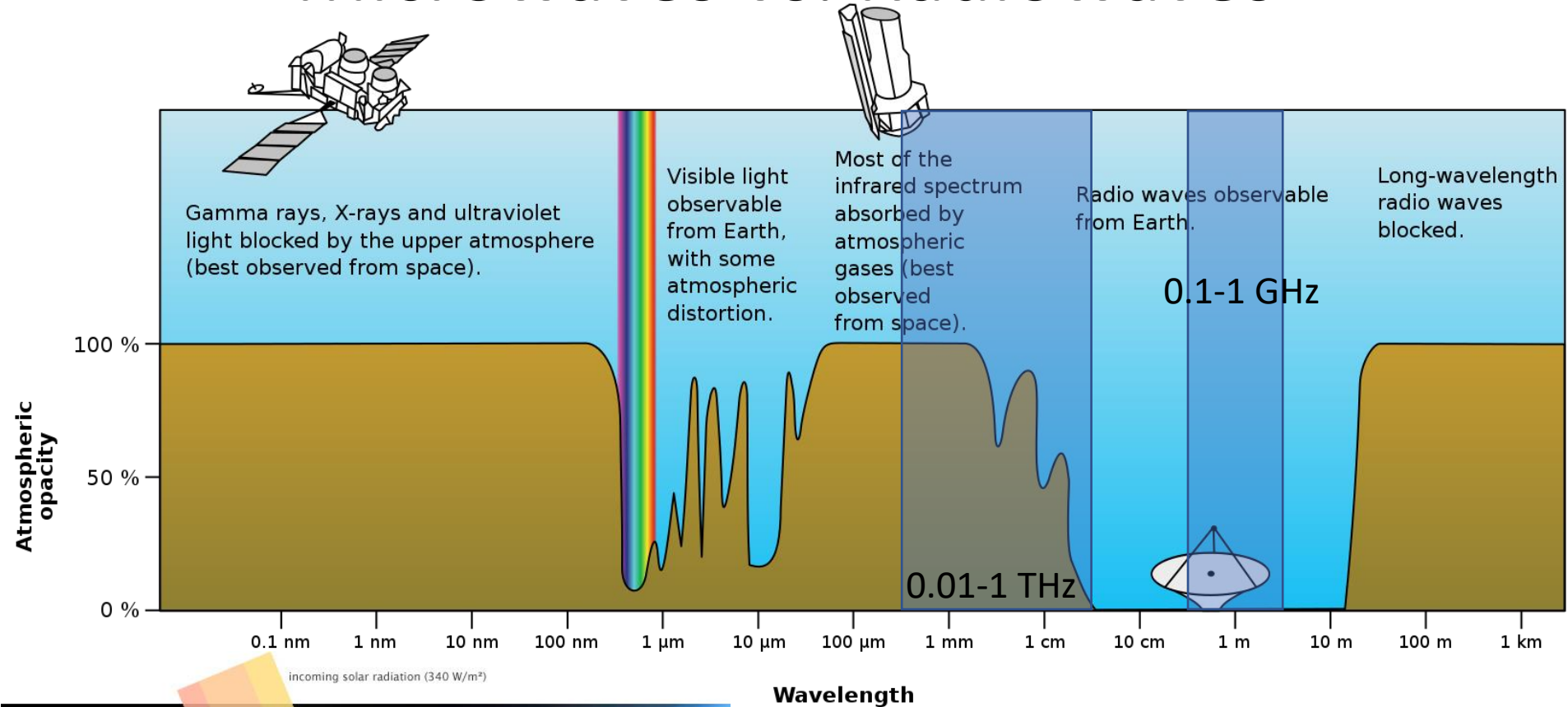
MAS, RF, pulse sequences

Superconductors/cryogenics



DNP: Practical aspects of irradiation

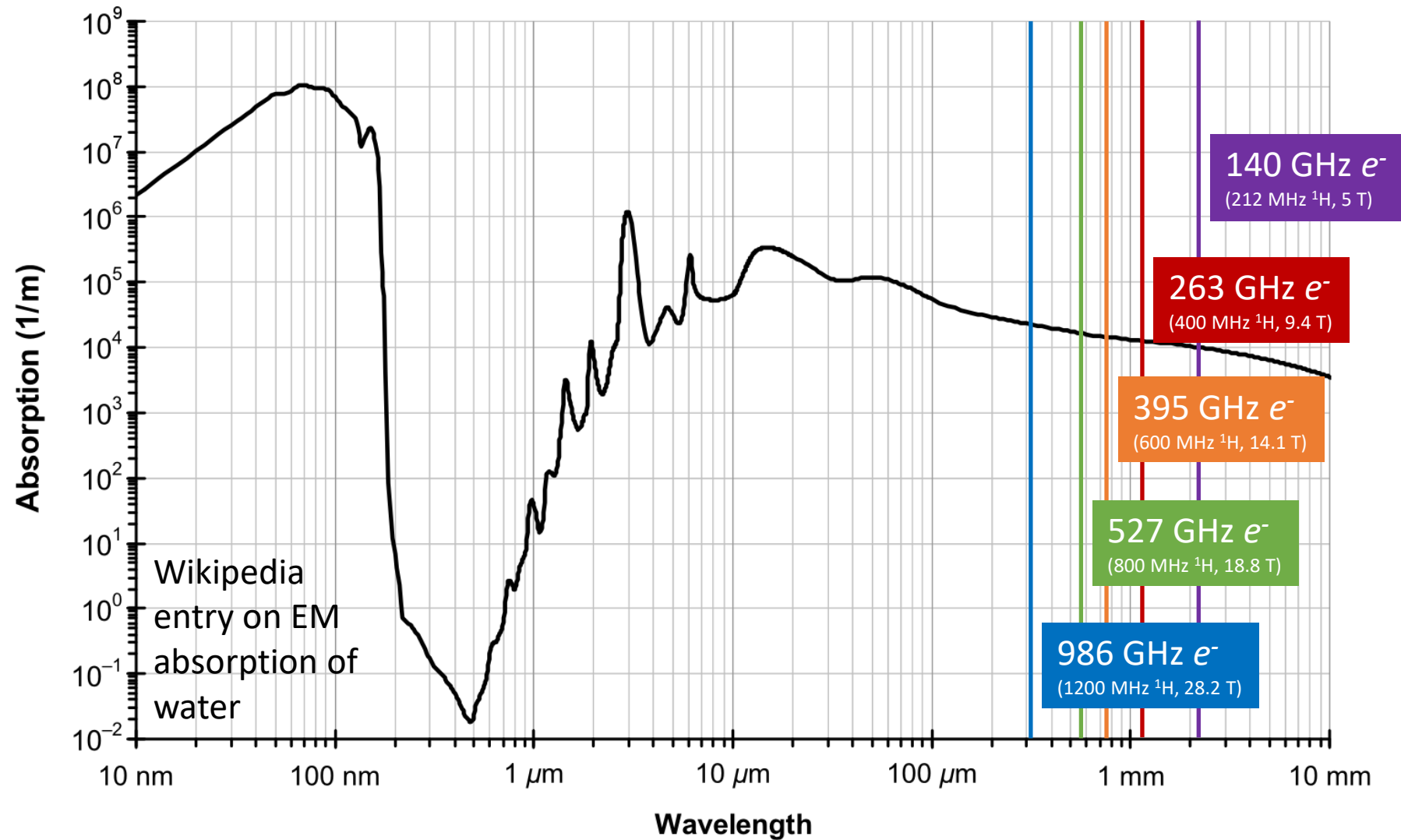
Microwaves vs. Radiowaves



Wavelength

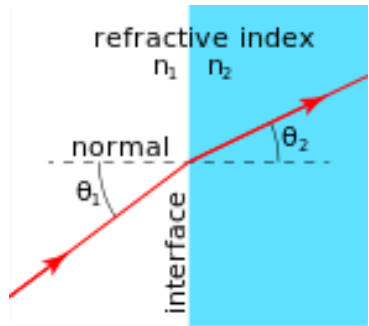
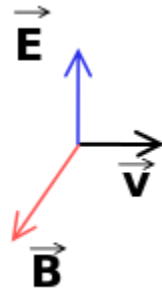
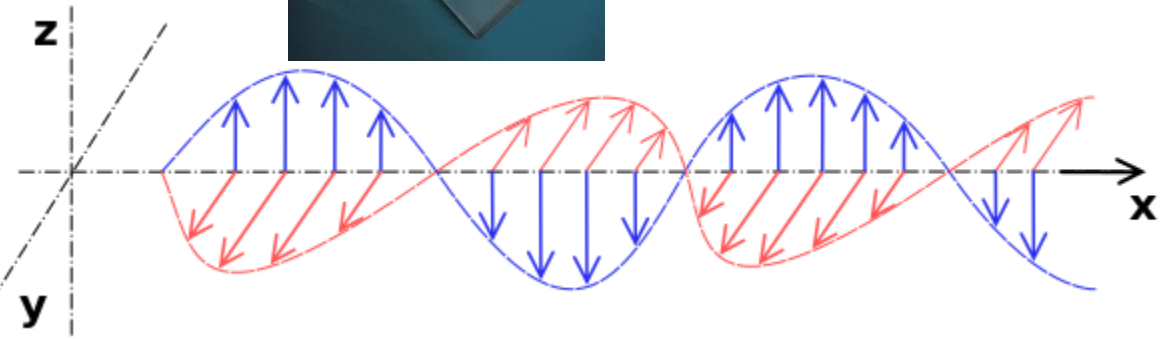
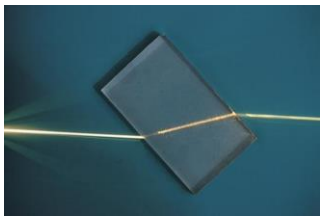
- ~29 percent of solar energy is reflected
- ~23 percent is absorbed by water vapor, dust, and ozone in the atmosphere
- ~48 percent passes through the atmosphere and is absorbed by the surface.

Microwaves and absorption by (liquid) water



2-4 fold loss in efficiency over conventional NMR range

Minireview of electromagnetic propagation



$$n = \frac{c}{v}$$

$$\lambda = \frac{\lambda_0}{n}$$

$$f = \frac{v}{\lambda}$$

- n is dependent on the electric susceptibility of a material and is frequency dependent
- Interactions of the incoming light with electrons in the material lead to their spontaneous emission of light at varying angles relative to the incoming beam
- 90° out of phase $\rightarrow n > 1$ (refraction)
- 180° out of phase \rightarrow interference (absorption)
- 270° out of phase \rightarrow anomalous refraction ($n < 1$)
- 0° or in phase \rightarrow amplification of light (lasers)
- For most materials at visible frequencies, a combination of refraction and absorption occurs

$$\underline{n} = n + ik$$

λ in the sample

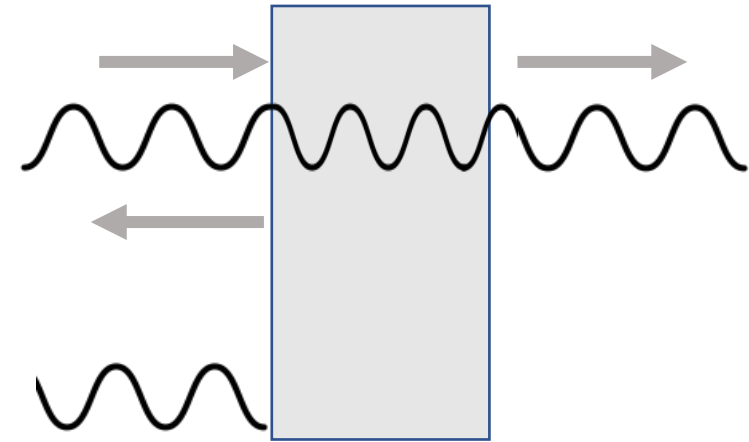
Extinction coefficient

$$\alpha = \frac{4\pi\kappa}{\lambda_0}$$

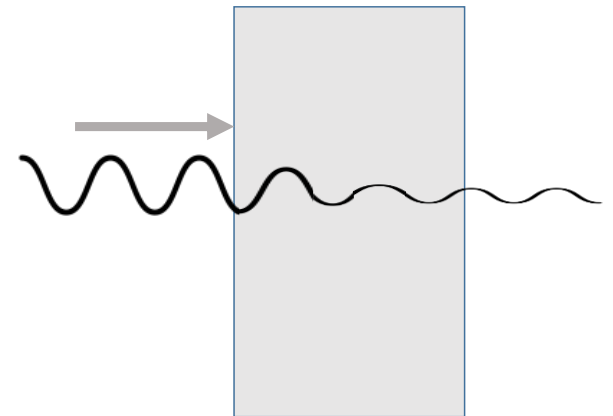
α is the attenuation coefficient

$$\delta_p = 1/\alpha$$

δ_p is the distance for attenuation by $1/e$



$n > 1$



High k

Ice vs. Water at wavelengths we care about

THE FLORIDA STATE UNIVERSITY

COLLEGE OF ARTS AND SCIENCES

COMPLEX INDICES OF REFRACTION FOR WATER AND ICE

FROM VISIBLE TO LONG WAVELENGTHS

By

MARK LEE MESENBRINK

A Thesis submitted to the
Department of Meteorology
in partial fulfillment of the
requirements for the degree of
Masters of Science

Degree Awarded:

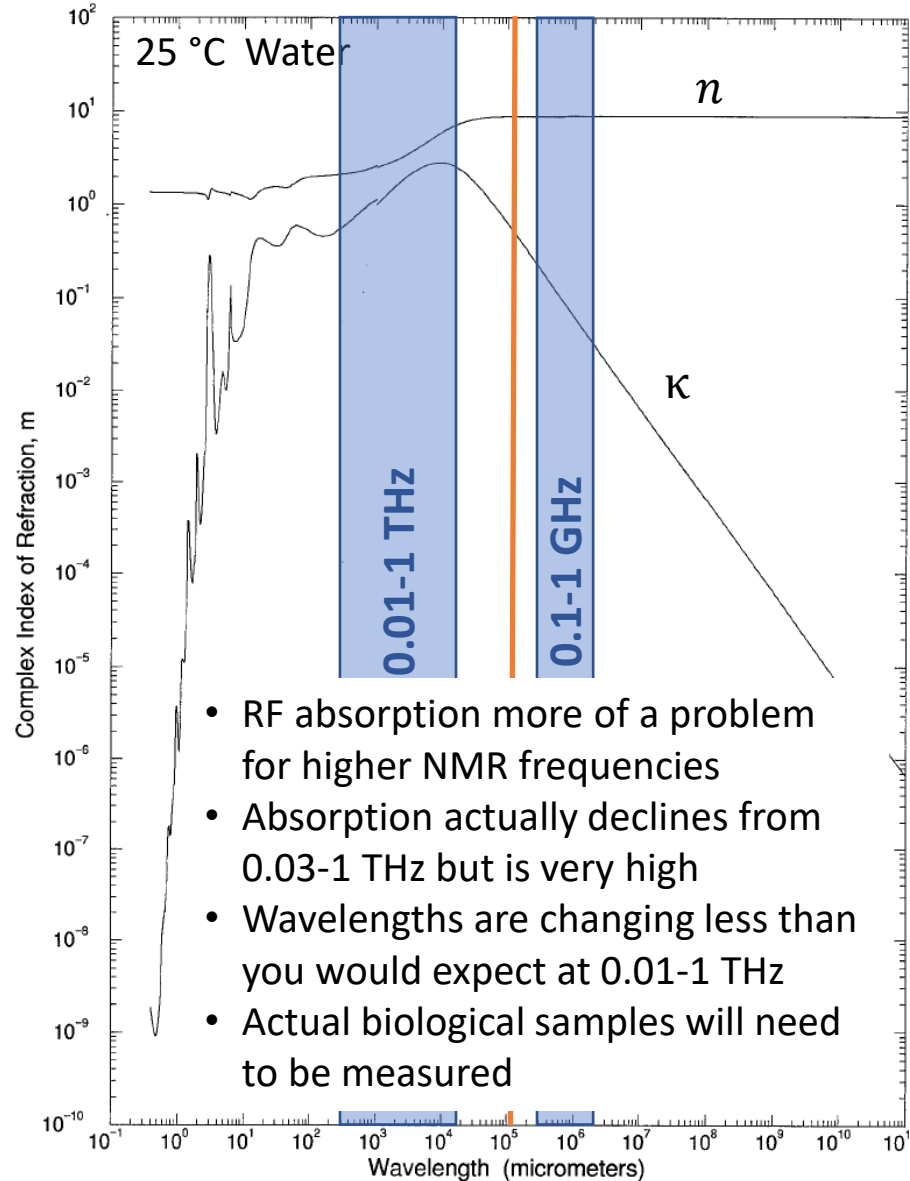
Spring Semester, 1996

ACKNOWLEDEMENTS

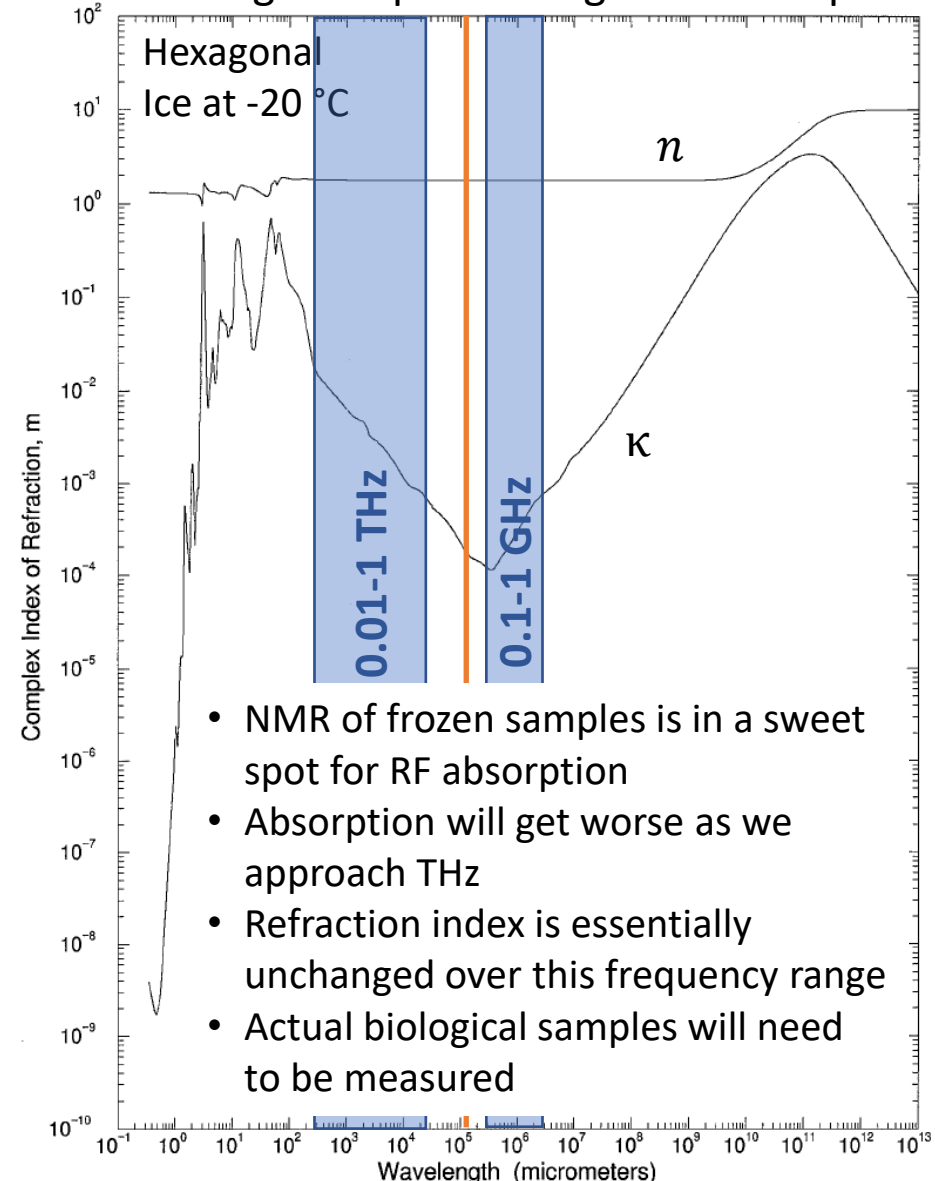
I would like to acknowledge the many people that have assisted and supported me with my research. My deepest and dearest thanks goes to Cyndi. Without her love, I would not have been able to keep focused. My Committee members, Dr. Peter Ray, Dr. Melody Owens and Dr. T. N. Krishnamurti, deserve many sincere thanks. Without their guidance and instruction, my research would never have been complete. I would like to also thank the three "behind the lines" people who made it all happen: Dr. Craig Bohren from Penn State University for his wisdom; Dr. Jesse Stephens for pointing me in the right directions; and Bret Whissel for his god-like knowledge of FORTRAN and countless other programs. Finally, I would like to thank the Air Force for allowing me the opportunity to further my education.

Ice vs. Water at wavelengths we care about

M. Mesenbrink, master's thesis, FSU, 1996



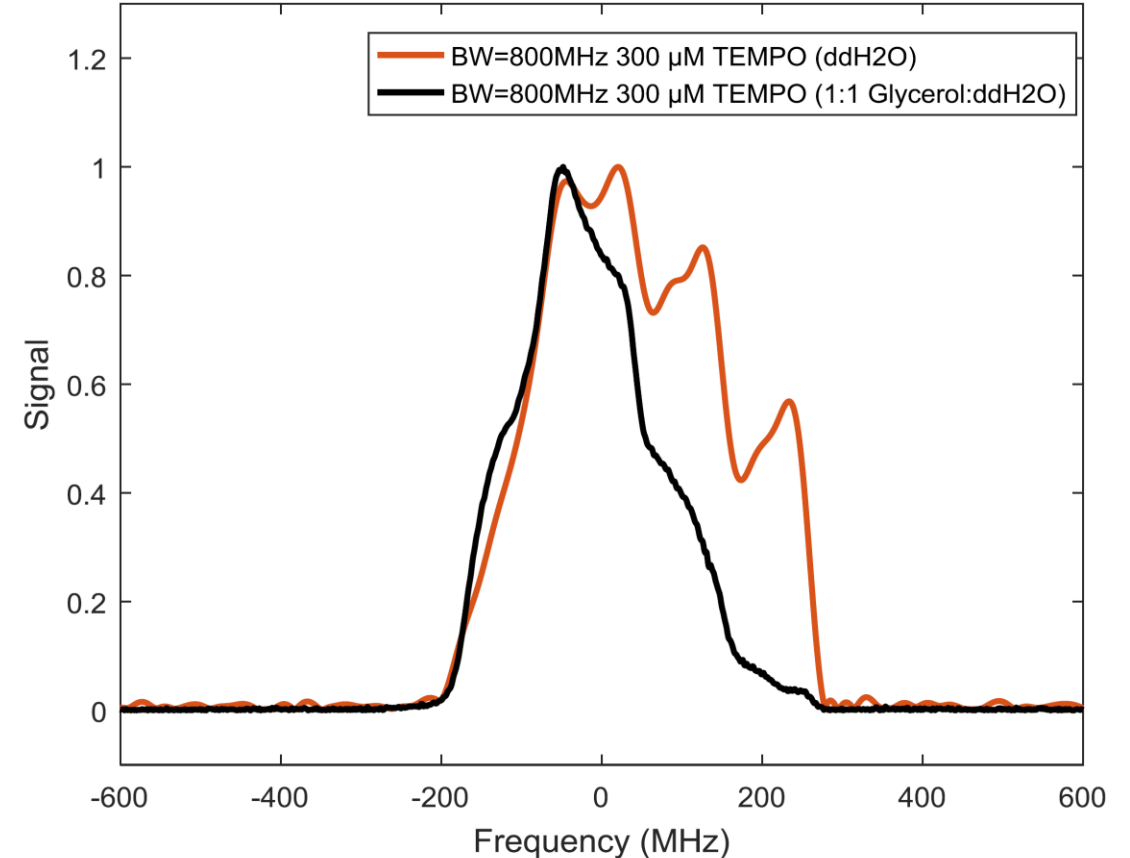
<https://www.youtube.com/watch?v=HwREvdUWSKE>
Finding The Speed of Light with Peeps and a Microwave



DNP: Practical aspects of freezing and temperature

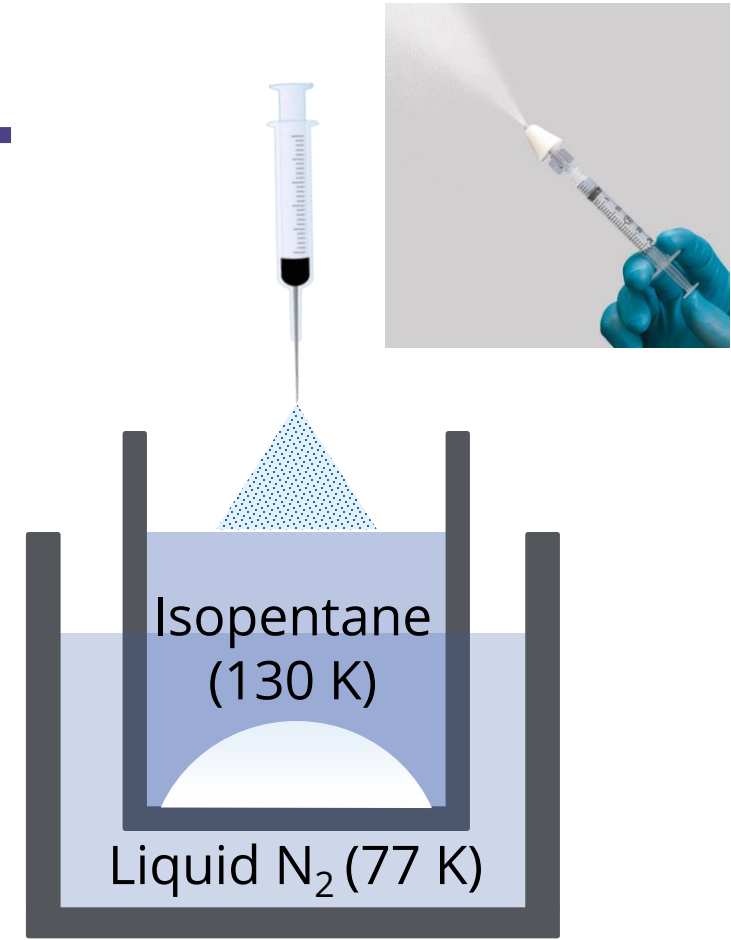
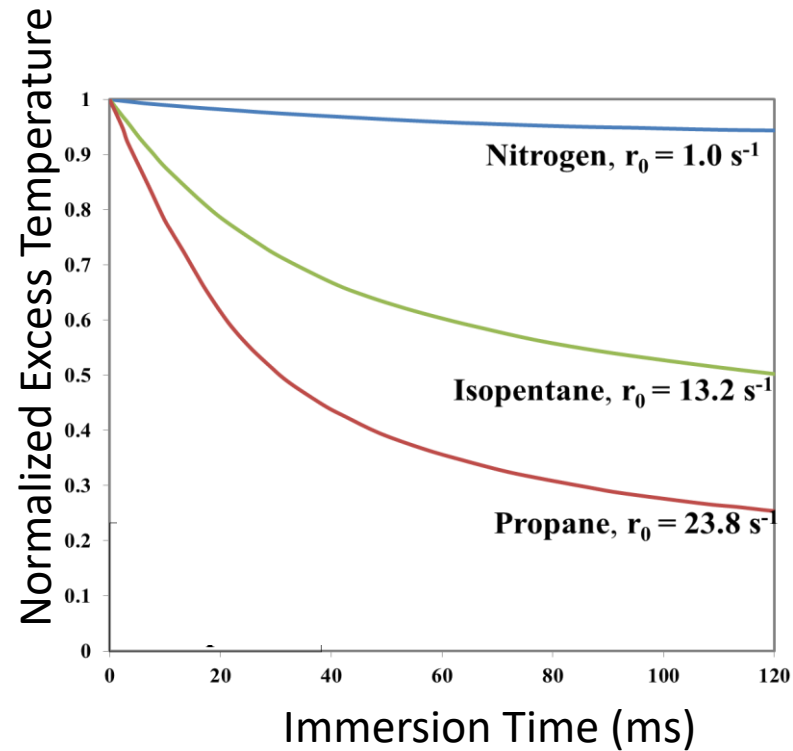
Sample freezing

- Ice crystals can lead to biradical aggregation as well as degrade the sample
- MAS DNP typically relies on freezing the sample on insertion of the rotor into the probe (which takes a few seconds)
- Glassing agents can prevent crystal formation but can create other issues
- Alternatively faster freezing can be done outside of the rotor
- Freezing can also alter the pH of the sample
- The fields of cryoEM and cell biology have extensive literature on cryoprotectants and freezing protocols



Sample freezing

- An efficient freezing agent can remove the need for a glassing agent
- Vitroblots for cryoEM typically use liquid ethane or propane
- Enzyme kinetics people often use isopentane as it is a liquid at room temperature
- EPR and NMR labs have demonstrated freezing via spraying onto cold metal surfaces



Glassing agents

- An effective glassing agent allows you to slowly freeze in the probe
- A popular (though not ideal!) glass is DNP juice (60/40 glycerol/water)
- Cell biology typically uses DMSO, betaine, or trehalose as cryoprotectants which also work well for DNP glasses (with caveats to be shown)
- For biological solids, membranes and crystallation additives (like PEG) act as glassing agents too
- *Dehydration*—via high glassing agent concentration or removal of water through ultracentrifugation/drying/lyophilization will cause *inhomogeneous broadening*. This is widespread in the DNP literature.
- My lab likes 10% DMSO or 10% betaine as a glassing agent as they preserve structure/viability of the samples. We also like minimal ^2H and full hydration.

Classical DNP Matrix Considerations

- Complete radical solubility
- Homogenous distribution of radical
- Dilute proton bath
- High protein concentration
- Preserve native environment of biological sample

~ 5-10 mM biradical

“DNP Juice”

60/30/10 (v/v) glycerol- d_8 / D_2O / H_2O
 % glassing agent % deuteration

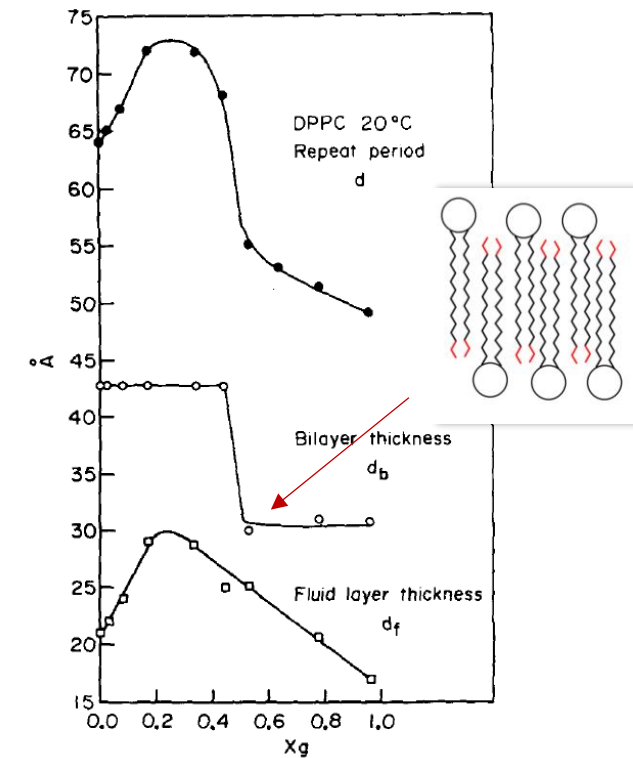
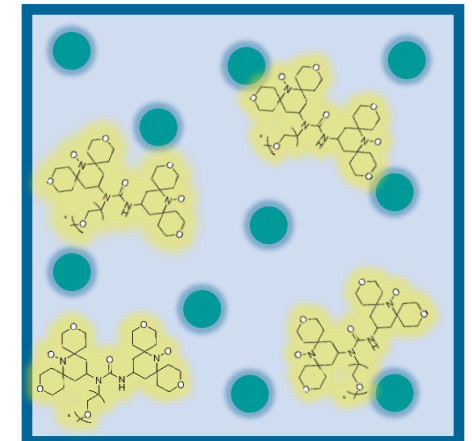
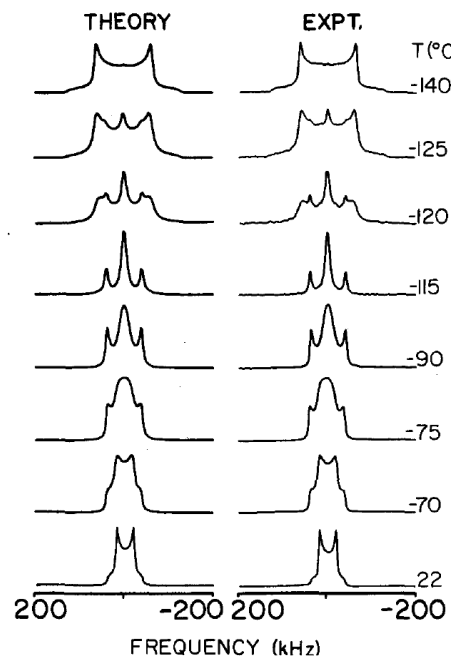
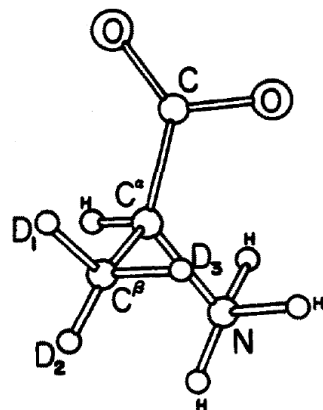
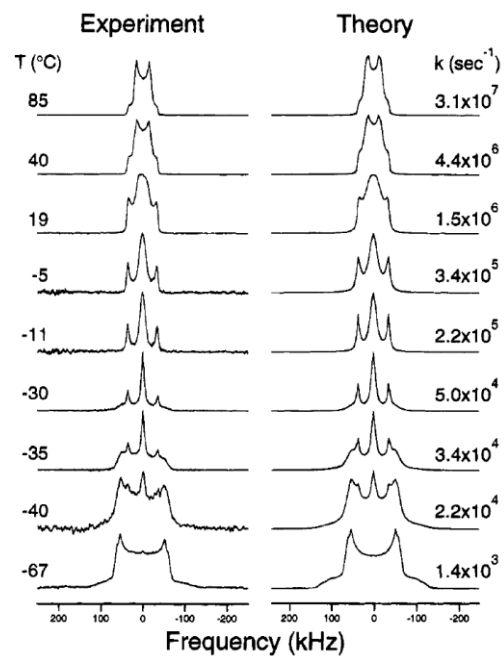


Fig. 4. X-ray parameters for DPPC as a function of mole fraction of glycerol (X_g). The solid circles (●) represent the repeat periods d and the open circles (○) and open squares (□) represent the bilayer widths and fluid layer thicknesses, respectively, as determined from electron density profiles (see Fig. 7).

R. V. McDaniel et al. , *Biochim Biophys Acta* .1983,731, 97-108



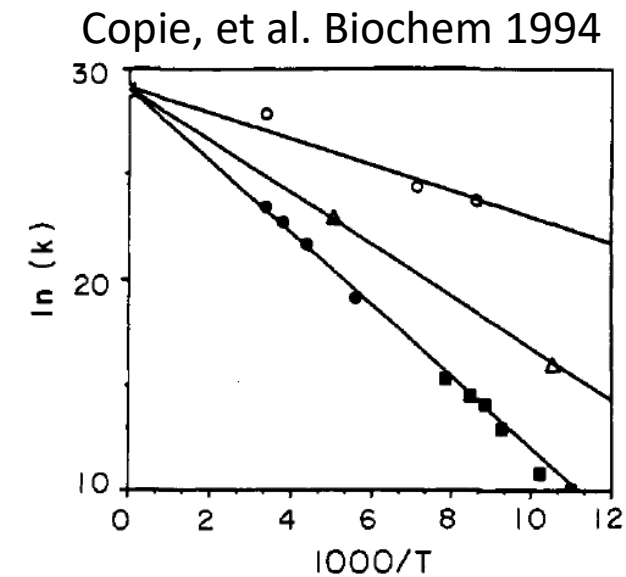
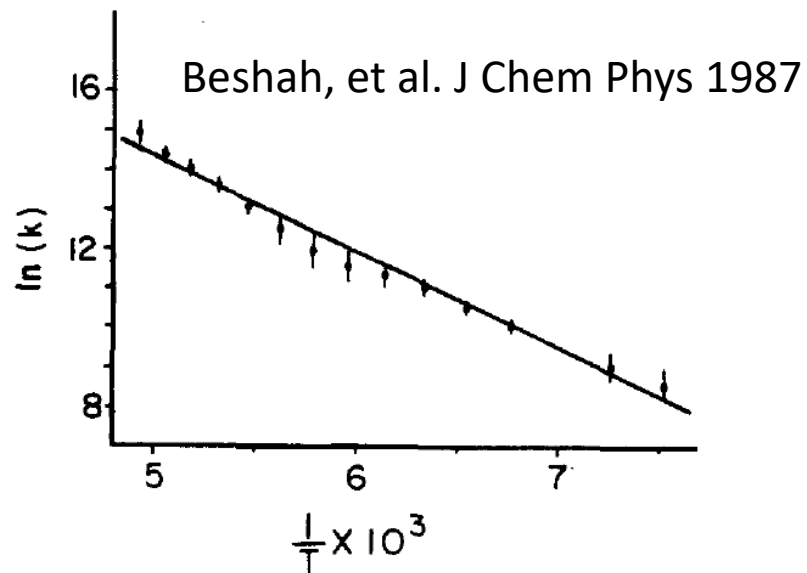
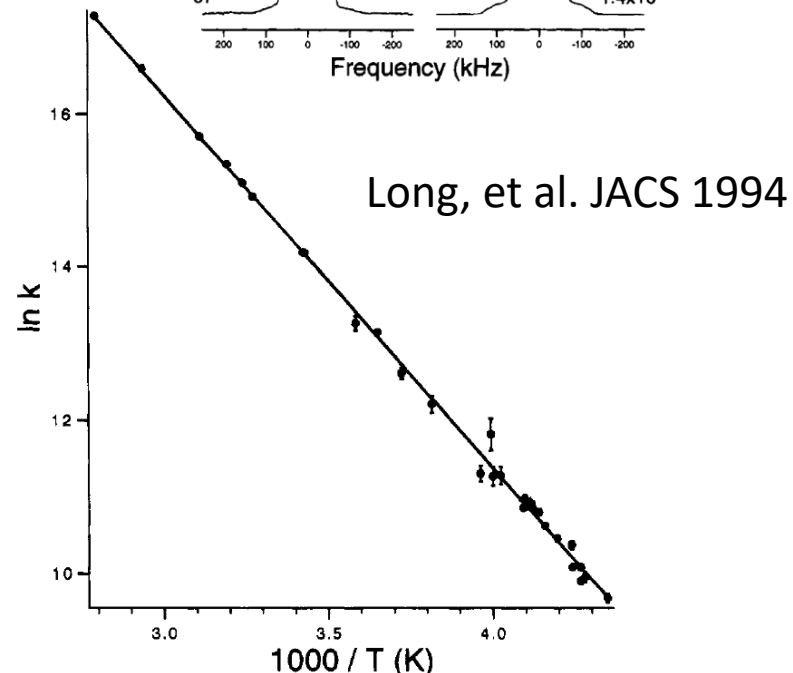
Biological dynamics also impact polarization



²H NMR of Bacteriorhodopsin and Retinal Model Compounds

Table 1: Rates and Activation Energies for Methyl Three-Site Hop

| T, K | 18-C: 6-s-cis ^a | 18-C: 6-s-trans ^b | 18-C: bR ^c | 16,17-C: 6-s-trans ^d | 16,17-C: bR ^e |
|----------------|----------------------------|------------------------------|-----------------------|---------------------------------|--------------------------|
| 91 | 2.25 × 10 ⁴ | | | | |
| 95 | | | | | 8.65 × 10 ⁵ |
| 98 | 5.06 × 10 ⁴ | | > 5 × 10 ⁷ | | |
| 101 | | | | 1.71 × 10 ⁵ | |
| 108 | 3.84 × 10 ⁵ | | | | |
| 113 | 1.30 × 10 ⁶ | | | | |
| 116 | | 2.1 × 10 ¹⁰ | | | |
| 117 | | | | 3.84 × 10 ⁵ | |
| 118 | 1.94 × 10 ⁶ | | | | |
| 123 | | | 5 × 10 ⁶ | | 2.96 × 10 ⁶ |
| 126 | | | | 1.95 × 10 ⁶ | |
| 128 | 4.38 × 10 ⁶ | | | | |
| 140 | | 4.0 × 10 ¹⁰ | | | |
| 139 | | | | 2.96 × 10 ⁶ | |
| 139 | | | | 2.96 × 10 ⁶ | |
| 158 | | | | | > 5 × 10 ⁷ |
| 179 | 2.0 × 10 ⁸ | | | | |
| 198 | | | 8 × 10 ⁹ | | |
| 228 | 2.6 × 10 ⁹ | | | | |
| 263 | 7.6 × 10 ⁹ | | | | |
| 297 | 1.5 × 10 ¹⁰ | 1.2 × 10 ¹² | | | |
| E(act), kJ/mol | 14.5 ± 1 | 5 ± 1 | 9 | 14 ± 2 | 13 ± 2 |



DNP: Practical aspects of ssNMR hardware

Sizes of Interactions: Solids

$$H_{total} = H_{external} + H_{internal}$$

$$H_{ext} = H_{Zeeman} + H_{Radio\ Frequency}$$

500 - 900 MHz 0.001 - 200 kHz

$$H_{Int} = H_{Dipole-Dipole} + H_{Chemical\ Shift} + H_{J-coupling}$$

0.05 - 40 kHz 20 - 40 kHz <200 Hz

Magic Angle Spinning

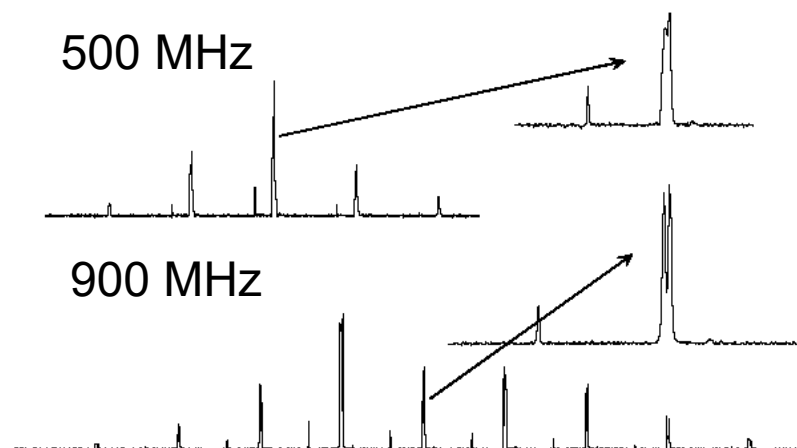
0.2 - 50 kHz

Challenges of biomolecular ssNMR

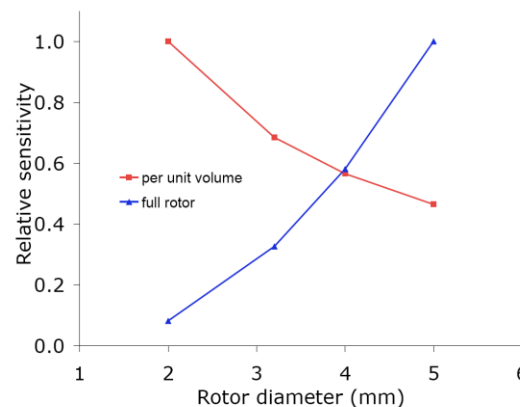
- Sensitivity → Optimizing for proteins which are inherently dilute
 - Temperature matters → Minimizing RF/MAS heating
 - Filtering out the signal of interest from a messy background → Double quantum filtering techniques
- Water is a major component of most samples

Encyclopedia of Magnetic Resonance (2010)

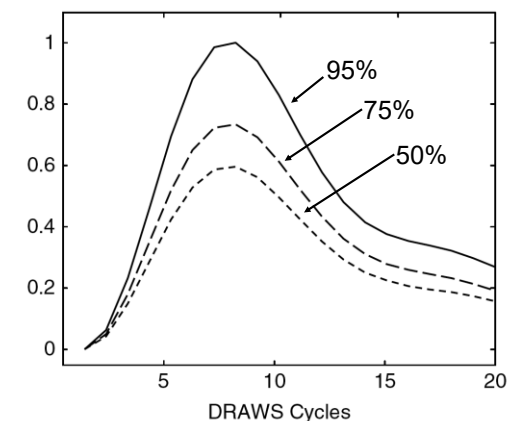
CSA field dependence



MAS vs sensitivity



RF homogeneity

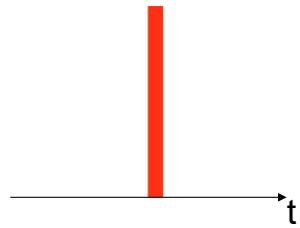
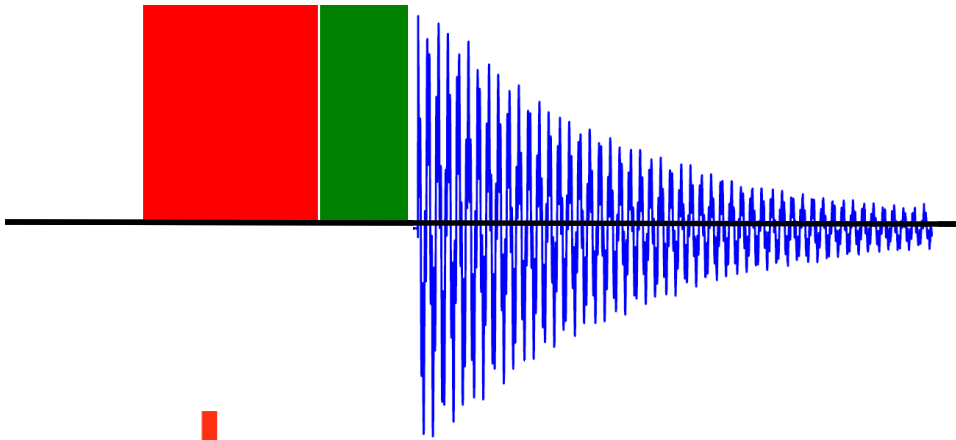


In dry air at 20 °C (68 °F), the speed of sound is 343 m/s (1235 km/h, or 770 mph, or 1129 ft/s, or approximately 5 seconds per mile)

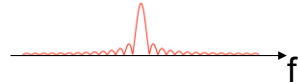
| MAS rate | Rotor Dia (mm) | Outer Speed (m/s) | km/h | Outer Speed (mph) |
|----------|----------------|-------------------|------|-------------------|
| 16000 | 4 | 201 | 724 | 450 |
| 50000 | 2.5 | 393 | 1414 | 880 |
| 68000 | 1.3 | 278 | 1000 | 622 |
| 70000 | 1.3 | 286 | 1029 | 640 |

RF Pulsing in NMR

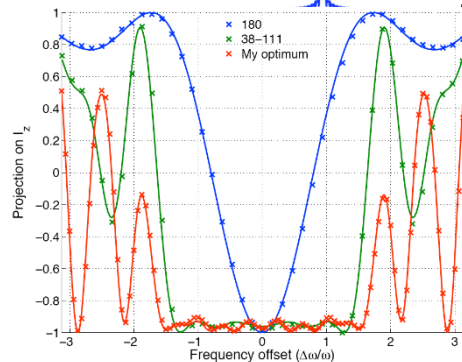
180° 90°



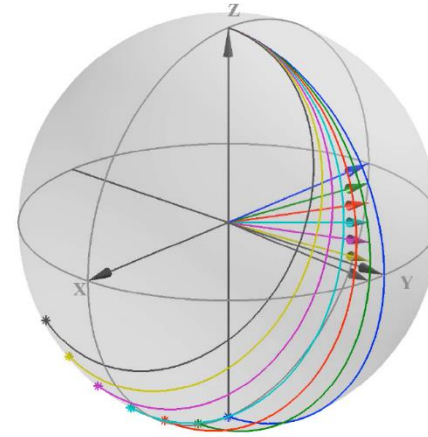
FFT



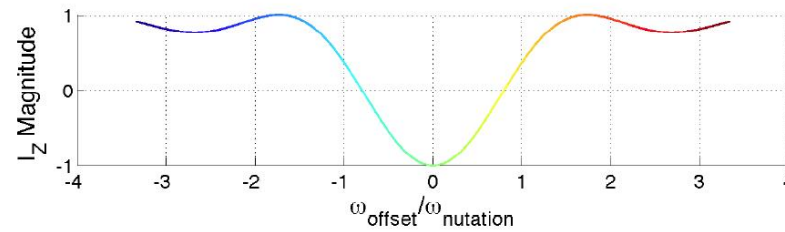
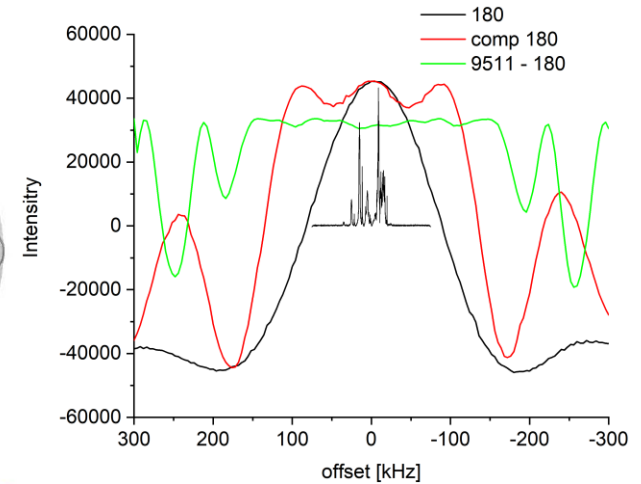
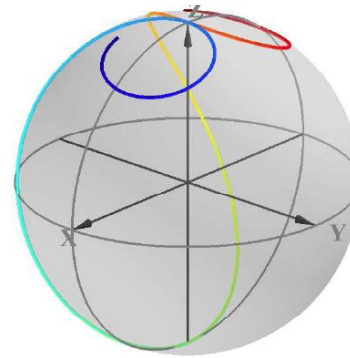
FFT



Inversion pulse: $\omega_{\text{offset}}/\omega_{\text{nutration}}$



- 0
- -0.1
- -0.2
- -0.3
- -0.4
- -0.5
- -0.6



Low-E MAS probes for dilute protein samples

RF Coil Design

Pencil rotors (longest)

Stators custom-designed

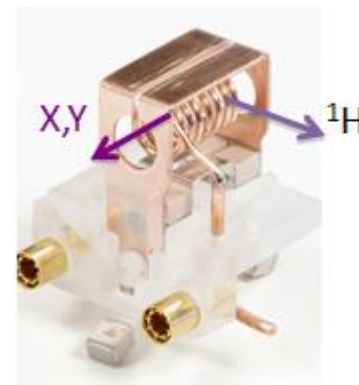
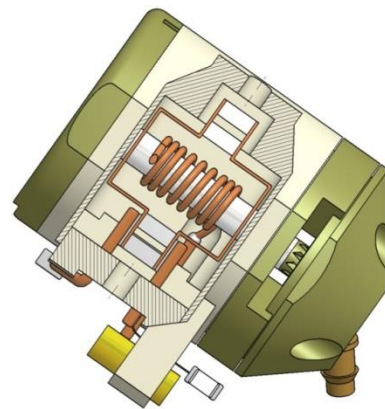
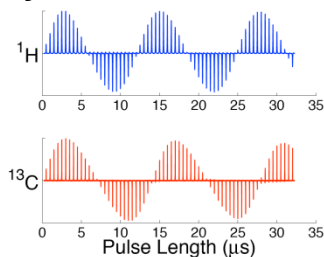
B_1 homogeneity over full 36 μ L rotor

(900 MHz probe):

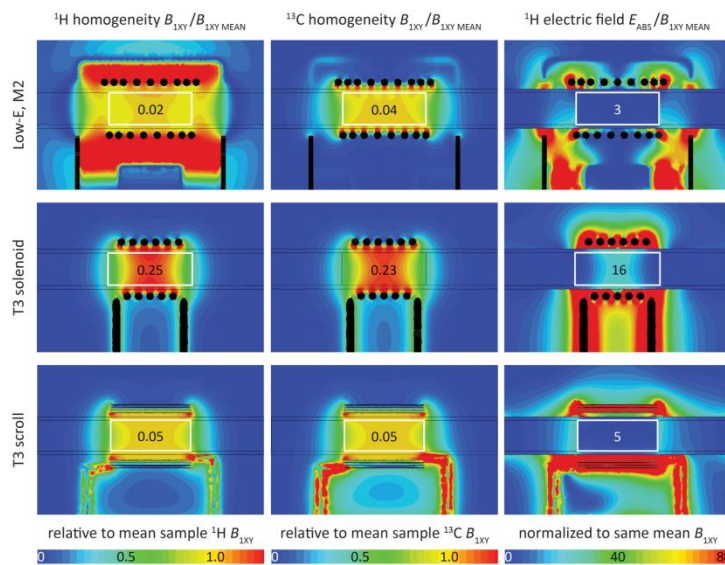
^1H 810°/90° = 97%

^{13}C 810°/90° = 88%

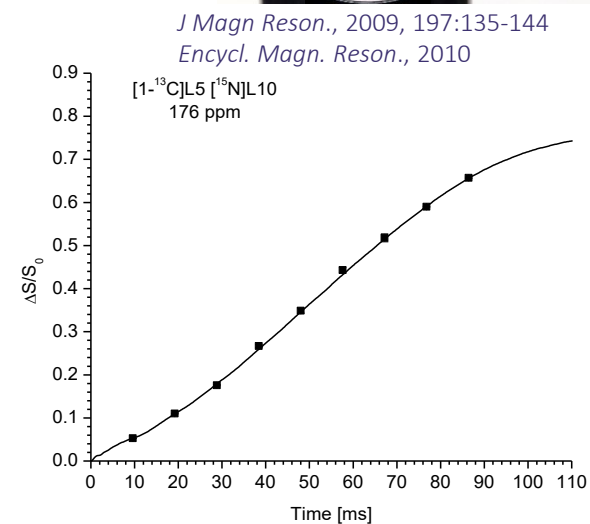
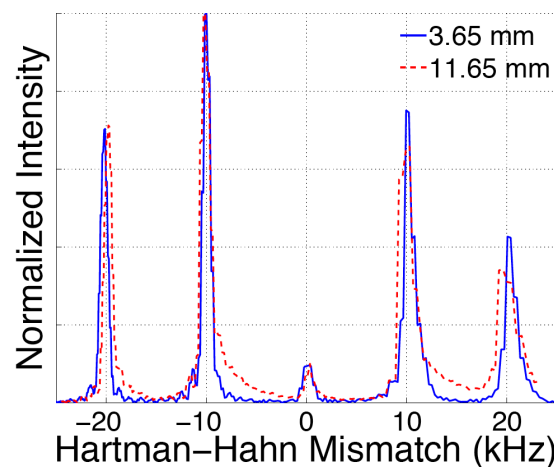
^{15}N 810°/90° = 82%



- High B_1 homogeneity
- Stable under high power
- Minimal RF heating of sample

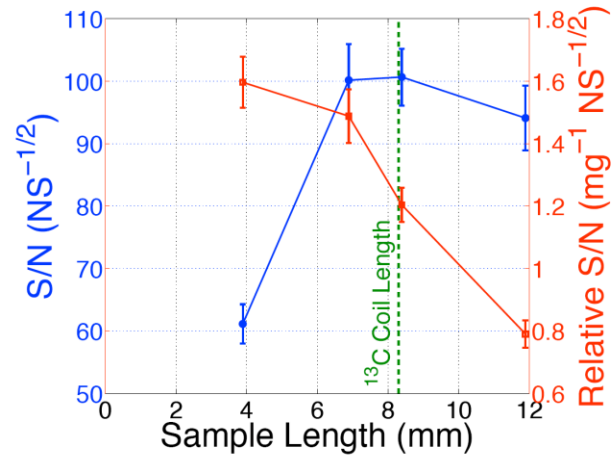


Standard deviations of B_1 field and sample-averaged values of E/B_1

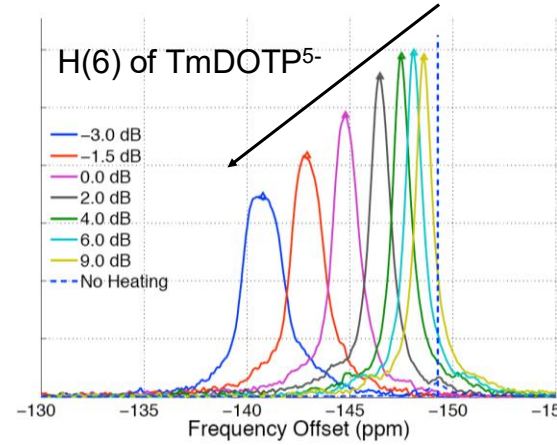


Characterizing a probe

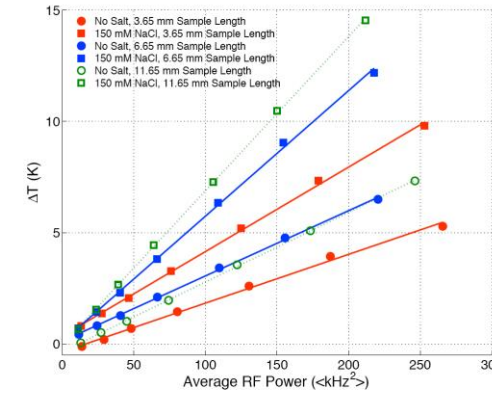
Rotor packing



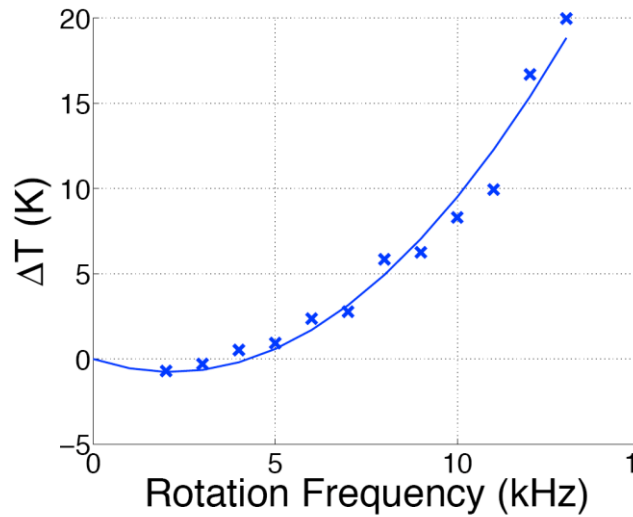
RF heating



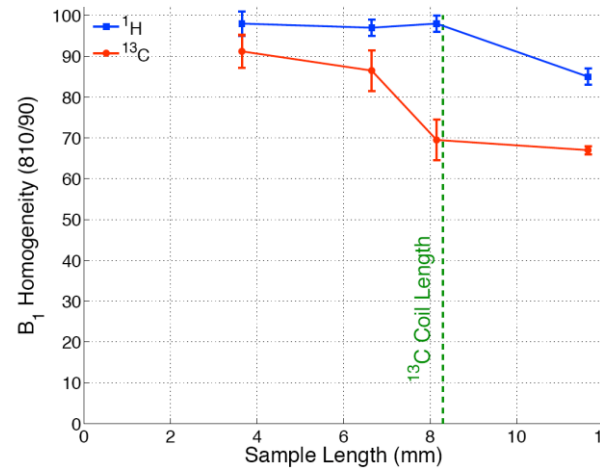
Dielectric effects



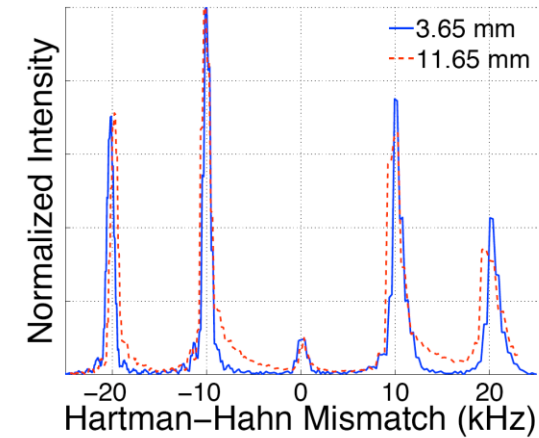
MAS heating



RF homogeneity



B1 field profiles



RF efficiency

| | ¹ H kHz/W | ¹³ C kHz/W |
|------------------------------|----------------------|-----------------------|
| Low-E MAS | 0.47 | 0.96 |
| MAS Scroll | 2.37 | 0.23 |
| Balanced Solenoid MAS | 1.10 | 0.71 |
| Crossed Coil | 0.63 | 0.12 |
| Z-Coil | 0.43 | |

Calibrating a probe:KBr

Setting the magic angle

J Magn Reson., 1982, 48:125-131

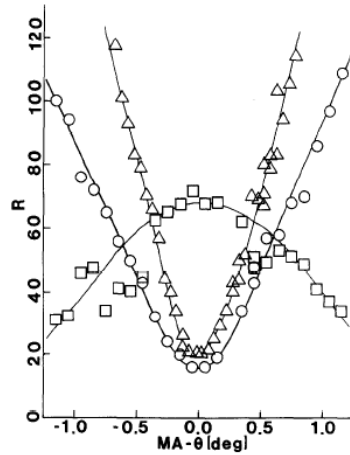


FIG. 3. Plot of peak height ratio vs deviation from magic angle. For KBr, $R = (\text{average ht second-order spinning sidebands})/(\text{height of central peak})$ with powdered (O) and crystalline (Δ) ples. For HMB = (\square), $R = (\text{height of aromatic peak})/(\text{height of methyl peak})$.

TABLE 1
CANDIDATES FOR ANGLE REFERENCE MATERIALS

| $I = 1/2$ Nuclide | Quadrupolar reference nuclide | $ \gamma_1 - \gamma_2 / \gamma_1 ^2$ |
|----------------------|----------------------------------|--------------------------------------|
| ^{13}C | ^{79}Br | 0.004 |

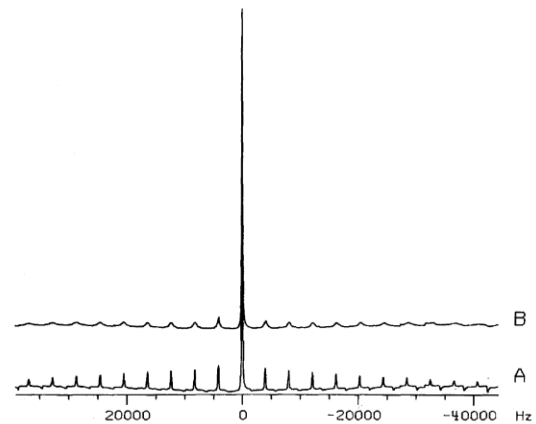
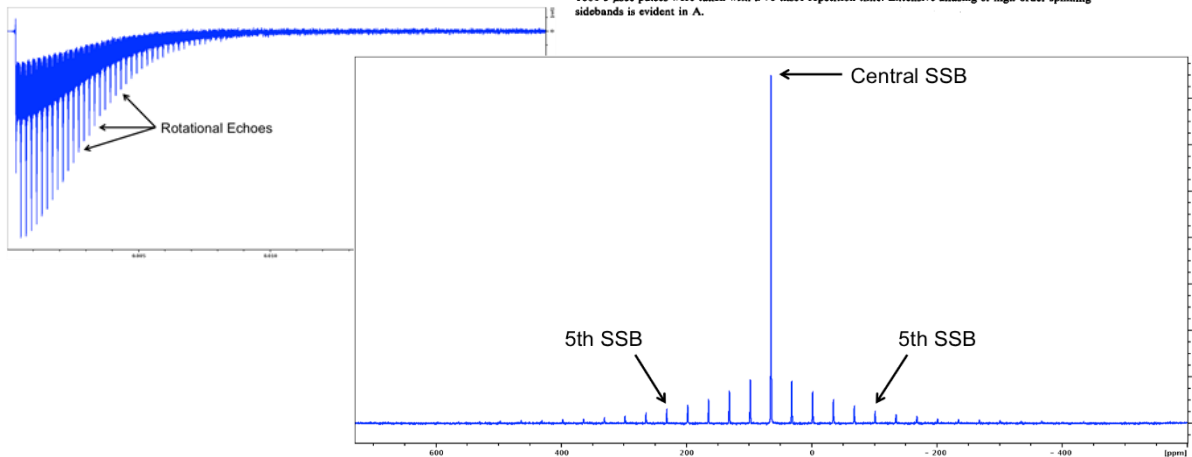
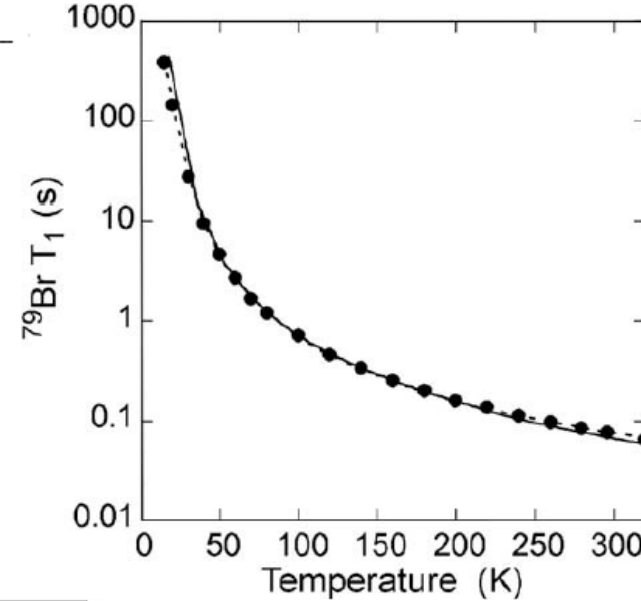


FIG. 2. FT/MAS ^{79}Br spectrum of KBr at the magic angle (A) and 0.5° off angle (B), at 37.6 MHz. 1000 3- μsec pulses were taken with a 70-msec repetition time. Extensive aliasing of high-order spinning sidebands is evident in A.

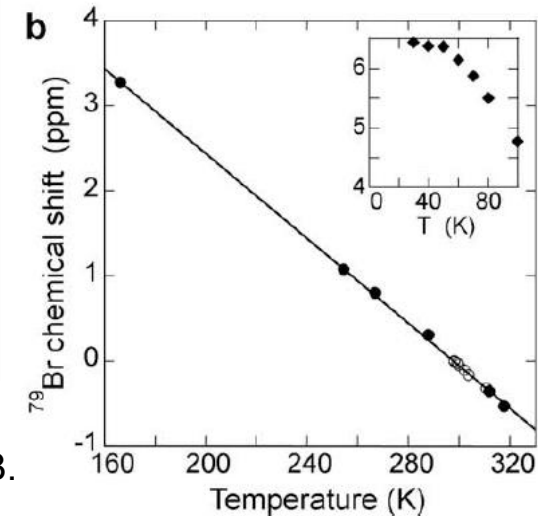
Calibrating temperature

J Magn Reson., 2009, 196:84-87



The FWHM of the central SSB should be $\sim 120\text{-}130$ Hz and the 5th SSB FWHM should be within 10% of the measured FWHM for the central SSB.

Roughly calibrate the field: 60.15 ppm for KBr



Calibrating a probe: Adamantane

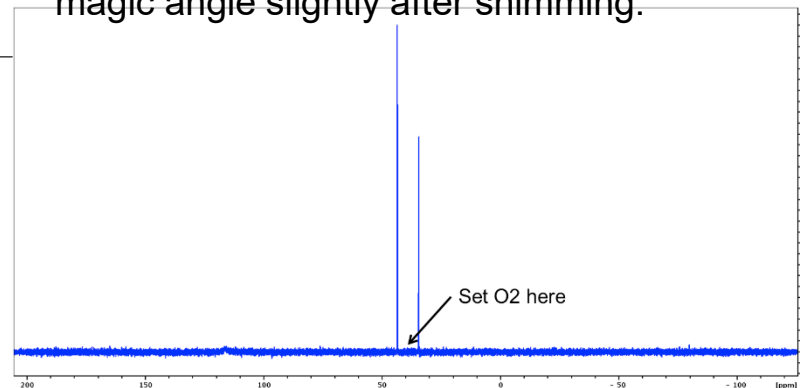
Shimming

J Magn Reson., 1997, 128:87-91

TABLE 3
Spherical Harmonic Shims in the Tilted Frame Expressed as Linear Combinations of Laboratory Frame Shims

| | |
|---|--|
| First order | |
| $B_{z_1}^{(1)} - \frac{1}{\sqrt{3}} B_{z_2}^{(1)} - \frac{\sqrt{2}}{\sqrt{3}} B_{z_3}^{(1)}$ | |
| $B_{z_2}^{(1)} - \frac{1}{\sqrt{3}} B_{z_1}^{(1)} + \frac{\sqrt{2}}{\sqrt{3}} B_{z_3}^{(1)}$ | |
| $B_{z_3}^{(1)} - B_{z_4}^{(1)}$ | |
| Second order | |
| $B_{z_1}^{(2)} - B_{z_2}^{(2)} - \frac{2\sqrt{2}}{3} B_{z_3}^{(2)}$ | |
| $B_{z_2}^{(2)} - \frac{1}{3} B_{z_1}^{(2)} + \frac{\sqrt{2}}{6} B_{z_3}^{(2)} - \frac{\sqrt{2}}{6} B_{z_4}^{(2)}$ | |
| $B_{z_3}^{(2)} - \frac{1}{\sqrt{3}} B_{z_1}^{(2)} - \frac{\sqrt{2}}{\sqrt{3}} B_{z_2}^{(2)}$ | |
| $B_{z_4}^{(2)} - \frac{2\sqrt{2}}{3} B_{z_1}^{(2)} + \frac{1}{3} B_{z_2}^{(2)} + \frac{2}{3} B_{z_3}^{(2)}$ | |
| $B_{z_5}^{(2)} - \frac{1}{\sqrt{3}} B_{z_1}^{(2)} + \frac{\sqrt{2}}{\sqrt{3}} B_{z_2}^{(2)}$ | |
| Third order | |
| $B_{z_1}^{(3)} - \frac{2}{3\sqrt{3}} B_{z_2}^{(3)} - \frac{1}{\sqrt{6}} B_{z_3}^{(3)} + \frac{5}{\sqrt{3}} B_{z_4}^{(3)} - \frac{5}{3\sqrt{6}} B_{z_5}^{(3)}$ | |
| $B_{z_2}^{(3)} - \frac{\sqrt{2}}{3\sqrt{3}} B_{z_1}^{(3)} + \frac{\sqrt{3}}{2} B_{z_3}^{(3)} + \frac{5}{6\sqrt{3}} B_{z_4}^{(3)}$ | |
| $B_{z_3}^{(3)} - \frac{10\sqrt{2}}{3} B_{z_1}^{(3)} + \frac{1}{6} B_{z_2}^{(3)} + \frac{5}{6} B_{z_4}^{(3)}$ | |
| $B_{z_4}^{(3)} - \frac{1}{3\sqrt{3}} B_{z_1}^{(3)} - \frac{\sqrt{2}}{3\sqrt{3}} B_{z_2}^{(3)}$ | |
| $B_{z_5}^{(3)} - \frac{1}{3} B_{z_1}^{(3)} + \frac{\sqrt{2}}{12} B_{z_2}^{(3)} - \frac{\sqrt{2}}{12} B_{z_3}^{(3)}$ | |
| $B_{z_6}^{(3)} - \frac{\sqrt{2}}{3\sqrt{3}} B_{z_1}^{(3)} + \frac{1}{2\sqrt{3}} B_{z_2}^{(3)} + \frac{2\sqrt{2}}{\sqrt{3}} B_{z_3}^{(3)} + \frac{5}{6\sqrt{3}} B_{z_4}^{(3)}$ | |
| $B_{z_7}^{(3)} - 2\sqrt{2} B_{z_1}^{(3)} + \frac{1}{2} B_{z_2}^{(3)} + \frac{1}{2} B_{z_3}^{(3)}$ | |
| Fourth order | |
| $B_{z_1}^{(4)} - \frac{7}{18} B_{z_2}^{(4)} + \sum_{m=1}^4 c_m T_{4m}$ | |
| Fifth order | |
| $B_{z_1}^{(5)} - \frac{1}{6\sqrt{3}} B_{z_2}^{(5)} + \sum_{m=1}^5 c_m T_{5m}$ | |

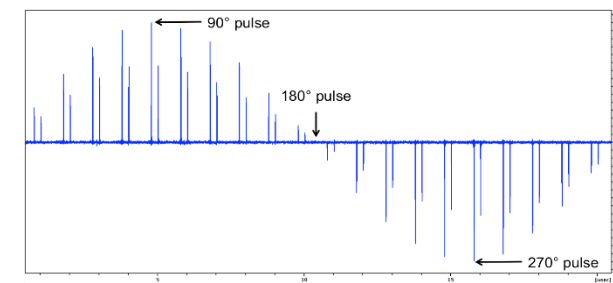
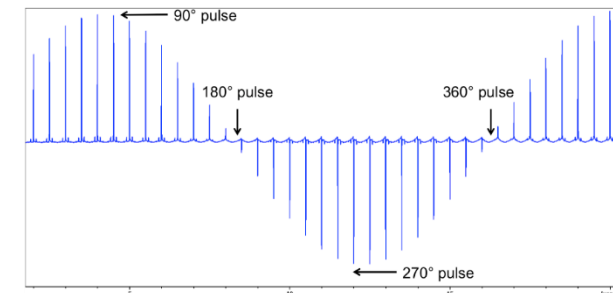
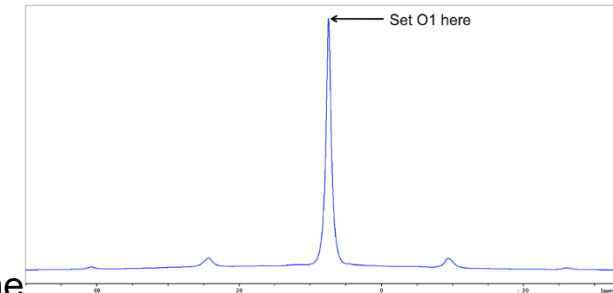
- Align magic angle axis with either x or y axis of shim set. Use simple pulse-acquire sequences
- Spin adamantane at 10 kHz, observe proton resonance (should be close to 2.3 ppm)
- Observe carbon with low power decouple on proton at 2.3 ppm (~50 mW), extend fid acquisition to 200-300 msec
- Set field for left peak at 38.48 ppm
- Shim using the X (or Y) shim and adjust; only the X OR Y shim should effect the shimming, NOT both; Z may help too
- Select the XZ (or YZ) shim and adjust
- Select the XZ² (or YZ²) shim and adjust
- Adjust field as needed to keep peak at 38.48 ppm as decoupling needs to be on resonance since low power
- If shims are way off, you may need to readjust magic angle slightly after shimming.



¹³C spectrum of adamantane, with proper shimming (FWHM ~ 4 Hz)

Calibrating RF

J Magn Reson., 2009, 196:84-87

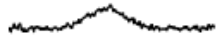


If console/amplifiers are linear, measuring 90 times at 50 W is sufficient to calculate power levels fairly closely for a range of experiments

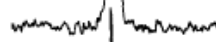
Calibrating a probe:CP and DCP

CP and magic angle spinning
J Magn Reson., 1977, 28:105-112

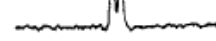
without dipolar decoupling
 or magic angle spinning



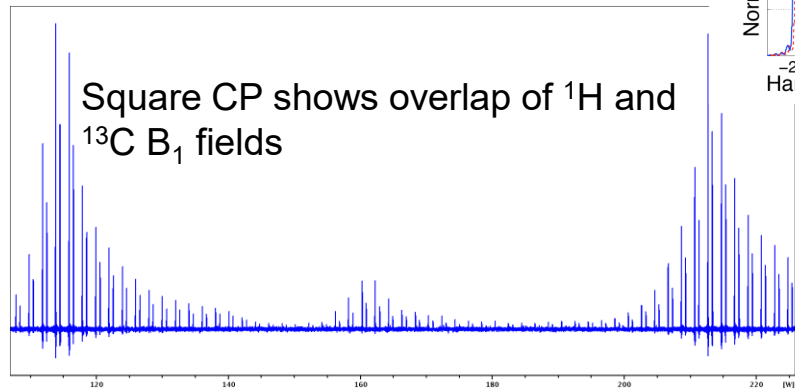
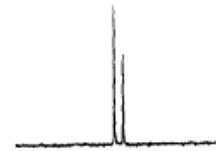
magic angle spinning only



dipolar decoupling only

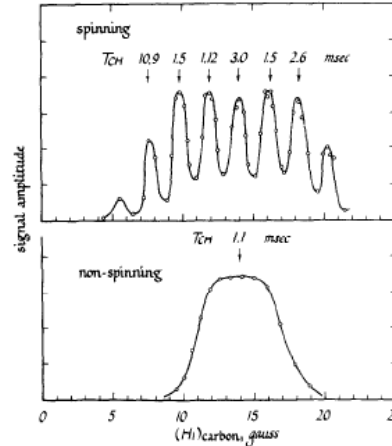


with dipolar decoupling
 and magic angle spinning

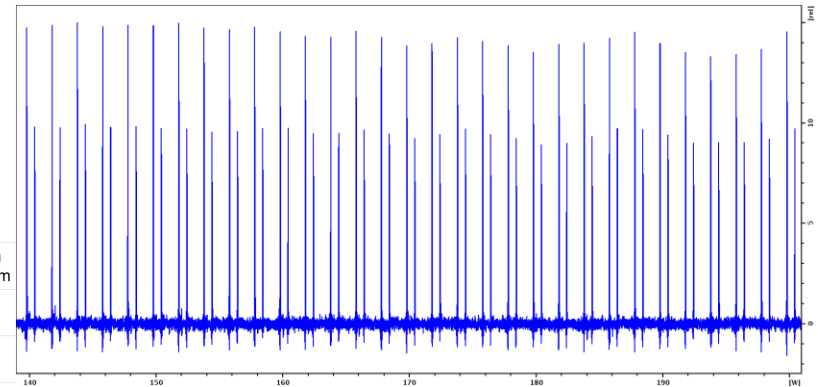
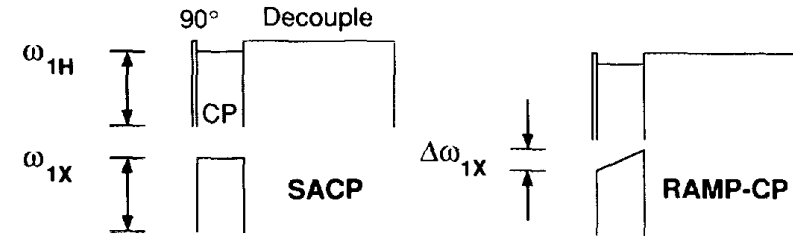
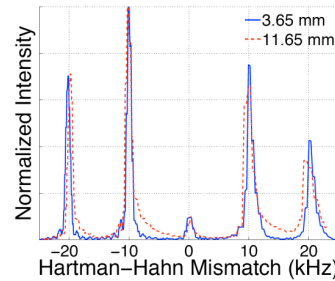


Square CP shows overlap of ^1H and ^{13}C B_1 fields

^{13}C power dependence at 10 kHz MAS for a commercial probe

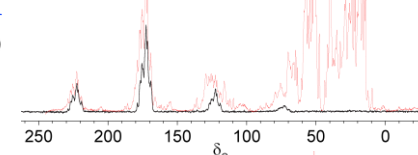


CP match on low-E probe
 (10 kHz MAS adamantane)



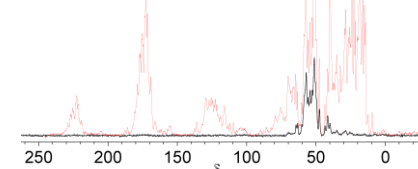
HNC0 Specific CP (black) vs CP (red)

$\nu_{1N}=52.5\text{kHz}$



HNCA Specific CP (black) vs CP (red)

$\nu_{1N}=54\text{kHz}$



Ramped CP overcomes the MAS
 dependence (to some extent)
J Magn Reson., 1994, 110:219-227

Specificity and efficiency of specific CP (DCP) sequences are dependent on homogeneity of RF and B_1 strength for ^{13}C and ^{15}N

DNP MAS probe cryogenic considerations



3.2 mm 600 MHz /395 GHz

Collaboration with Bruker

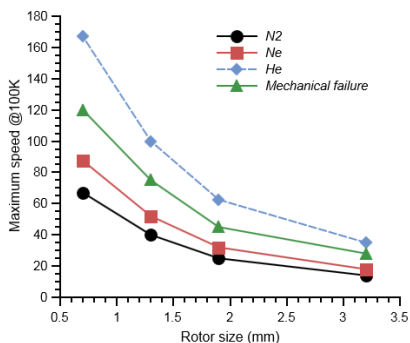
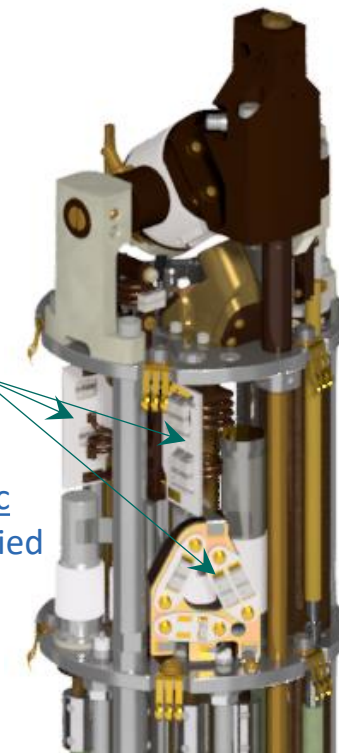
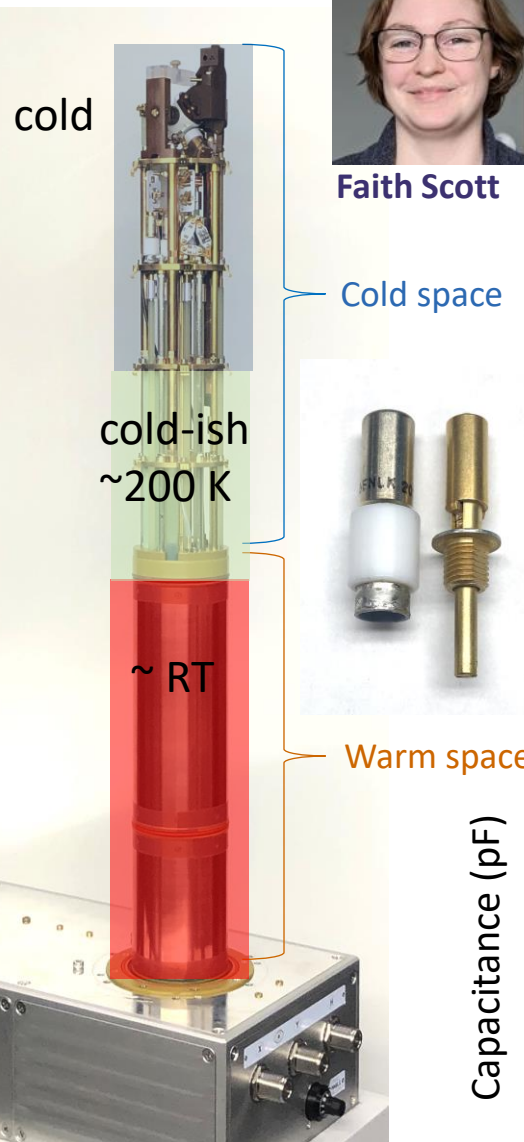
- ✓ Compatible with Bruker LT MAS cooling cabinet
- ✓ **¹HXY RF circuit cloned** from ¹H-detection probes
- ✓ **Large choice of X-Y isotopes by change of tuning cards:**
¹³C, ¹⁵N, ²H, ¹⁷O, ³¹P, ¹⁴N, metalloproteins, etc.
- ✓ Switches between 3- and 2-resonance circuits
- ✓ ¹H channel 2x more efficient
- ✓ Magic angle stable at 95K
- ✓ **Internal cold space is half as small**
 - ✓ <1 hour to warmup (vs. 2-3 hours)
 - ✓ <25" to cool down (vs. 45")
- ✓ Stable, predictable tuning at 95K
- ✓ Weighs ~1/3 less



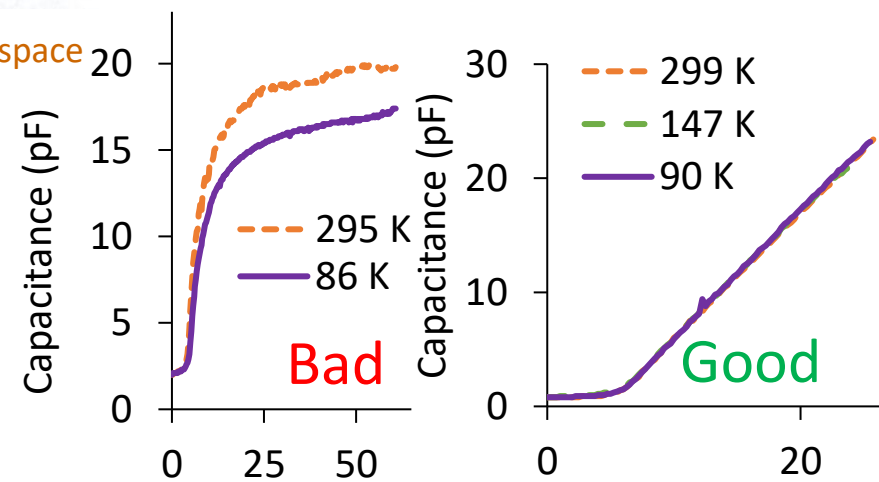
Faith Scott



Peter Gor'kov

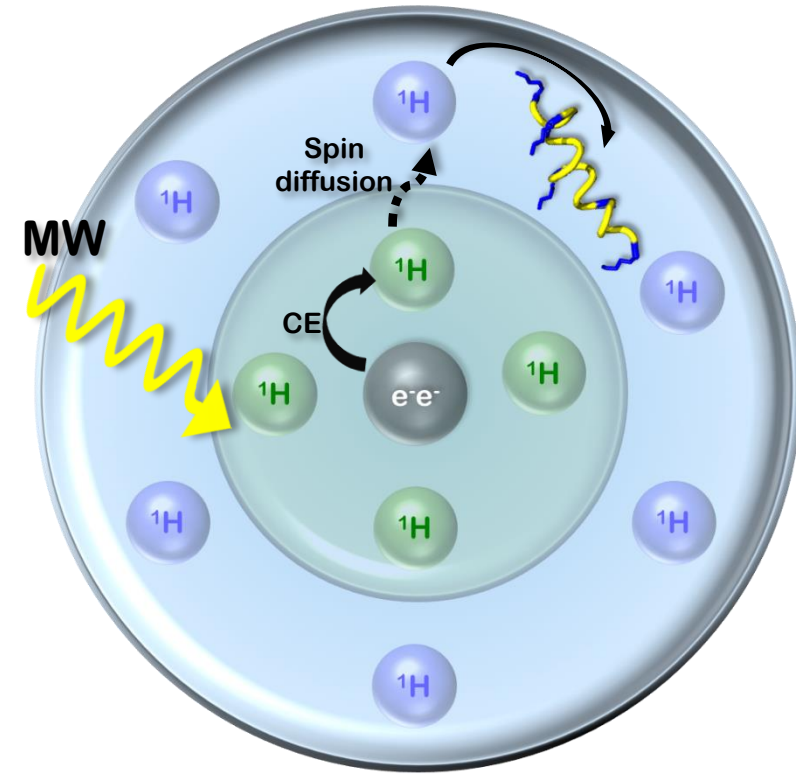


3.2 mm probe w/o outer dewar



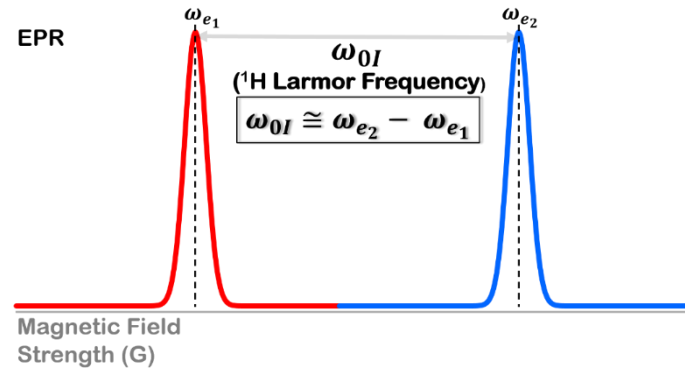
DNP: Practical aspects of determining optimal enhancements

Optimizing enhancements at high field

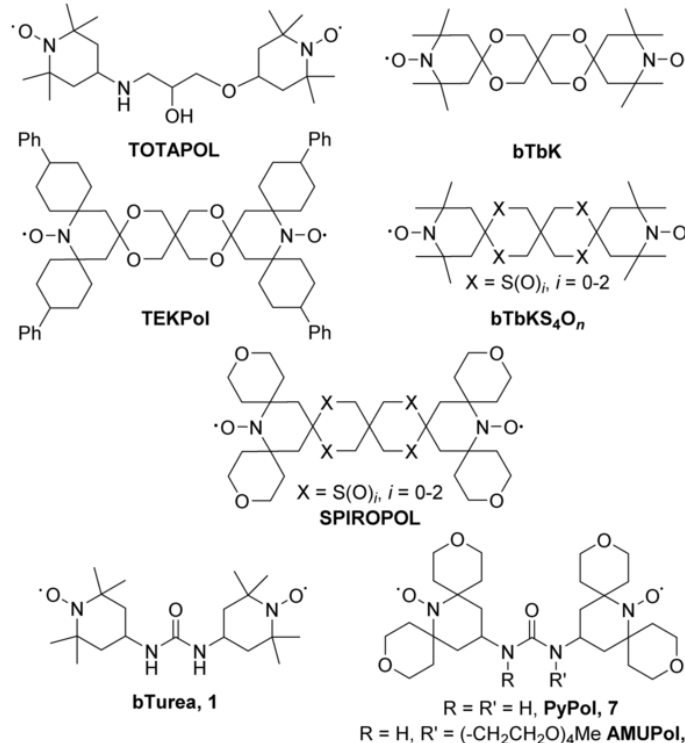


A. Smith et al. *Anal. Chem.* 2016, 88, 122–132
 C. Sauvée et al. *Chem. Eur. J.* 2016, 22, 5598–5606
 C. Sauvée et al., *Angew. Chem. Int. Ed.* 2013, 52, 10858–10861

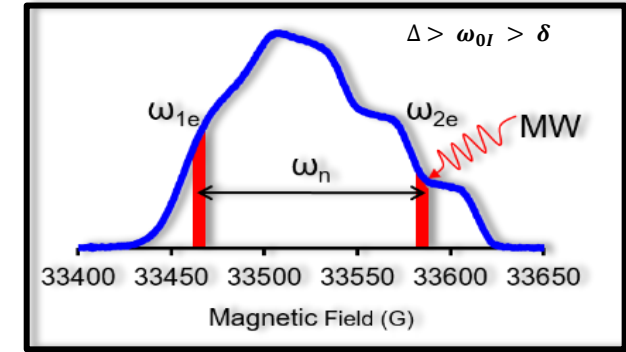
Proline enhancement of ~160 on our instrument (AMUPol) operating at ~95 K



Developing Water Soluble Nitroxide Biradicals



“Wide line radical”

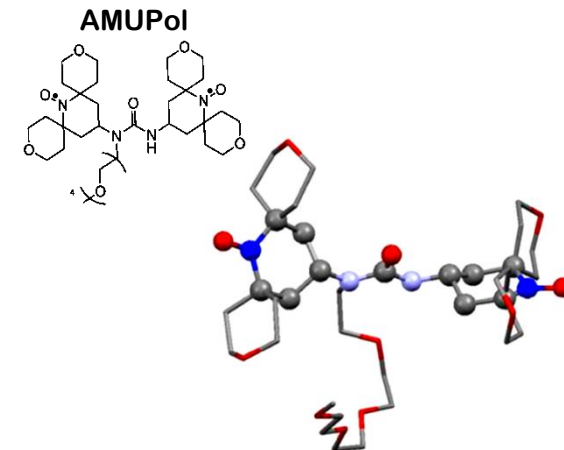


Inhomogeneous broadening

- g-anisotropy
- hyperfine interaction

Optimal DNP enhancements

- Perpendicular g-tensor orientation
- strong dipolar coupled e-
- rigid structure



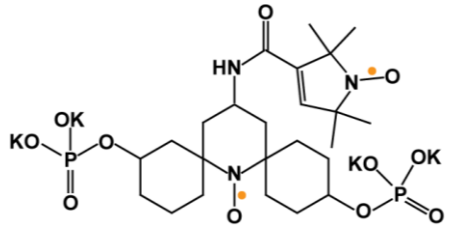
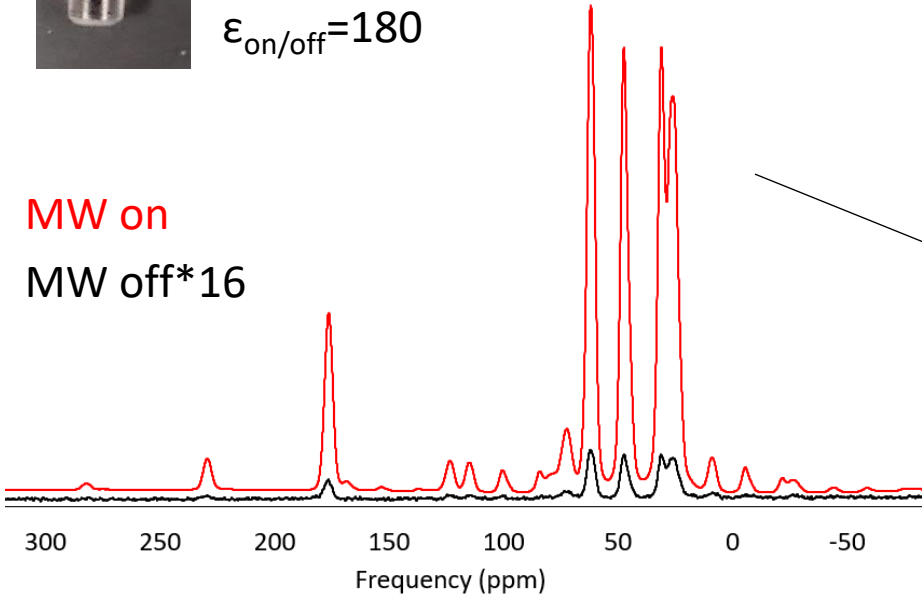
Optimizing enhancements at high field



150 mM ^{13}C -proline
 10 mM Amupol
 60% d_8 -glycerol/30%
 D_2O /10% H_2O
 Standard-wall sapphire rotor
 $\epsilon_{\text{on/off}}=180$

Sauvee, C., et al. (2013)
Angew. Chem. Int., 41
 $D \sim 35 \text{ MHz}$
 $|J| \sim 15 \text{ MHz}$

MW on
 MW off*16



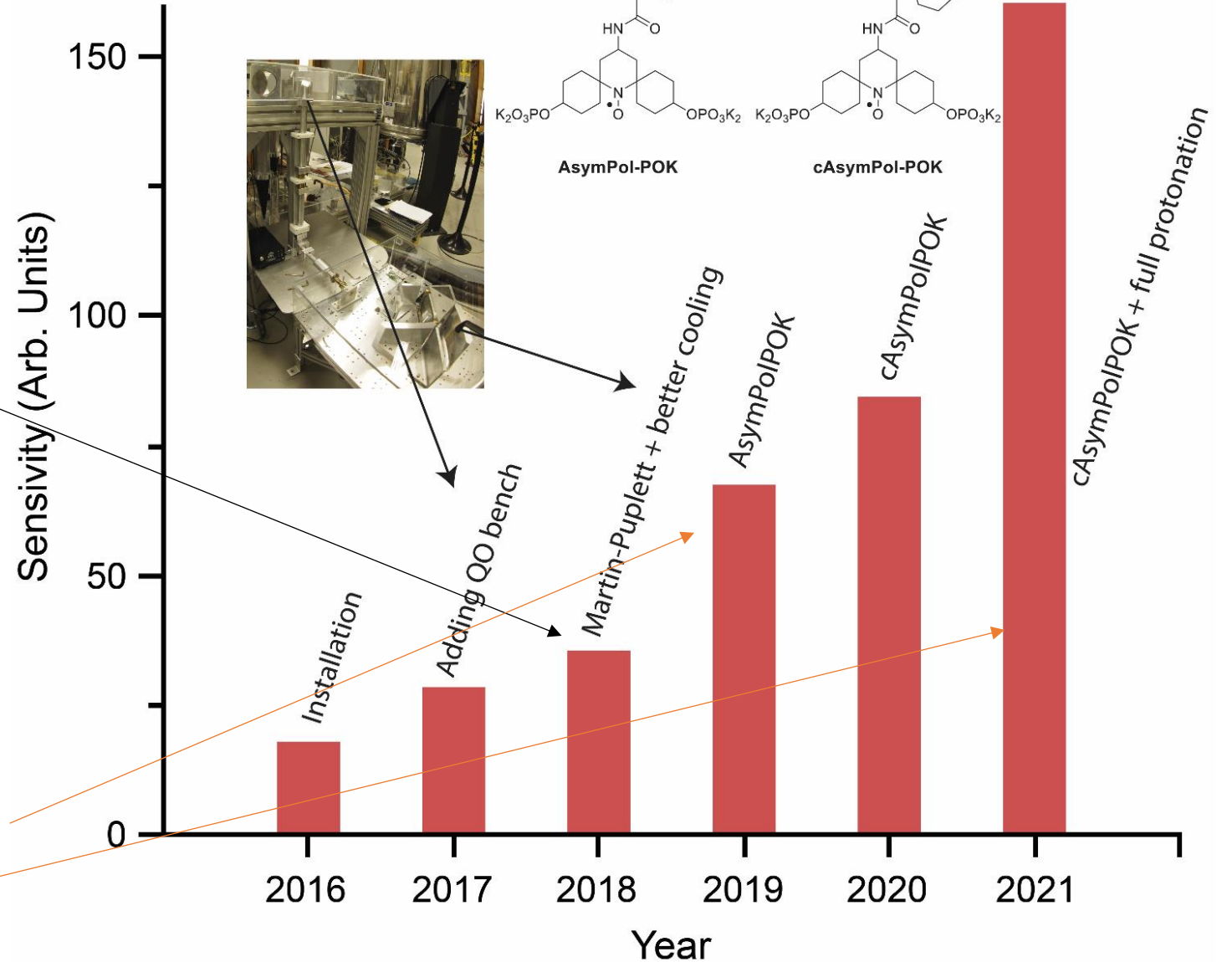
$D \sim 56 \text{ MHz}$
 $|J| \sim 70 \text{ MHz}$

- Faster DNP buildup time
- Insensitive to protonation

AsymPolPOK

Mentink-Vigier, F., et al. (2018) *J. Am. Chem. Soc.*, 141

Harrabi, R et al. (2022) *Ang. Chemie* 61 e202114103



What should our standard be?



150 mM ^{13}C -proline

10 mM AMUpol

60% d_8 -glycerol/30%

D_2O /10% H_2O

Standard-wall sapphire rotor

$\epsilon_{\text{on/off}}=180$

Sauvee, C., et al. (2013)

Angew. Chem. Int., 41

$D \sim 35$ MHz

$|J| \sim 15$ MHz

Considerations:

Biradical: AMUPol vs AsymPolPOK vs TinyPol

MAS Temperature: 90 K vs 100 K and higher

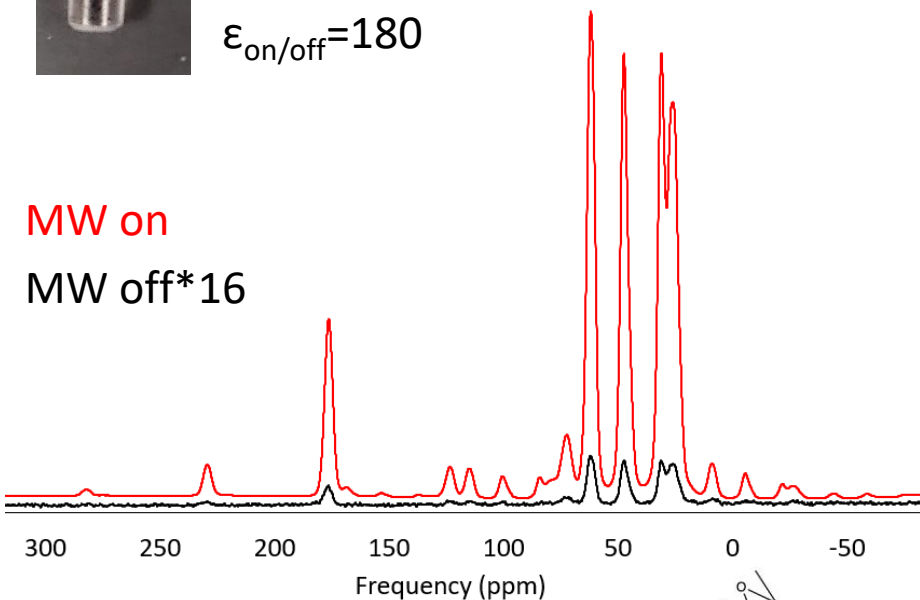
Glassing agent (MW absorption)

O_2 content

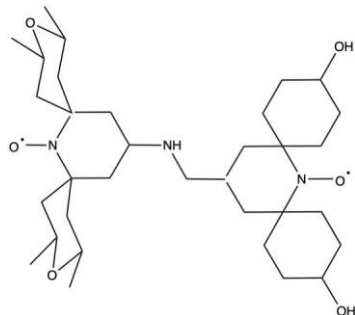
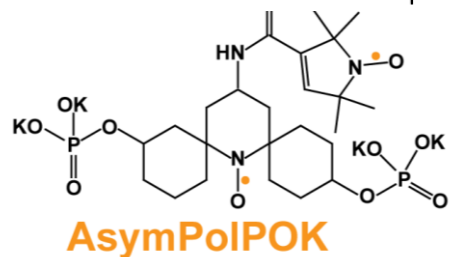
Sample integrity

MW on

MW off*16



Frequency (ppm)



Mentink-Vigier, F., et al. (2018) *J. Am. Chem. Soc.*, 141

Harrabi, R et al. (2022) *Ang. Chemie* 61 e202114103

Lund, A., et al. (2020) *Chem. Sci.*, 11

Our observations:

TinyPol and AsymPolPOK give roughly equivalent sensitivity

TinyPol wins for on/off; AsymPolPOK wins for buildup time

Both enable high levels of protonation

DNP juice is unreliable

Very sensitive to temperature

Absorbs MW

Hard to control O_2 concentration

Denatures proteins/impacts lipid organization

Other glassing agents work really well

Read the cryobiology literature

MW absorption is reduced relative to DNP juice

DNP buildup times are an order of magnitude faster

BUT don't expect your model compounds to look as good

Summary of DNP conditions (using proline)

$\epsilon_{on/off}$: deuterate, use tinypol or asympolPOK

| Biradical | ^2H | Juice | DMSO | Betaine |
|--------------|--------------|------------|-----------|------------|
| none | yes | -- | -- | -- |
| | no | -- | -- | -- |
| 10amupol | yes | 86 | 61 | 39 |
| | no | 43 | 22 | 12 |
| 5asympolpok | yes | 75 | 78 | 58 |
| | no | 75 | 84 | 79 |
| 10asympolpok | yes | 62 | 92 | 82 |
| | no | 60 | 63 | 72 |
| 10tiny pol | yes | 157 | 73 | 118 |
| | no | 141 | 61 | 50 |

Overall improvement: no ^2H needed!, asympolPOK

| Biradical | ^2H . | Juice | DMSO | Betaine |
|--------------|----------------|------------|------------|------------|
| none | yes | 1 | 2 | 4 |
| | no | 2 | 6 | 7 |
| amupol | yes | 151 | 43 | 74 |
| | no | 121 | 75 | 45 |
| 5asympolpok | yes | 162 | 217 | 191 |
| | no | 197 | 238 | 168 |
| 10asympolpok | yes | 279 | 395 | 93 |
| | no | 426 | 484 | 112 |
| tiny pol | yes | 230 | 135 | 128 |
| | no | 223 | 91 | 123 |



Luiza Caldas Nogueira

DNP Improvement: no ^2H , asympolPOK

| Biradical | ^2H . | Juice | DMSO | Betaine |
|--------------|----------------|------------|-----------|-----------|
| none | yes | 0.6 | 0.3 | 0.6 |
| | no | 1 | 1 | 1 |
| amupol | yes | 97 | 14 | 11 |
| | no | 78 | 8 | 7 |
| 5asympolpok | yes | 103 | 39 | 14 |
| | no | 126 | 43 | 17 |
| 10asympolpok | yes | 179 | 72 | 28 |
| | no | 272 | 88 | 25 |
| tiny pol | yes | 147 | 24 | 19 |
| | no | 143 | 17 | 18 |

Considerations:

Field: (we have a 600 MHz / 396 GHz instrument)

MAS rate and Temperature (10.4 kHz and 90 K)

Solvent/Glassing agent (MW absorption, Temp/phase behavior)

O_2 content (solubility, degassing)

Enhancement vs. Improvement--SNR/sqrt(T_b)

Methyl-containing glassing agents degrade enhancement but improve SNR/sqrt(T_b) and likely reflect performance in biological samples

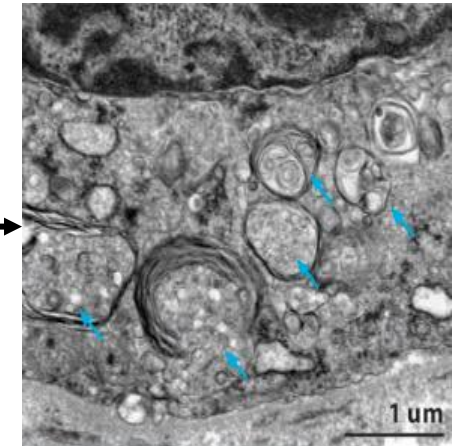
Sample integrity

DNP: What makes me want to add a
gyrotron to all my magnets

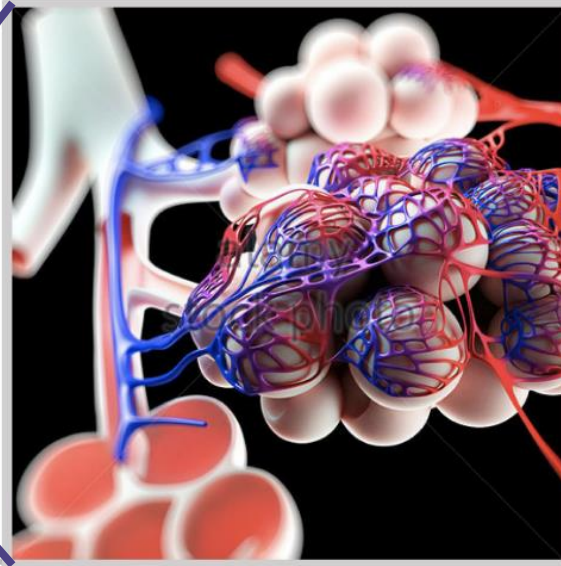
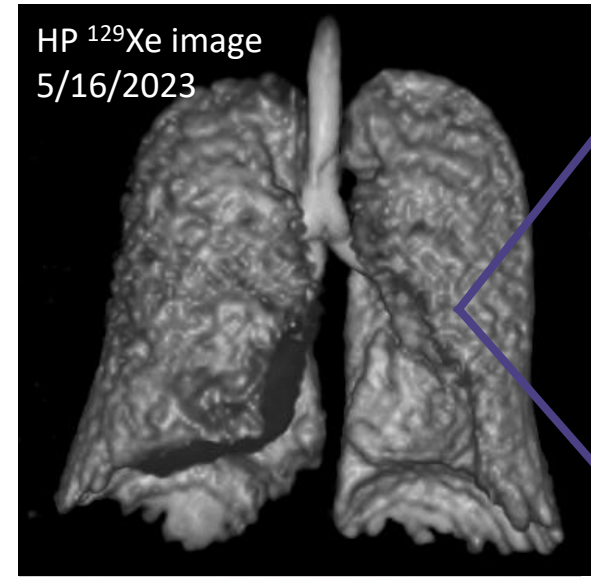
Pulmonary surfactant and lipid trafficking

- Surface area $\sim 300 \text{ cm}^2$ per cm^3 ($\sim 40\text{x}$ that of skin)
- Type II epithelial cells secrete pulmonary surfactant (PS) as lamellar bodies to lower surface tension
- Lamellar Body \rightarrow Tubular Myelin \rightarrow Air/Water interface (monolayer with reservoir beneath)
- PS is highly dynamic with lipid half lives of 5-10 hrs
- Surfactant protein B (SP-B) is absolutely required for lamellar body formation, trafficking into tubular myelin, and the recycling of PS

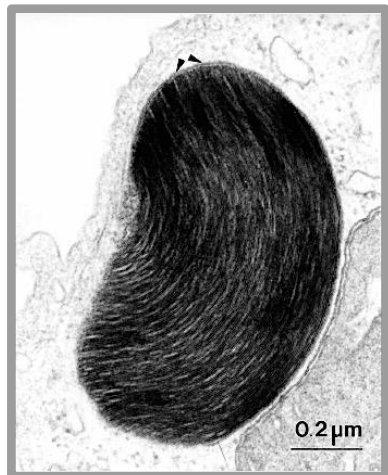
Knockout of SP-B in mice is lethal



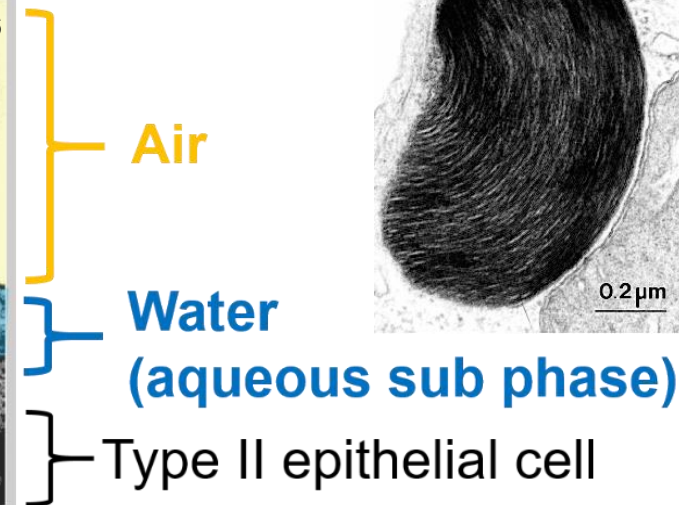
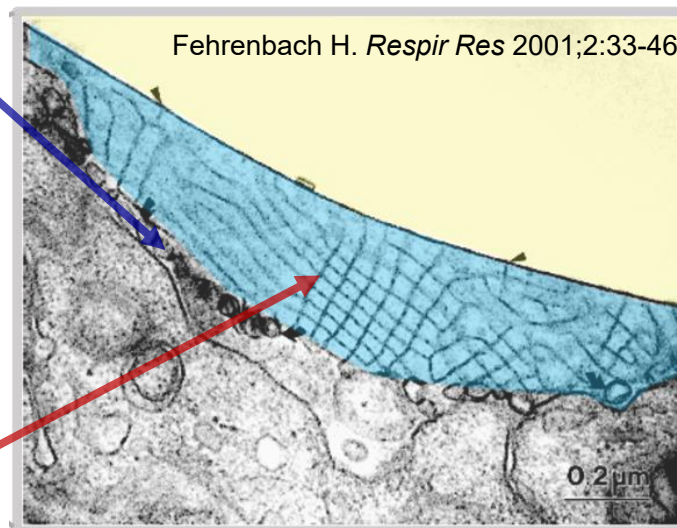
Whitsett JA. Annu. Rev. Med. 2010;61:105-119



PS Lamellar Body



Tubular Myelin

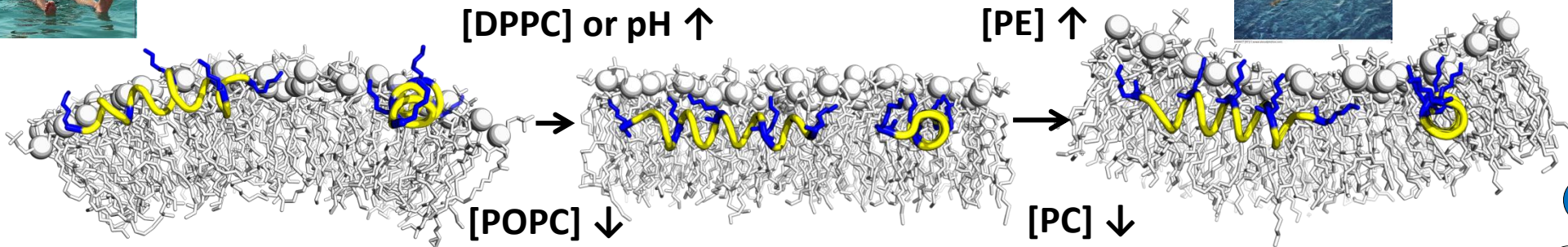


Partitioning, pH, and helicity of KL₄



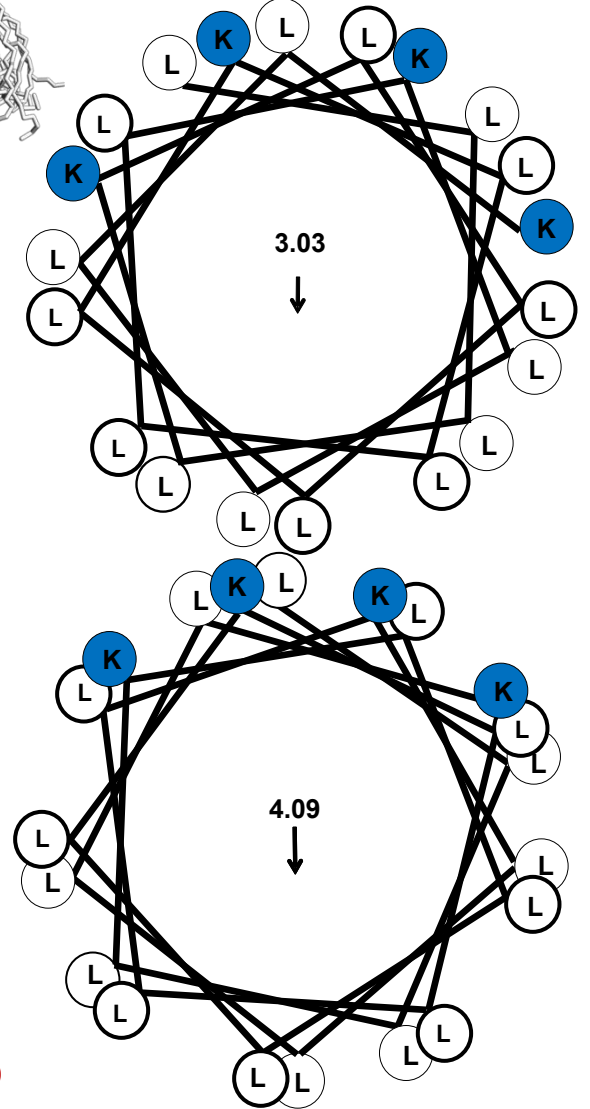
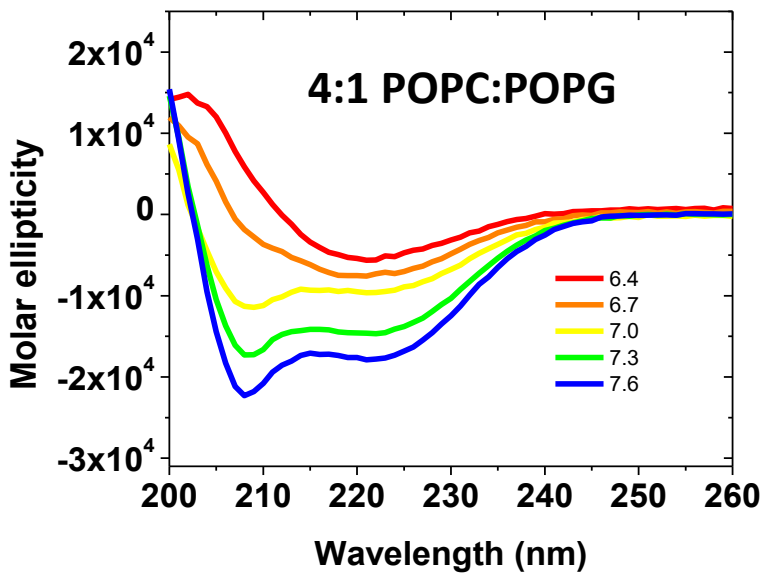
Otonye Braide-Moncoeur

KL₄KL₄KL₄KL₄



Current Opinion in Chemical Biology 32: 22-28 (2015)
BBA - Biomembranes 1838: 3212-3219 (2014)
BBA - Biomembranes 1798: 216-222 (2009)
Biophysical Journal 96: 4085-98 (2009)
Biochemistry. 47: 8292-8300 (2008)

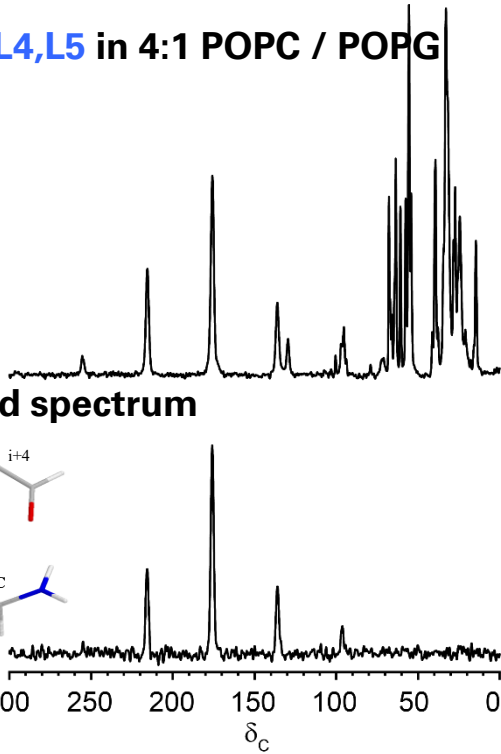
- Deeper peptide partitioning in DPPC:POPG stabilizes a planar lipid assembly
- More shallow partitioning in POPC:POPG leads to positive curvature strain
- This enables differentiation of lipids for selective trafficking of DPPC to the air/water interface
- pH has marked effect on helicity



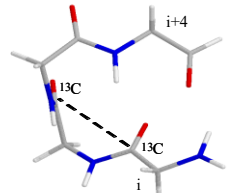
Optimal behavior (and clinically relevant) in lipids at 1:50 peptide:lipid ratio

pH-dependent characterization of KL₄

KL₄ 1-¹³C-L4,L5 in 4:1 POPC / POPG
CPMAS

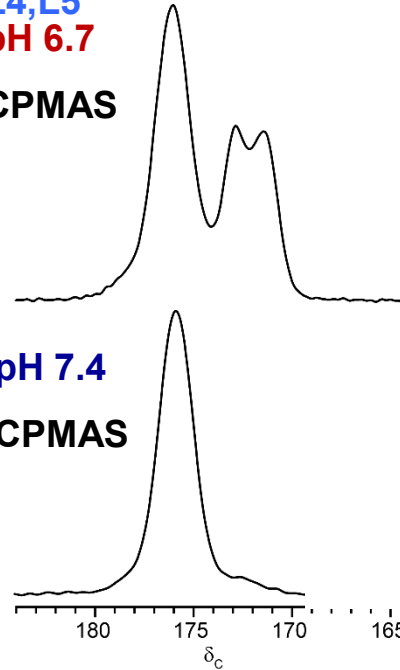


DQ filtered spectrum



KL₄ in 4:1 POPC / POPG
L4,L5
pH 6.7

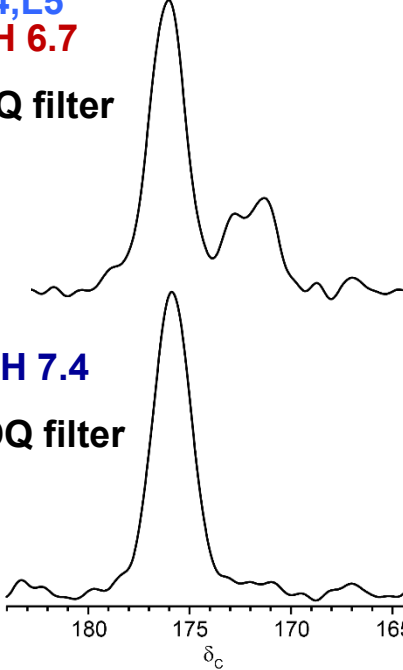
CPMAS



pH 7.4
CPMAS

L4,L5
pH 6.7

DQ filter



pH 7.4
DQ filter

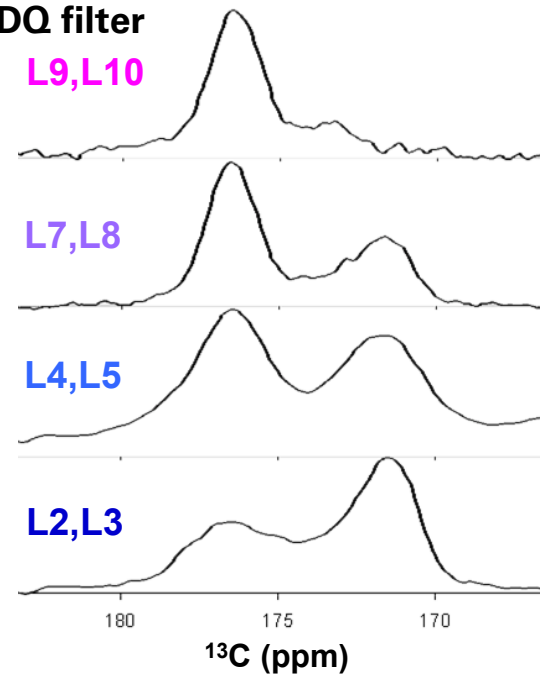
KL₄ in 4:1 DPPC / POPG, pH 6.7
DQ filter

L9,L10

L7,L8

L4,L5

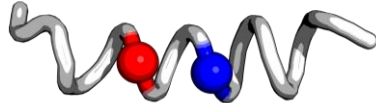
L2,L3



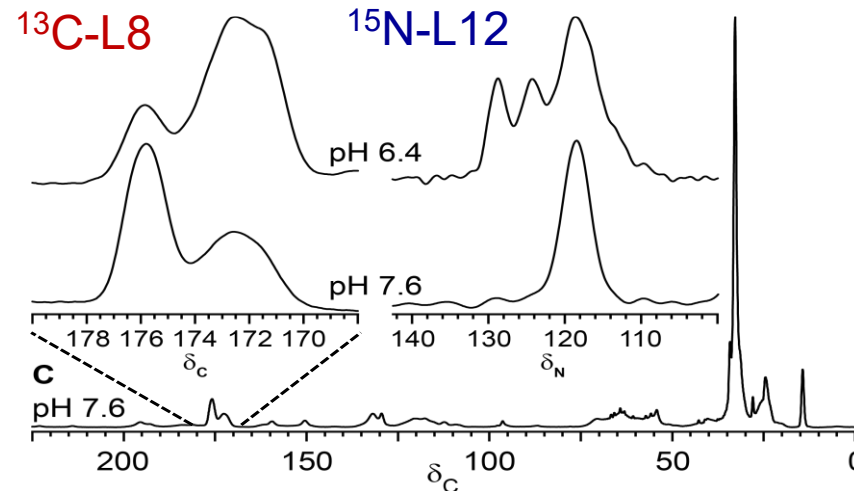
DNP CPMAS, ~95 K

Sample frozen in rotor on
insertion into probe

KL₄ 1-¹³C-L8, ¹⁵N-L12



i, i+4



KL₄ K₁L₂L₃L₄L₅L₆L₇L₈L₉L₁₀L₁₁L₁₂L₁₃L₁₄L₁₅L₁₆L₁₇L₁₈L₁₉L₂₀L₂₁L₂₂L₂₃L₂₄L₂₅L₂₆L₂₇L₂₈L₂₉L₃₀L₃₁L₃₂L₃₃L₃₄L₃₅L₃₆L₃₇L₃₈L₃₉L₄₀L₄₁L₄₂L₄₃L₄₄L₄₅L₄₆L₄₇L₄₈L₄₉L₅₀L₅₁L₅₂L₅₃L₅₄L₅₅L₅₆L₅₇L₅₈L₅₉L₆₀L₆₁L₆₂L₆₃L₆₄L₆₅L₆₆L₆₇L₆₈L₆₉L₇₀L₇₁L₇₂L₇₃L₇₄L₇₅L₇₆L₇₇L₇₈L₇₉L₈₀L₈₁L₈₂L₈₃L₈₄L₈₅L₈₆L₈₇L₈₈L₈₉L₉₀L₉₁L₉₂L₉₃L₉₄L₉₅L₉₆L₉₇L₉₈L₉₉L₁₀₀L₁₀₁L₁₀₂L₁₀₃L₁₀₄L₁₀₅L₁₀₆L₁₀₇L₁₀₈L₁₀₉L₁₁₀L₁₁₁L₁₁₂L₁₁₃L₁₁₄L₁₁₅L₁₁₆L₁₁₇L₁₁₈L₁₁₉L₁₂₀L₁₂₁L₁₂₂L₁₂₃L₁₂₄L₁₂₅L₁₂₆L₁₂₇L₁₂₈L₁₂₉L₁₃₀L₁₃₁L₁₃₂L₁₃₃L₁₃₄L₁₃₅L₁₃₆L₁₃₇L₁₃₈L₁₃₉L₁₄₀L₁₄₁L₁₄₂L₁₄₃L₁₄₄L₁₄₅L₁₄₆L₁₄₇L₁₄₈L₁₄₉L₁₅₀L₁₅₁L₁₅₂L₁₅₃L₁₅₄L₁₅₅L₁₅₆L₁₅₇L₁₅₈L₁₅₉L₁₆₀L₁₆₁L₁₆₂L₁₆₃L₁₆₄L₁₆₅L₁₆₆L₁₆₇L₁₆₈L₁₆₉L₁₇₀L₁₇₁L₁₇₂L₁₇₃L₁₇₄L₁₇₅L₁₇₆L₁₇₇L₁₇₈L₁₇₉L₁₈₀L₁₈₁L₁₈₂L₁₈₃L₁₈₄L₁₈₅L₁₈₆L₁₈₇L₁₈₈L₁₈₉L₁₉₀L₁₉₁L₁₉₂L₁₉₃L₁₉₄L₁₉₅L₁₉₆L₁₉₇L₁₉₈L₁₉₉L₂₀₀L₂₀₁L₂₀₂L₂₀₃L₂₀₄L₂₀₅L₂₀₆L₂₀₇L₂₀₈L₂₀₉L₂₁₀L₂₁₁L₂₁₂L₂₁₃L₂₁₄L₂₁₅L₂₁₆L₂₁₇L₂₁₈L₂₁₉L₂₂₀L₂₂₁L₂₂₂L₂₂₃L₂₂₄L₂₂₅L₂₂₆L₂₂₇L₂₂₈L₂₂₉L₂₃₀L₂₃₁L₂₃₂L₂₃₃L₂₃₄L₂₃₅L₂₃₆L₂₃₇L₂₃₈L₂₃₉L₂₄₀L₂₄₁L₂₄₂L₂₄₃L₂₄₄L₂₄₅L₂₄₆L₂₄₇L₂₄₈L₂₄₉L₂₅₀L₂₅₁L₂₅₂L₂₅₃L₂₅₄L₂₅₅L₂₅₆L₂₅₇L₂₅₈L₂₅₉L₂₆₀L₂₆₁L₂₆₂L₂₆₃L₂₆₄L₂₆₅L₂₆₆L₂₆₇L₂₆₈L₂₆₉L₂₇₀L₂₇₁L₂₇₂L₂₇₃L₂₇₄L₂₇₅L₂₇₆L₂₇₇L₂₇₈L₂₇₉L₂₈₀L₂₈₁L₂₈₂L₂₈₃L₂₈₄L₂₈₅L₂₈₆L₂₈₇L₂₈₈L₂₈₉L₂₉₀L₂₉₁L₂₉₂L₂₉₃L₂₉₄L₂₉₅L₂₉₆L₂₉₇L₂₉₈L₂₉₉L₃₀₀L₃₀₁L₃₀₂L₃₀₃L₃₀₄L₃₀₅L₃₀₆L₃₀₇L₃₀₈L₃₀₉L₃₁₀L₃₁₁L₃₁₂L₃₁₃L₃₁₄L₃₁₅L₃₁₆L₃₁₇L₃₁₈L₃₁₉L₃₂₀L₃₂₁L₃₂₂L₃₂₃L₃₂₄L₃₂₅L₃₂₆L₃₂₇L₃₂₈L₃₂₉L₃₃₀L₃₃₁L₃₃₂L₃₃₃L₃₃₄L₃₃₅L₃₃₆L₃₃₇L₃₃₈L₃₃₉L₃₄₀L₃₄₁L₃₄₂L₃₄₃L₃₄₄L₃₄₅L₃₄₆L₃₄₇L₃₄₈L₃₄₉L₃₅₀L₃₅₁L₃₅₂L₃₅₃L₃₅₄L₃₅₅L₃₅₆L₃₅₇L₃₅₈L₃₅₉L₃₆₀L₃₆₁L₃₆₂L₃₆₃L₃₆₄L₃₆₅L₃₆₆L₃₆₇L₃₆₈L₃₆₉L₃₇₀L₃₇₁L₃₇₂L₃₇₃L₃₇₄L₃₇₅L₃₇₆L₃₇₇L₃₇₈L₃₇₉L₃₈₀L₃₈₁L₃₈₂L₃₈₃L₃₈₄L₃₈₅L₃₈₆L₃₈₇L₃₈₈L₃₈₉L₃₉₀L₃₉₁L₃₉₂L₃₉₃L₃₉₄L₃₉₅L₃₉₆L₃₉₇L₃₉₈L₃₉₉L₄₀₀L₄₀₁L₄₀₂L₄₀₃L₄₀₄L₄₀₅L₄₀₆L₄₀₇L₄₀₈L₄₀₉L₄₁₀L₄₁₁L₄₁₂L₄₁₃L₄₁₄L₄₁₅L₄₁₆L₄₁₇L₄₁₈L₄₁₉L₄₂₀L₄₂₁L₄₂₂L₄₂₃L₄₂₄L₄₂₅L₄₂₆L₄₂₇L₄₂₈L₄₂₉L₄₃₀L₄₃₁L₄₃₂L₄₃₃L₄₃₄L₄₃₅L₄₃₆L₄₃₇L₄₃₈L₄₃₉L₄₄₀L₄₄₁L₄₄₂L₄₄₃L₄₄₄L₄₄₅L₄₄₆L₄₄₇L₄₄₈L₄₄₉L₄₅₀L₄₅₁L₄₅₂L₄₅₃L₄₅₄L₄₅₅L₄₅₆L₄₅₇L₄₅₈L₄₅₉L₄₆₀L₄₆₁L₄₆₂L₄₆₃L₄₆₄L₄₆₅L₄₆₆L₄₆₇L₄₆₈L₄₆₉L₄₇₀L₄₇₁L₄₇₂L₄₇₃L₄₇₄L₄₇₅L₄₇₆L₄₇₇L₄₇₈L₄₇₉L₄₈₀L₄₈₁L₄₈₂L₄₈₃L₄₈₄L₄₈₅L₄₈₆L₄₈₇L₄₈₈L₄₈₉L₄₉₀L₄₉₁L₄₉₂L₄₉₃L₄₉₄L₄₉₅L₄₉₆L₄₉₇L₄₉₈L₄₉₉L₅₀₀L₅₀₁L₅₀₂L₅₀₃L₅₀₄L₅₀₅L₅₀₆L₅₀₇L₅₀₈L₅₀₉L₅₁₀L₅₁₁L₅₁₂L₅₁₃L₅₁₄L₅₁₅L₅₁₆L₅₁₇L₅₁₈L₅₁₉L₅₂₀L₅₂₁L₅₂₂L₅₂₃L₅₂₄L₅₂₅L₅₂₆L₅₂₇L₅₂₈L₅₂₉L₅₃₀L₅₃₁L₅₃₂L₅₃₃L₅₃₄L₅₃₅L₅₃₆L₅₃₇L₅₃₈L₅₃₉L₅₄₀L₅₄₁L₅₄₂L₅₄₃L₅₄₄L₅₄₅L₅₄₆L₅₄₇L₅₄₈L₅₄₉L₅₅₀L₅₅₁L₅₅₂L₅₅₃L₅₅₄L₅₅₅L₅₅₆L₅₅₇L₅₅₈L₅₅₉L₅₆₀L₅₆₁L₅₆₂L₅₆₃L₅₆₄L₅₆₅L₅₆₆L₅₆₇L₅₆₈L₅₆₉L₅₇₀L₅₇₁L₅₇₂L₅₇₃L₅₇₄L₅₇₅L₅₇₆L₅₇₇L₅₇₈L₅₇₉L₅₈₀L₅₈₁L₅₈₂L₅₈₃L₅₈₄L₅₈₅L₅₈₆L₅₈₇L₅₈₈L₅₈₉L₅₉₀L₅₉₁L₅₉₂L₅₉₃L₅₉₄L₅₉₅L₅₉₆L₅₉₇L₅₉₈L₅₉₉L₆₀₀L₆₀₁L₆₀₂L₆₀₃L₆₀₄L₆₀₅L₆₀₆L₆₀₇L₆₀₈L₆₀₉L₆₁₀L₆₁₁L₆₁₂L₆₁₃L₆₁₄L₆₁₅L₆₁₆L₆₁₇L₆₁₈L₆₁₉L₆₂₀L₆₂₁L₆₂₂L₆₂₃L₆₂₄L₆₂₅L₆₂₆L₆₂₇L₆₂₈L₆₂₉L₆₃₀L₆₃₁L₆₃₂L₆₃₃L₆₃₄L₆₃₅L₆₃₆L₆₃₇L₆₃₈L₆₃₉L₆₄₀L₆₄₁L₆₄₂L₆₄₃L₆₄₄L₆₄₅L₆₄₆L₆₄₇L₆₄₈L₆₄₉L₆₅₀L₆₅₁L₆₅₂L₆₅₃L₆₅₄L₆₅₅L₆₅₆L₆₅₇L₆₅₈L₆₅₉L₆₆₀L₆₆₁L₆₆₂L₆₆₃L₆₆₄L₆₆₅L₆₆₆L₆₆₇L₆₆₈L₆₆₉L₆₇₀L₆₇₁L₆₇₂L₆₇₃L₆₇₄L₆₇₅L₆₇₆L₆₇₇L₆₇₈L₆₇₉L₆₈₀L₆₈₁L₆₈₂L₆₈₃L₆₈₄L₆₈₅L₆₈₆L₆₈₇L₆₈₈L₆₈₉L₆₉₀L₆₉₁L₆₉₂L₆₉₃L₆₉₄L₆₉₅L₆₉₆L₆₉₇L₆₉₈L₆₉₉L₇₀₀L₇₀₁L₇₀₂L₇₀₃L₇₀₄L₇₀₅L₇₀₆L₇₀₇L₇₀₈L₇₀₉L₇₁₀L₇₁₁L₇₁₂L₇₁₃L₇₁₄L₇₁₅L₇₁₆L₇₁₇L₇₁₈L₇₁₉L₇₂₀L₇₂₁L₇₂₂L₇₂₃L₇₂₄L₇₂₅L₇₂₆L₇₂₇L₇₂₈L₇₂₉L₇₃₀L₇₃₁L₇₃₂L₇₃₃L₇₃₄L₇₃₅L₇₃₆L₇₃₇L₇₃₈L₇₃₉L₇₄₀L₇₄₁L₇₄₂L₇₄₃L₇₄₄L₇₄₅L₇₄₆L₇₄₇L₇₄₈L₇₄₉L₇₅₀L₇₅₁L₇₅₂L₇₅₃L₇₅₄L₇₅₅L₇₅₆L₇₅₇L₇₅₈L₇₅₉L₇₆₀L₇₆₁L₇₆₂L₇₆₃L₇₆₄L₇₆₅L₇₆₆L₇₆₇L₇₆₈L₇₆₉L₇₇₀L₇₇₁L₇₇₂L₇₇₃L₇₇₄L₇₇₅L₇₇₆L₇₇₇L₇₇₈L₇₇₉L₇₈₀L₇₈₁L₇₈₂L₇₈₃L₇₈₄L₇₈₅L₇₈₆L₇₈₇L₇₈₈L₇₈₉L₇₉₀L₇₉₁L₇₉₂L₇₉₃L₇₉₄L₇₉₅L₇₉₆L₇₉₇L₇₉₈L₇₉₉L₈₀₀L₈₀₁L₈₀₂L₈₀₃L₈₀₄L₈₀₅L₈₀₆L₈₀₇L₈₀₈L₈₀₉L₈₁₀L₈₁₁L₈₁₂L₈₁₃L₈₁₄L₈₁₅L₈₁₆L₈₁₇L₈₁₈L₈₁₉L₈₂₀L₈₂₁L₈₂₂L₈₂₃L₈₂₄L₈₂₅L₈₂₆L₈₂₇L₈₂₈L₈₂₉L₈₃₀L₈₃₁L₈₃₂L₈₃₃L₈₃₄L₈₃₅L₈₃₆L₈₃₇L₈₃₈L₈₃₉L₈₄₀L₈₄₁L₈₄₂L₈₄₃L₈₄₄L₈₄₅L₈₄₆L₈₄₇L₈₄₈L₈₄₉L₈₅₀L₈₅₁L₈₅₂L₈₅₃L₈₅₄L₈₅₅L₈₅₆L₈₅₇L₈₅₈L₈₅₉L₈₆₀L₈₆₁L₈₆₂L₈₆₃L₈₆₄L₈₆₅L₈₆₆L₈₆₇L₈₆₈L₈₆₉L₈₇₀L₈₇₁L₈₇₂L₈₇₃L₈₇₄L₈₇₅L₈₇₆L₈₇₇L₈₇₈L₈₇₉L₈₈₀L₈₈₁L₈₈₂L₈₈₃L₈₈₄L₈₈₅L₈₈₆L₈₈₇L₈₈₈L₈₈₉L₈₉₀L₈₉₁L₈₉₂L₈₉₃L₈₉₄L₈₉₅L₈₉₆L₈₉₇L₈₉₈L₈₉₉L₉₀₀L₉₀₁L₉₀₂L₉₀₃L₉₀₄L₉₀₅L₉₀₆L₉₀₇L₉₀₈L₉₀₉L₉₁₀L₉₁₁L₉₁₂L₉₁₃L₉₁₄L₉₁₅L₉₁₆L₉₁₇L₉₁₈L₉₁₉L₉₂₀L₉₂₁L₉₂₂L₉₂₃L₉₂₄L₉₂₅L₉₂₆L₉₂₇L₉₂₈L₉₂₉L₉₃₀L₉₃₁L₉₃₂L₉₃₃L₉₃₄L₉₃₅L₉₃₆L₉₃₇L₉₃₈L₉₃₉L₉₄₀L₉₄₁L₉₄₂L₉₄₃L₉₄₄L₉₄₅L₉₄₆L₉₄₇L₉₄₈L₉₄₉L₉₅₀L₉₅₁L₉₅₂L₉₅₃L₉₅₄L₉₅₅L₉₅₆L₉₅₇L₉₅₈L₉₅₉L₉₆₀L₉₆₁L₉₆₂L₉₆₃L₉₆₄L₉₆₅L₉₆₆L₉₆₇L₉₆₈L₉₆₉L₉₇₀L₉₇₁L₉₇₂L₉₇₃L₉₇₄L₉₇₅L₉₇₆L₉₇₇L₉₇₈L₉₇₉L₉₈₀L₉₈₁L₉₈₂L₉₈₃L₉₈₄L₉₈₅L₉₈₆L₉₈₇L₉₈₈L₉₈₉L₉₉₀L₉₉₁L₉₉₂L₉₉₃L₉₉₄L₉₉₅L₉₉₆L₉₉₇L₉₉₈L₉₉₉L₁₀₀₀L₁₀₀₁L₁₀₀₂L₁₀₀₃L₁₀₀₄L₁₀₀₅L₁₀₀₆L₁₀₀₇L₁₀₀₈L₁₀₀₉L₁₀₁₀L₁₀₁₁L₁₀₁₂L₁₀₁₃L₁₀₁₄L₁₀₁₅L₁₀₁₆L₁₀₁₇L₁₀₁₈L₁₀₁₉L₁₀₂₀L₁₀₂₁L₁₀₂₂L₁₀₂₃L₁₀₂₄L₁₀₂₅L₁₀₂₆L₁₀₂₇L₁₀₂₈L₁₀₂₉L₁₀₃₀L₁₀₃₁L₁₀₃₂L₁₀₃₃L₁₀₃₄L₁₀₃₅L₁₀₃₆L₁₀₃₇L₁₀₃₈L₁₀₃₉L₁₀₄₀L₁₀₄₁L₁₀₄₂L₁₀₄₃L₁₀₄₄L₁₀₄₅L₁₀₄₆L₁₀₄₇L₁₀₄₈L₁₀₄₉L₁₀₅₀L₁₀₅₁L₁₀₅₂L₁₀₅₃L₁₀₅₄L₁₀₅₅L₁₀₅₆L₁₀₅₇L₁₀₅₈L₁₀₅₉L₁₀₆₀L₁₀₆₁L₁₀₆₂L₁₀₆₃L₁₀₆₄L₁₀₆₅L₁₀₆₆L₁₀₆₇L₁₀₆₈L₁₀₆₉L₁₀₇₀L₁₀₇₁L₁₀₇₂L₁₀₇₃L₁₀₇₄L₁₀₇₅L₁₀₇₆L₁₀₇₇L₁₀₇₈L₁₀₇₉L₁₀₈₀L₁₀₈₁L₁₀₈₂L₁₀₈₃L₁₀₈₄L₁₀₈₅L₁₀₈₆L₁₀₈₇L₁₀₈₈L₁₀₈₉L₁₀₉₀L₁₀₉₁L₁₀₉₂L₁₀₉₃L₁₀₉₄L₁₀₉₅L₁₀₉₆L₁₀₉₇L₁₀₉₈L₁₀₉₉L₁₁₀₀L₁₁₀₁L₁₁₀₂L₁₁₀₃L₁₁₀₄L₁₁₀₅L₁₁₀₆L₁₁₀₇L₁₁₀₈L₁₁₀₉L₁₁₁₀L₁₁₁₁L₁₁₁₂L₁₁₁₃L₁₁₁₄L₁₁₁₅L₁₁₁₆L₁₁₁₇L₁₁₁₈L₁₁₁₉L₁₁₂₀L₁₁₂₁L₁₁₂₂L₁₁₂₃L₁₁₂₄L₁₁₂₅L₁₁₂₆L₁₁₂₇L₁₁₂₈L₁₁₂₉L₁₁₃₀L₁₁₃₁L₁₁₃₂L₁₁₃₃L₁₁₃₄L₁₁₃₅L₁₁₃₆L₁₁₃₇L₁₁₃₈L₁₁₃₉L₁₁₄₀L₁₁₄₁L₁₁₄₂L₁₁₄₃L₁₁₄₄L₁₁₄₅L₁₁₄₆L₁₁₄₇L₁₁₄₈L₁₁₄₉L₁₁₅₀L₁₁₅₁L₁₁₅₂L₁₁₅₃L₁₁₅₄L₁₁₅₅L₁₁₅₆L₁₁₅₇L₁₁₅₈L₁₁₅₉L₁₁₆₀L₁₁₆₁L₁₁₆₂L₁₁₆₃L₁₁₆₄L₁₁₆₅L₁₁₆₆L₁₁₆₇L₁₁₆₈L₁₁₆₉L₁₁₇₀L₁₁₇₁L₁₁₇₂L₁₁₇₃L₁₁₇₄L₁₁₇₅L₁₁₇₆L₁₁₇₇L₁₁₇₈L₁₁₇₉L₁₁₈₀L₁₁₈₁L₁₁₈₂L₁₁₈₃L₁₁₈₄L₁₁₈₅L₁₁₈₆L₁₁₈₇L₁₁₈₈L₁₁₈₉L_{1190</}

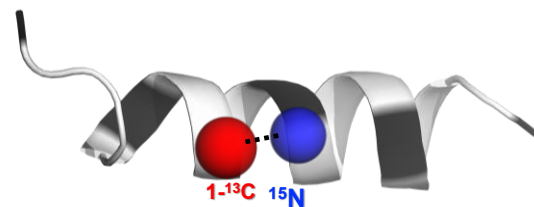
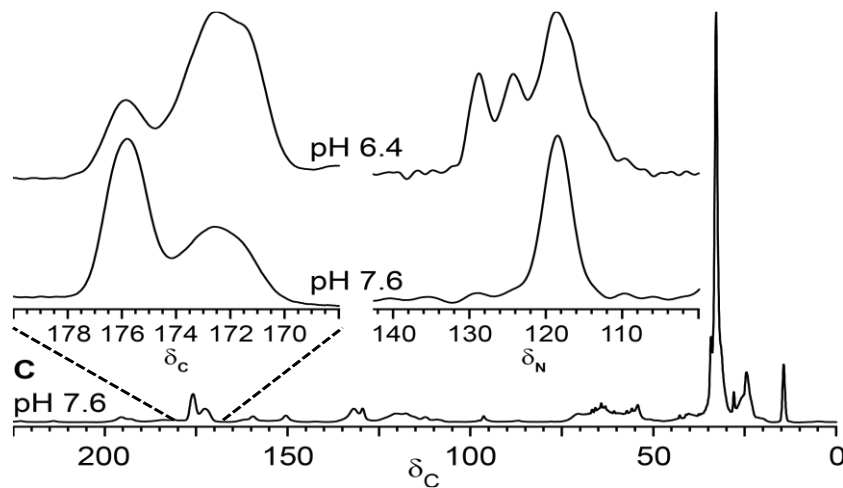
Buffers / pH are also important to consider

Biochem J.
167: 593-600 (1977)

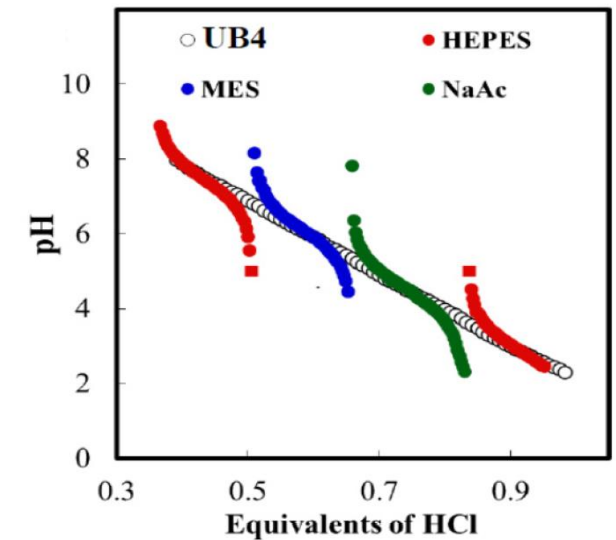
| Buffer | $\Delta\text{pH}_{\text{app.}}$ for pH 8.1–8.2 at 20°C Manual freeze | $\Delta\text{pH}_{\text{app.}}$ for pH 6.9–7.4 at 20°C | | | Average pH change (without albumin) |
|----------------------|---|--|------------------|----------------|-------------------------------------|
| | | Rapid freeze | Manual freeze | | |
| | | | Alone | With albumin | |
| Tris | $+1.6 \pm 0.5$ | $+2.1 \pm 0.3$ | $+3.3 \pm 0.4^*$ | $+0.1 \pm 0.2$ | +2.3 |
| Taps | $+1.8 \pm 0.6$ | $+2.0 \pm 0.5$ | $+0.9 \pm 0.7$ | — | +1.6 |
| Morpholine | $+1.3 \pm 0.2$ | — | — | — | +1.3 |
| Hepps | $+0.6 \pm 0.2$ | — | — | — | +0.6 |
| Bicine | $+0.4 \pm 0.2$ | -0.4 ± 0.2 | $-0.4 \pm 0.1^*$ | 0 ± 0.1 | -0.1 |
| Tricine | — | 0 ± 0.2 | -0.4 ± 0.1 | $+0.1 \pm 0.2$ | -0.2 |
| Hepes | — | — | -0.4 ± 0.2 | $+0.4 \pm 0.1$ | -0.4 |
| Potassium phosphate | -1.2 ± 0.1 | -1.4 ± 0.7 | $-1.1 \pm 0.3^*$ | $+0.1 \pm 0.1$ | -1.2 |
| Sodium phosphate | — | -1.8 ± 0.2 | $-1.9 \pm 0.5^*$ | -0.3 ± 0.1 | -1.8 |
| Sodium pyrophosphate | -2.5 ± 0.2 | -2.9 ± 0.3 | $-2.9 \pm 0.7^*$ | -1.2 ± 0.5 | -2.8 |

AIMS Biophysics
2:336-342 (2015)

| Buffer | pKa at 25°C | dpKa/°C at pH 7.0 |
|----------|-------------|-------------------------|
| Bis-Tris | 6.46 | N/A |
| HEPES | 7.55 | -0.014 |
| MES | 6.15 | -0.011 |
| NaAc | 4.76 | Negligible ¹ |
| Tricine | 8.05 | -0.021 |
| Tris | 8.06 | -0.028 |

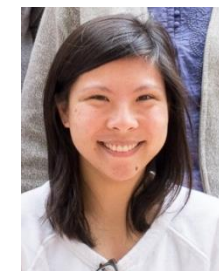


8/2/1 DPPC/POPG/cholesterol MLVs
with 2 mol% KL₄

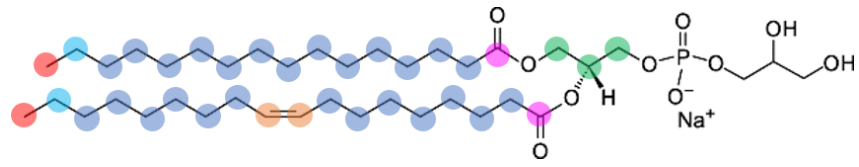
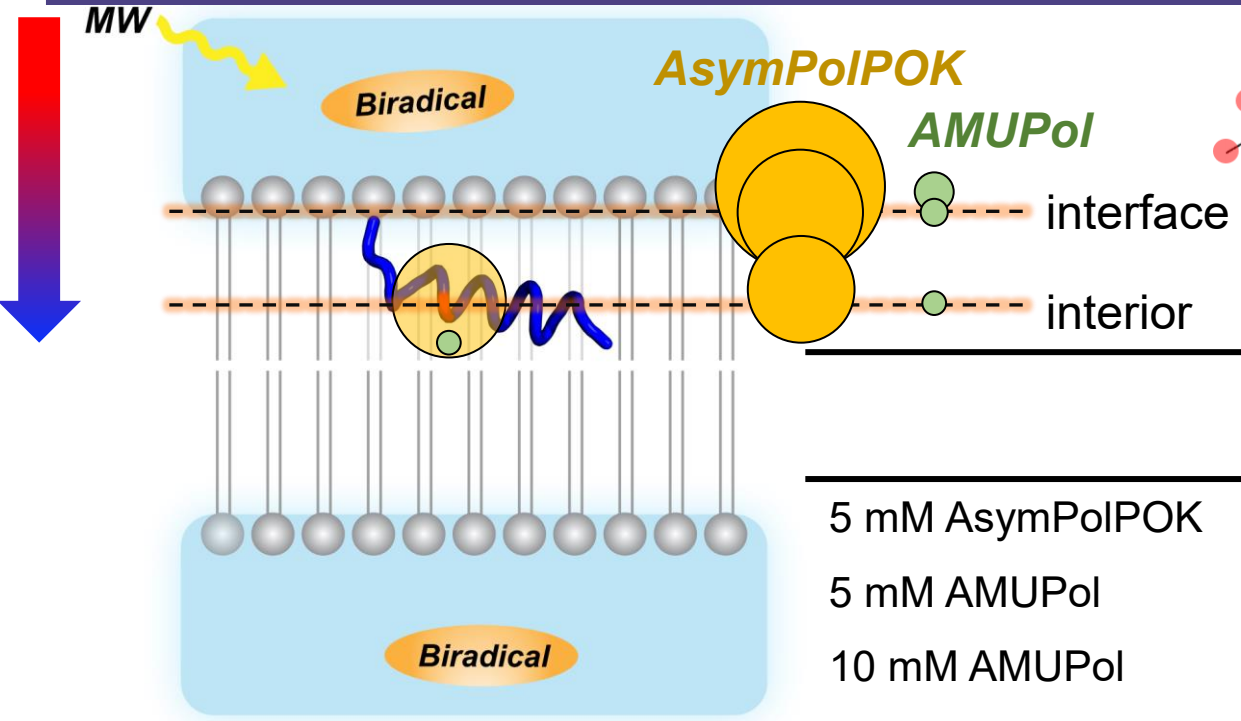
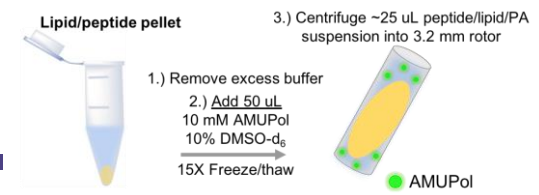


Archives Biochem. Biophysics 384: 398-406 (2000)
Biotechnol. Prog. 26:727-733 (2010)

KL₄ DNP enhancements



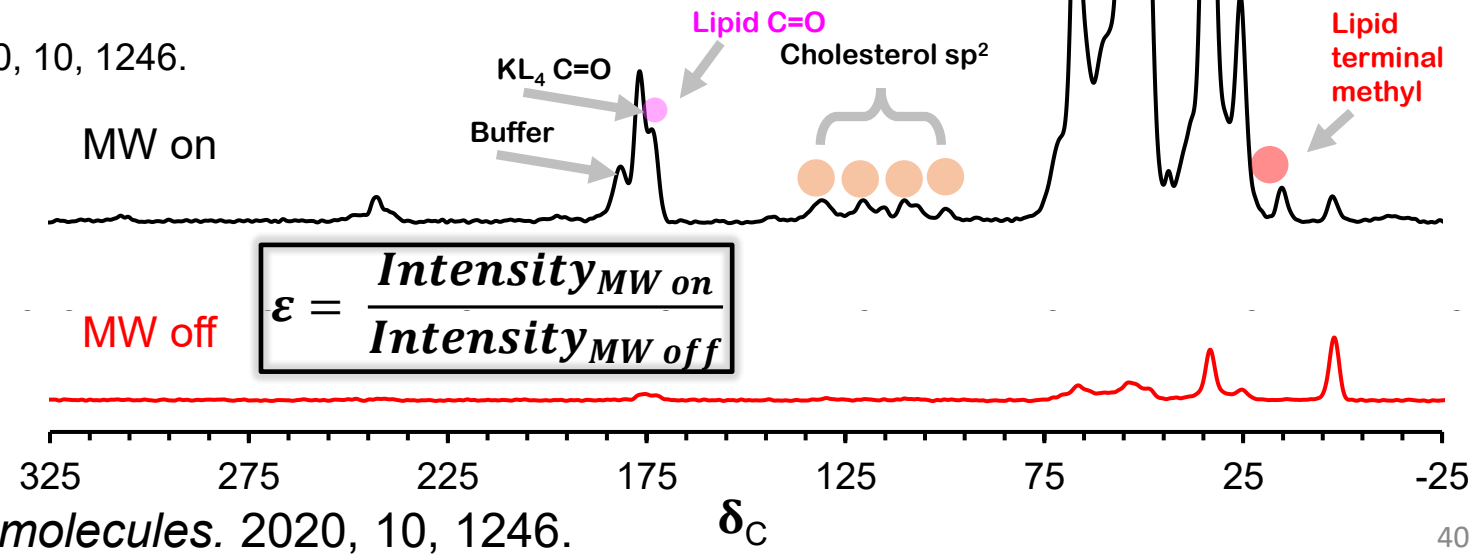
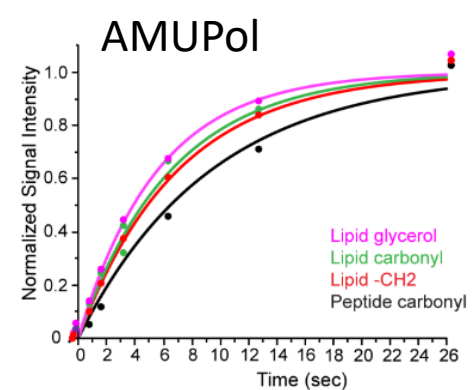
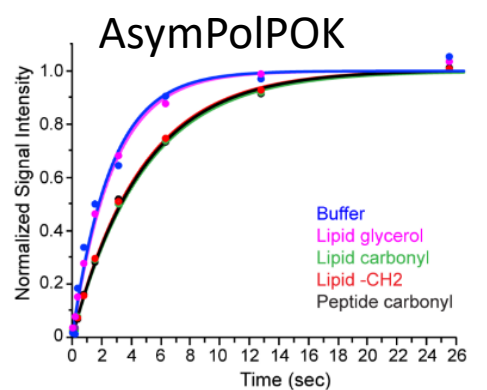
Nhi Tran



With AsymPolIPOK, only the water is deuterated!

| | Buffer | Lipid glycerol | Lipid C=O | KL4 C=O | -CH ₂ |
|------------------|--------|----------------|-----------|---------|------------------|
| 5 mM AsymPolIPOK | 93±27 | 57±2 | 42±6 | 38±3 | 36±0.5 |
| 5 mM AMUPol | 20±10 | 13±0.5 | 9±1.2 | 8±1.2 | 8±0.1 |
| 10 mM AMUPol | 50 | 24 | 13 | 14 | 14 |

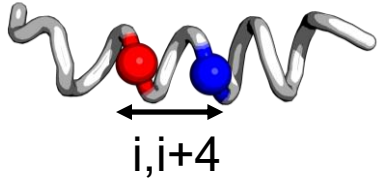
Biomolecules. 2020, 10, 1246.



Biomolecules. 2020, 10, 1246.

$^{13}\text{C}\{^{15}\text{N}\}$ REDOR: Conventional ssNMR & DNP

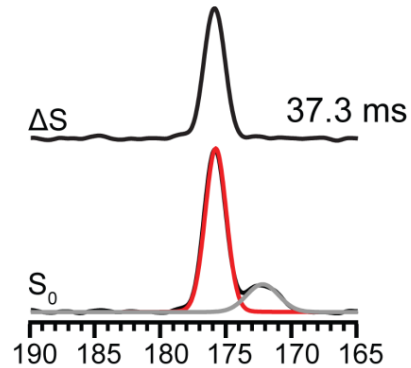
KL₄ 1- ^{13}C -Leu8, ^{15}N -Leu12, pH 7.4



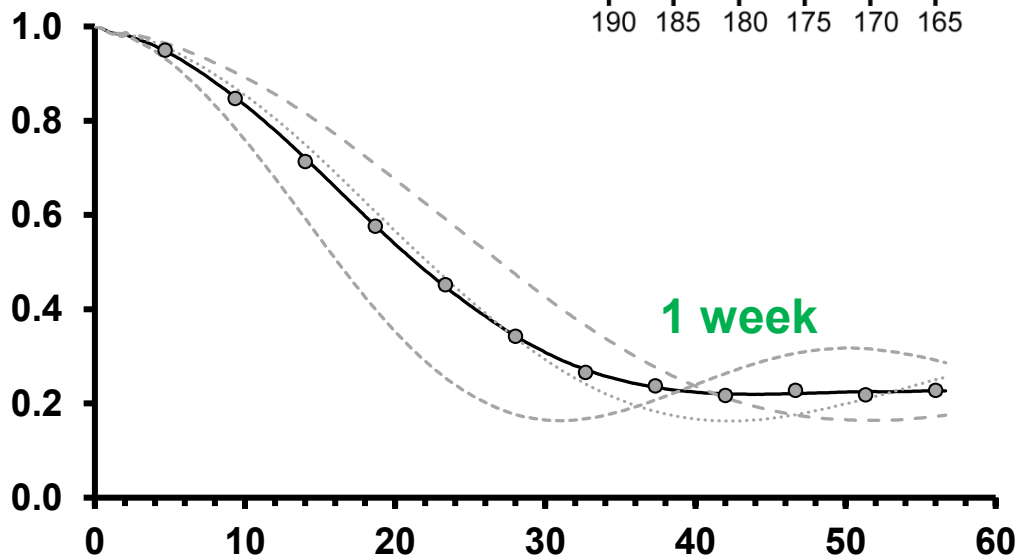
Luiza Caldas
Nogueira



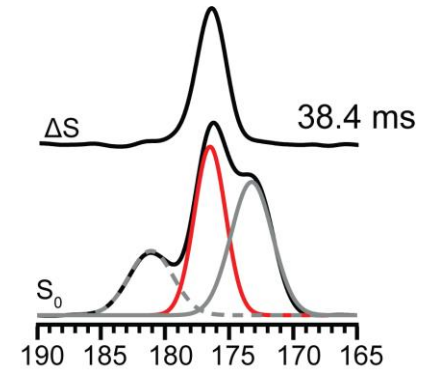
Diana
Tymochko



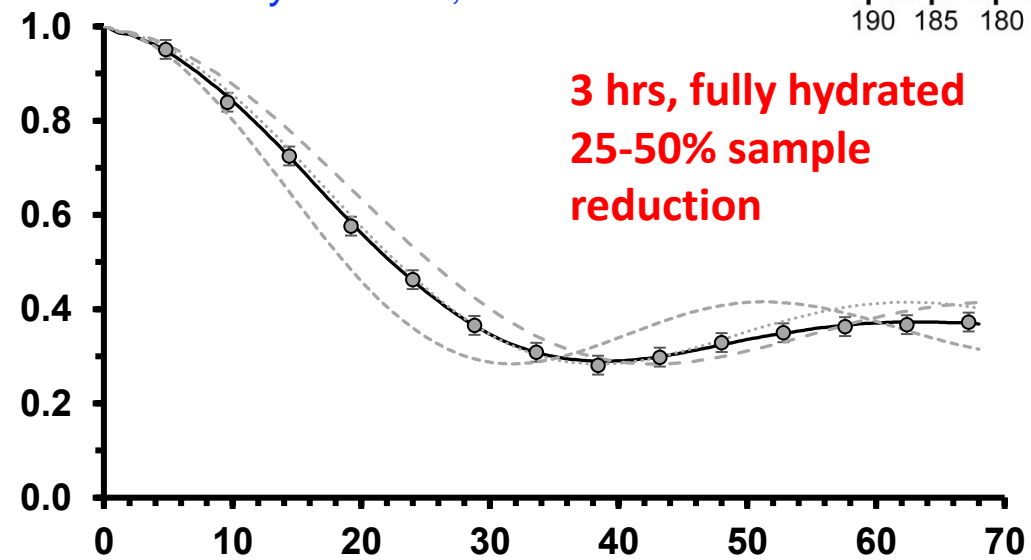
Lyophilized peptide/lipid
238K, 750 MHz, 12 kHz



Hydrated peptide/lipid
100K, 600 MHz/395 GHz,
5mM AsymPolIPOK, 10 kHz



3 hrs, fully hydrated
25-50% sample
reduction



Measuring multiple conformers

7802

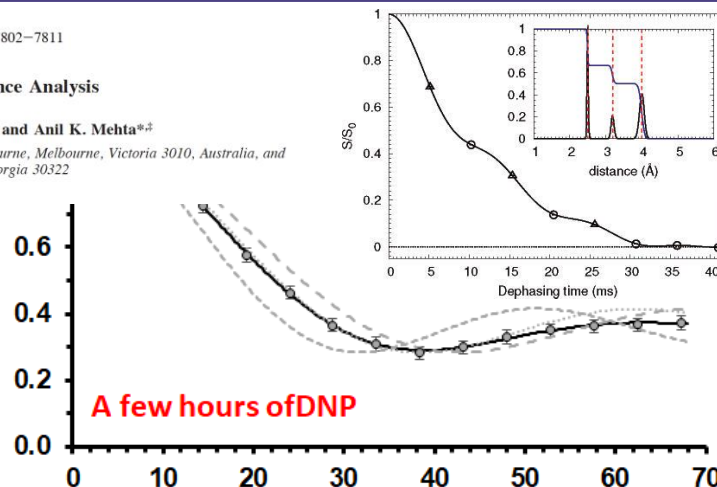
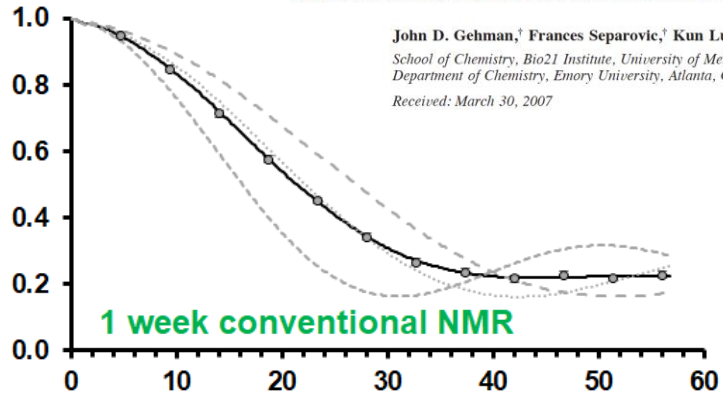
J. Phys. Chem. B 2007, 111, 7802–7811

Boltzmann Statistics Rotational-Echo Double-Resonance Analysis

John D. Gehman,[†] Frances Separovic,[†] Kun Lu,[‡] and Anil K. Mehta^{*‡}

School of Chemistry, Bio21 Institute, University of Melbourne, Melbourne, Victoria 3010, Australia, and Department of Chemistry, Emory University, Atlanta, Georgia 30322

Received: March 30, 2007



Direct BS-REDOR transform

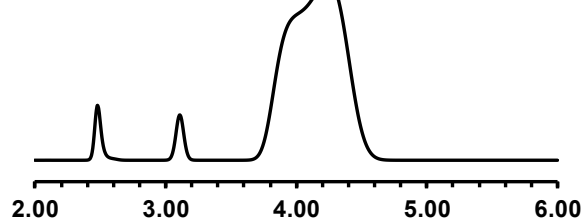
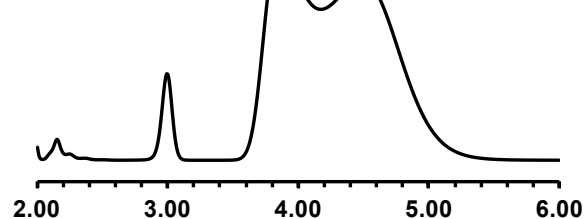


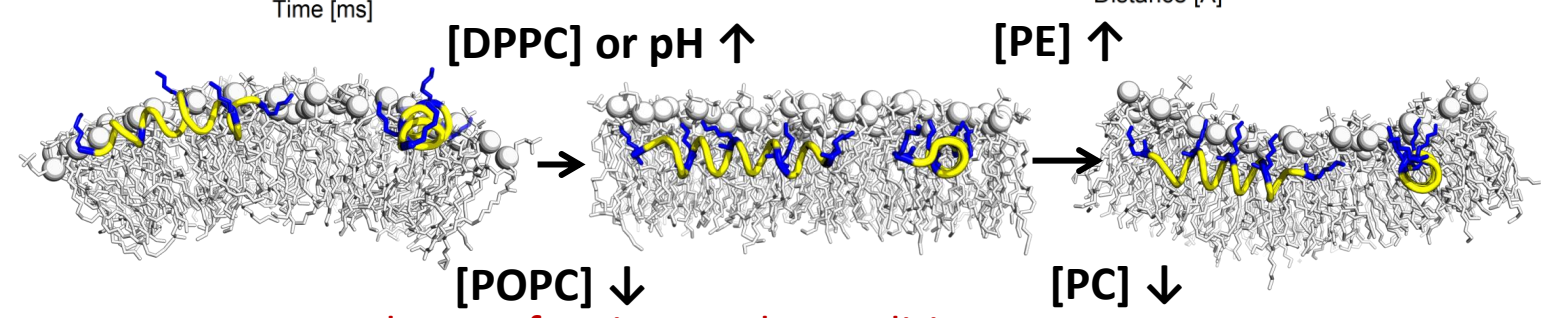
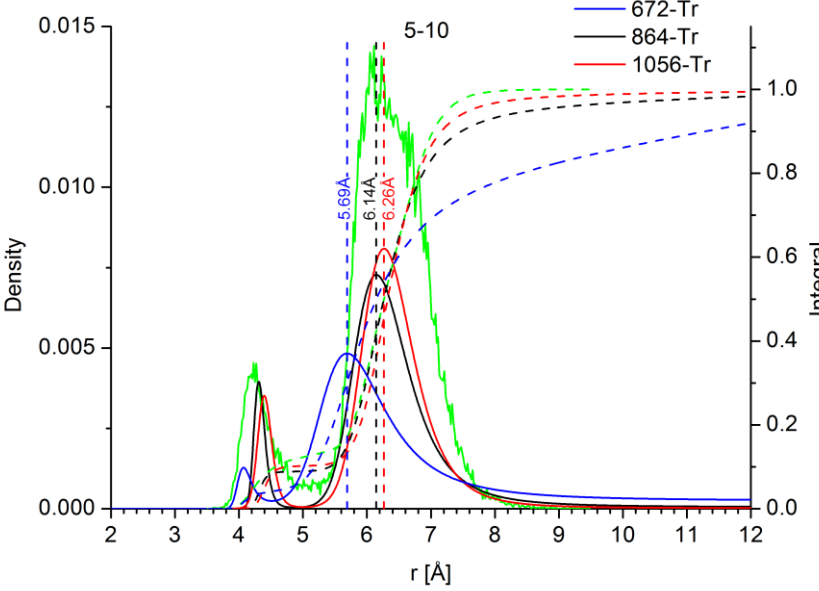
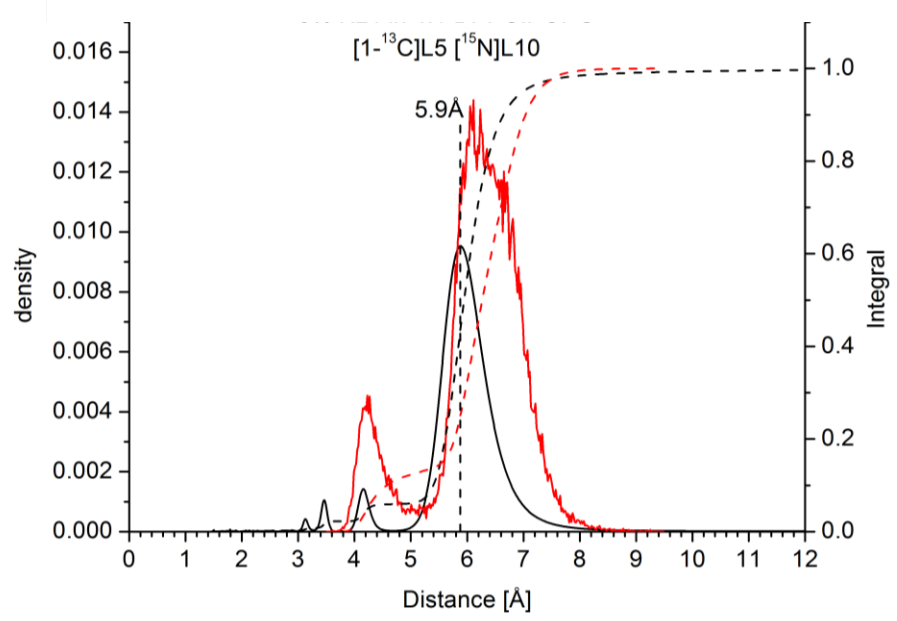
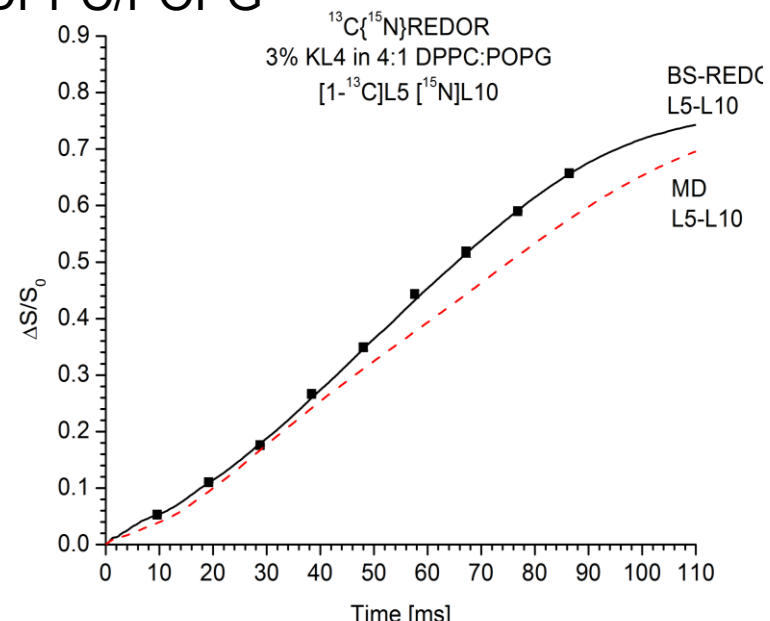
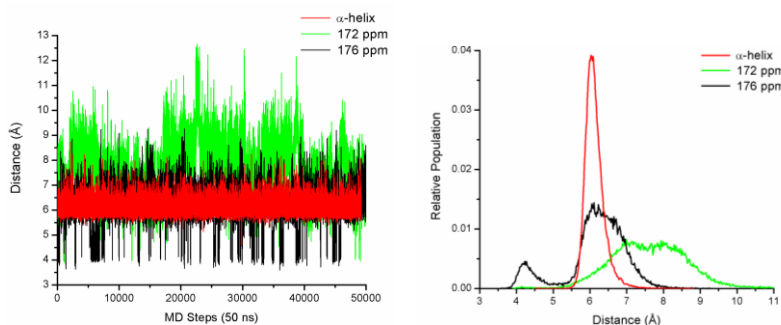
Table 1: Distances from ^{15}N for ideal and x-ray structures.

| ^{13}CO | α -helix -52°, -53° | α -helix GCN4 1CE9.pdb | π -helix -57°, -70° | 2QD1 resid 342- 353 |
|------------------|-------------------------------|-------------------------------------|----------------------------|---------------------------|
| i-1 | 1.38 Å | 1.33 Å | 1.38 Å | 1.32 Å |
| i-2 | 3.30 Å | 3.29 Å | 3.59 Å | 3.54 Å |
| i-3 | 3.64 Å | 3.71 Å | 4.21 Å | 5.18 Å |
| i-4 | 3.84 Å | 4.19 Å | 3.08 Å | 4.18 Å |
| i-5 | 5.73 Å | 6.05 Å | 3.06 Å | 4.39 Å |
| i+1 | 2.5 Å | 2.5 Å | 2.5 Å | 2.5 Å |

- RF inhomogeneity / natural abundance background corrected by L-curve

MD guidance of next experiments

KL₄ 1-¹³C-Leu5, ¹⁵N-Leu10, pH 7.4 in DPPC/POPG

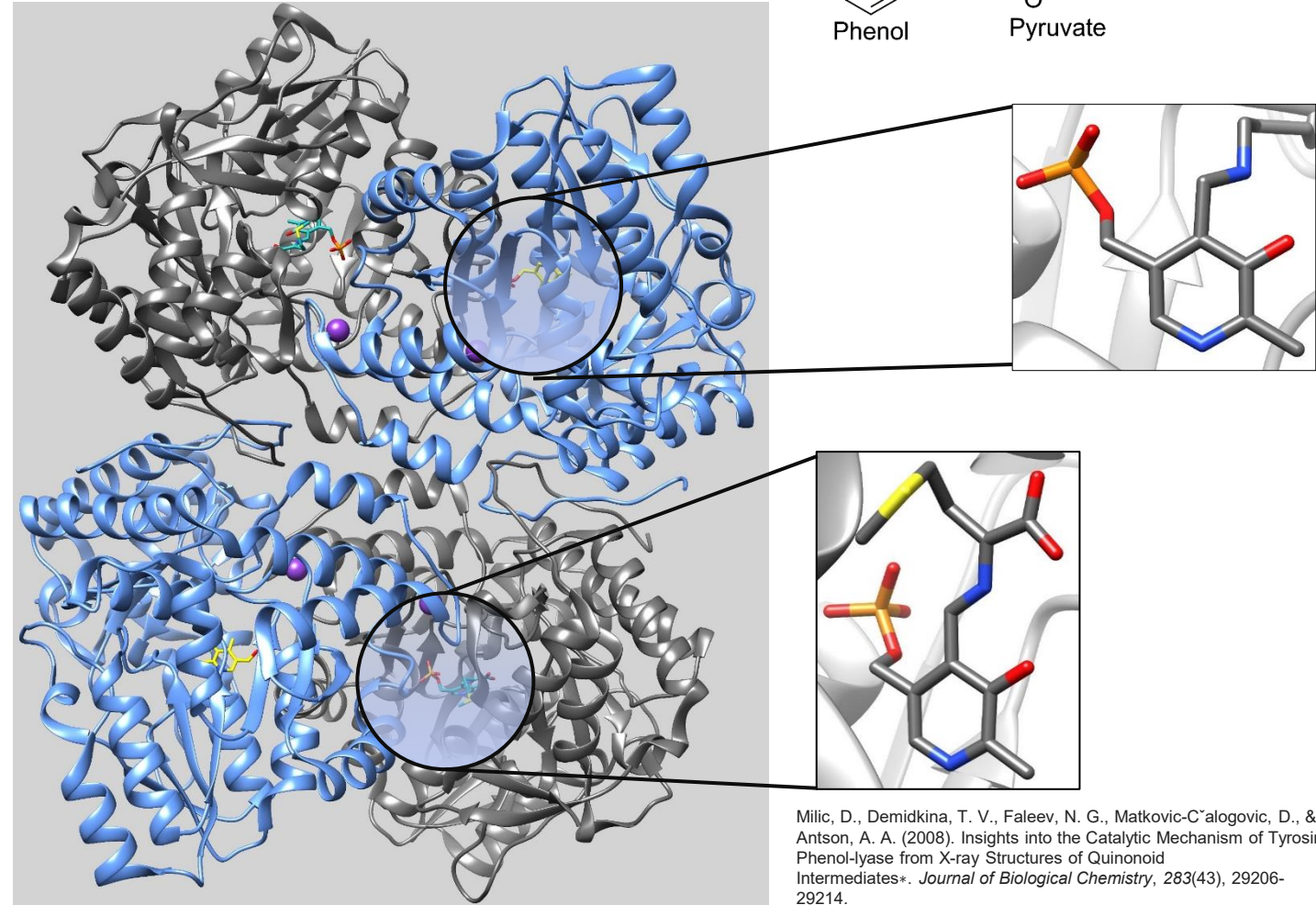
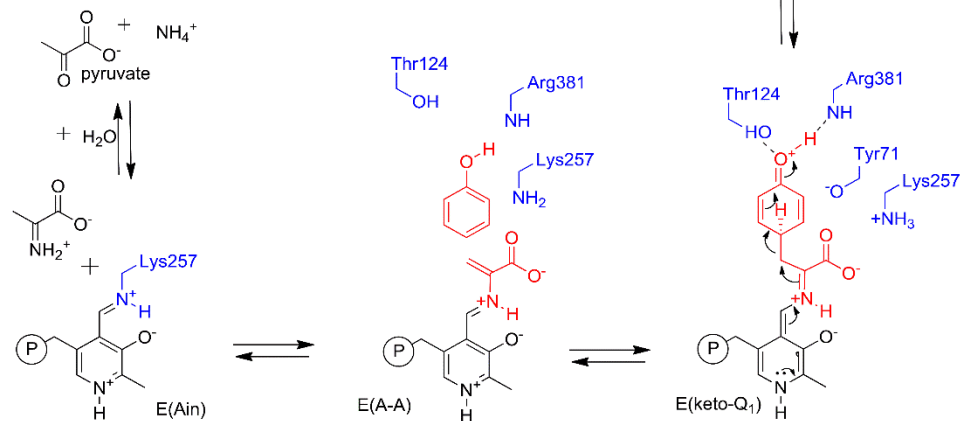
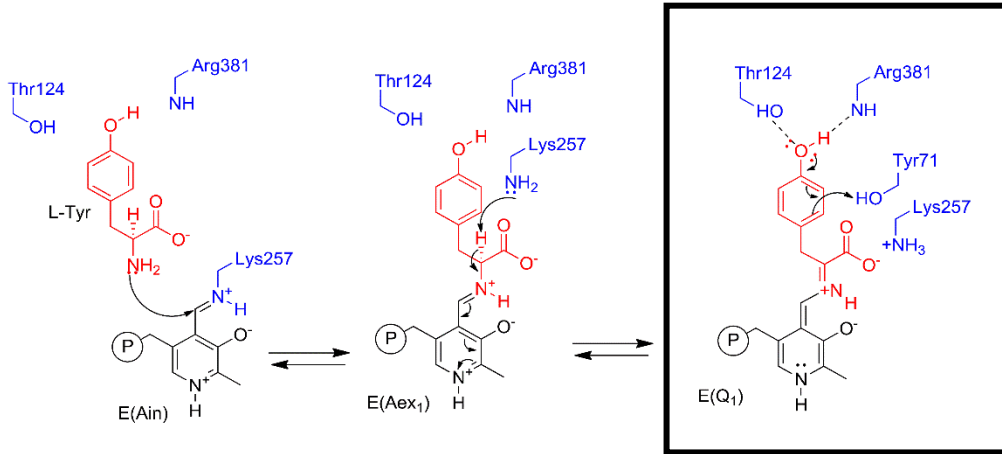
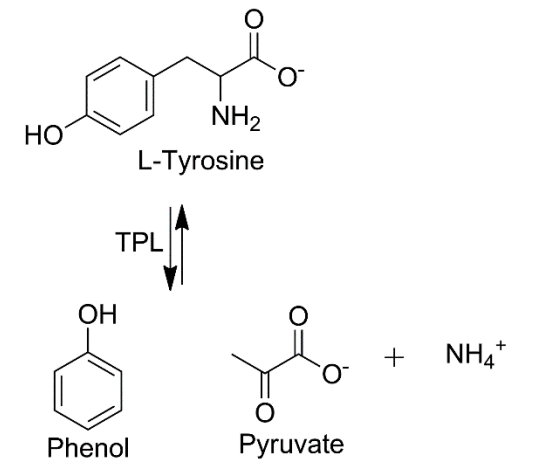


Measurements underway for six sample conditions,
 ~40 constraints per condition (~120 days with DNP under ideal operations)

- MD predicts fluctuations in hydrogen bonding patterns with a bimodal distance distribution
- MD guides experimental REDOR measurements needed to complete our model of KL₄ coupling partitioning and helicity
- Differences between initial MD and experimental data now refining MD (iterative fitting)

Tyrosine Phenol-Lyase (TPL)

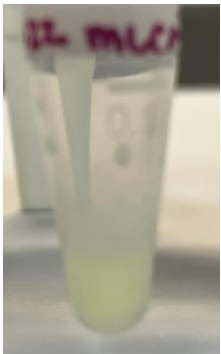
Tetramer complex
206 kDa effective asymmetric unit



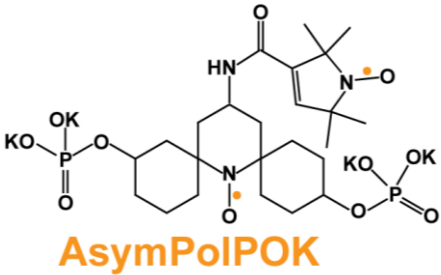
Milic, D., Demidkina, T. V., Faleev, N. G., Matkovic-C'alogovic, D., & Antson, A. A. (2008). Insights into the Catalytic Mechanism of Tyrosine Phenol-lyase from X-ray Structures of Quinonoid Intermediates*. *Journal of Biological Chemistry*, 283(43), 29206-29214.

Phillips, R. S., Craig, S., Kovalevsky, A., Gerlits, O., Weiss, K., Iorgu, A. I., ... & Hay, S. (2019). Pressure and temperature effects on the formation of aminoacrylate intermediates of tyrosine phenol-lyase demonstrate reaction dynamics. *ACS Catalysis*, 10(3), 1692-1703.

Sample preparation and evaluation: TPL example

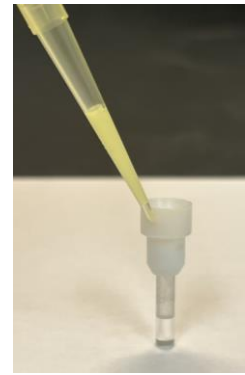


10x solution in crystallization buffer



Mentink-Vigier, F., et al. (2018) *J.Am.Chem.Soc.*, 141

- D ~ 56 MHz
- |J| ~ 70 MHz
- 5 mM final concentration
- Faster DNP buildup time
- Insensitive to protonation



Protein microcrystals
 10% DMSO as glassing agent
 optimized crystallization conditions



Rittik Ghosh

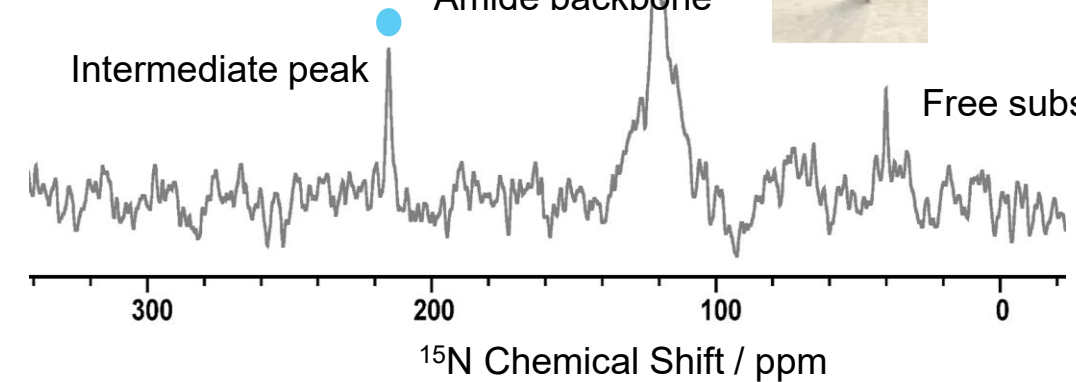


Luiza Caldas Nogueira

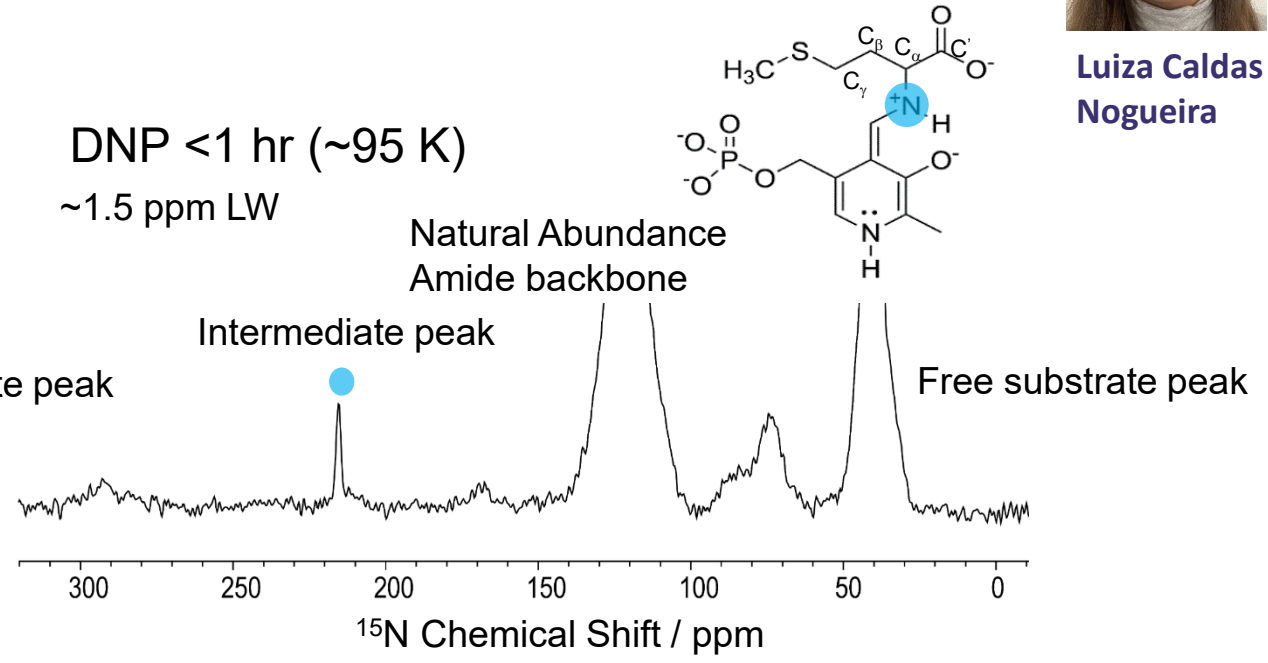
¹⁵N, ¹³C L-Methionine added to unlabeled protein

ssNMR ~40 hrs (~283 K)

4mm rotor; 9.4 T



DNP <1 hr (~95 K)
 ~1.5 ppm LW

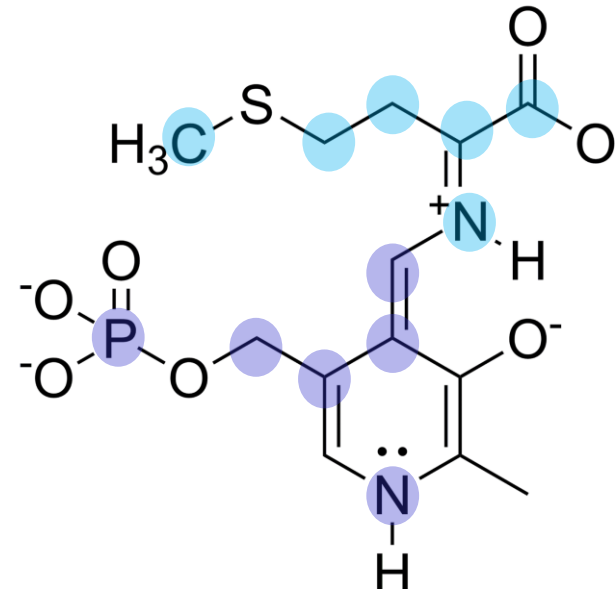


TPL quinonoid intermediate

Tetramer complex

206 kDa effective asymmetric unit

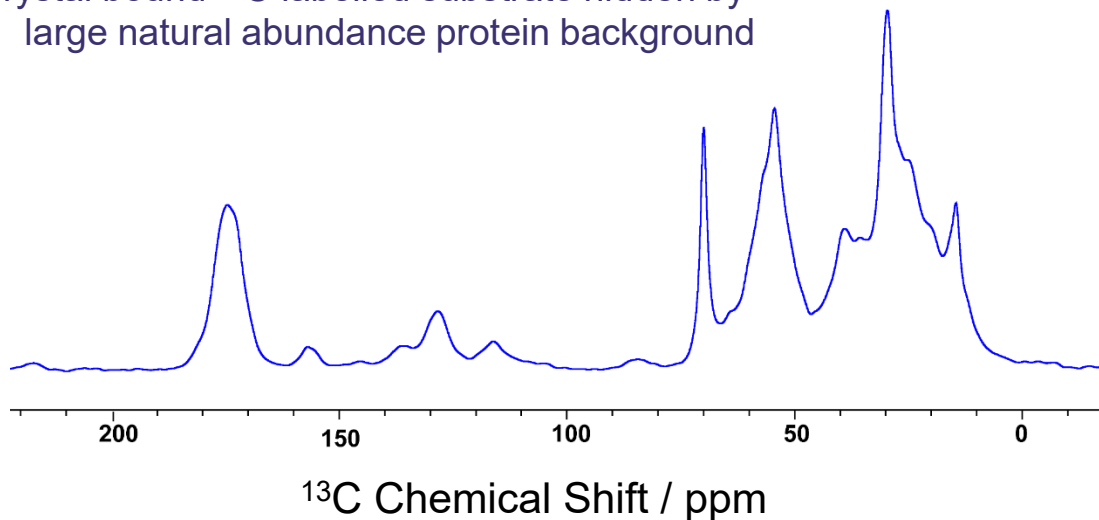
- NA TPL in *either* protonated or deuterated crystallization buffer, 10% DMSO
- 5 mM AsymPolPOK, $\epsilon > 50$
- Buildup times shorter with ^2H , but ϵ constant
- ^{15}N , ^{13}C L-Methionine added (substrate analog)



Why doesn't the L-Met turnover ?

What can this tell us about the mechanism for the natural substrate L-Tyr ?

Crystal bound ^{13}C labelled substrate hidden by large natural abundance protein background



TPL quinonoid intermediate

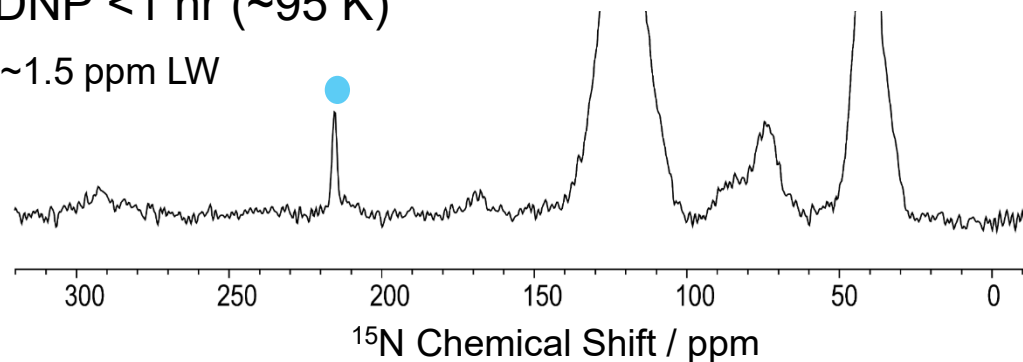
- NA TPL in *either* protonated or deuterated crystallization buffer, 10% DMSO
- 5 mM AsymPolIPOK, $\epsilon > 50$ and DNP buildup < 1 sec
- Buildup times shorter with ^2H , but ϵ constant
- ^{15}N , ^{13}C L-Methionine added



Rittik Ghosh Luiza Caldas
Nogueira

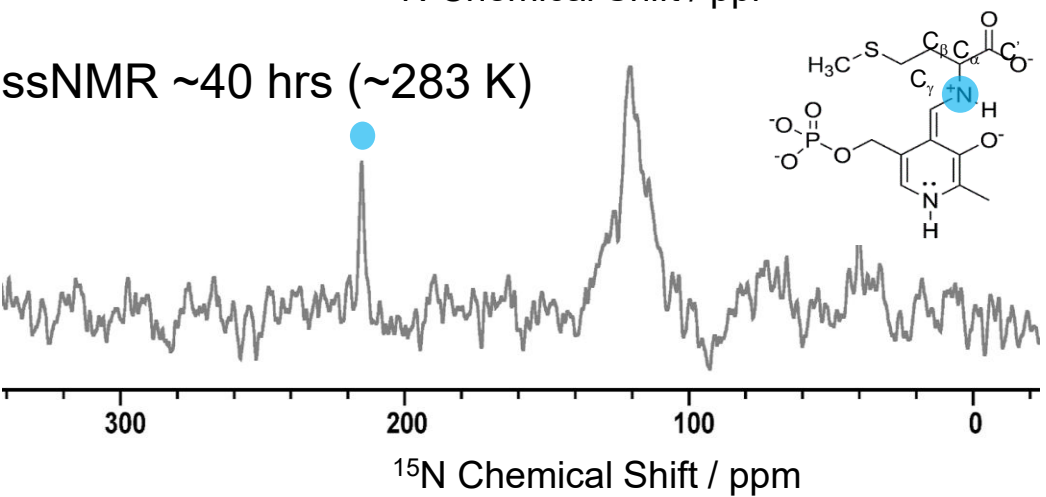
DNP < 1 hr (~ 95 K)

~ 1.5 ppm LW

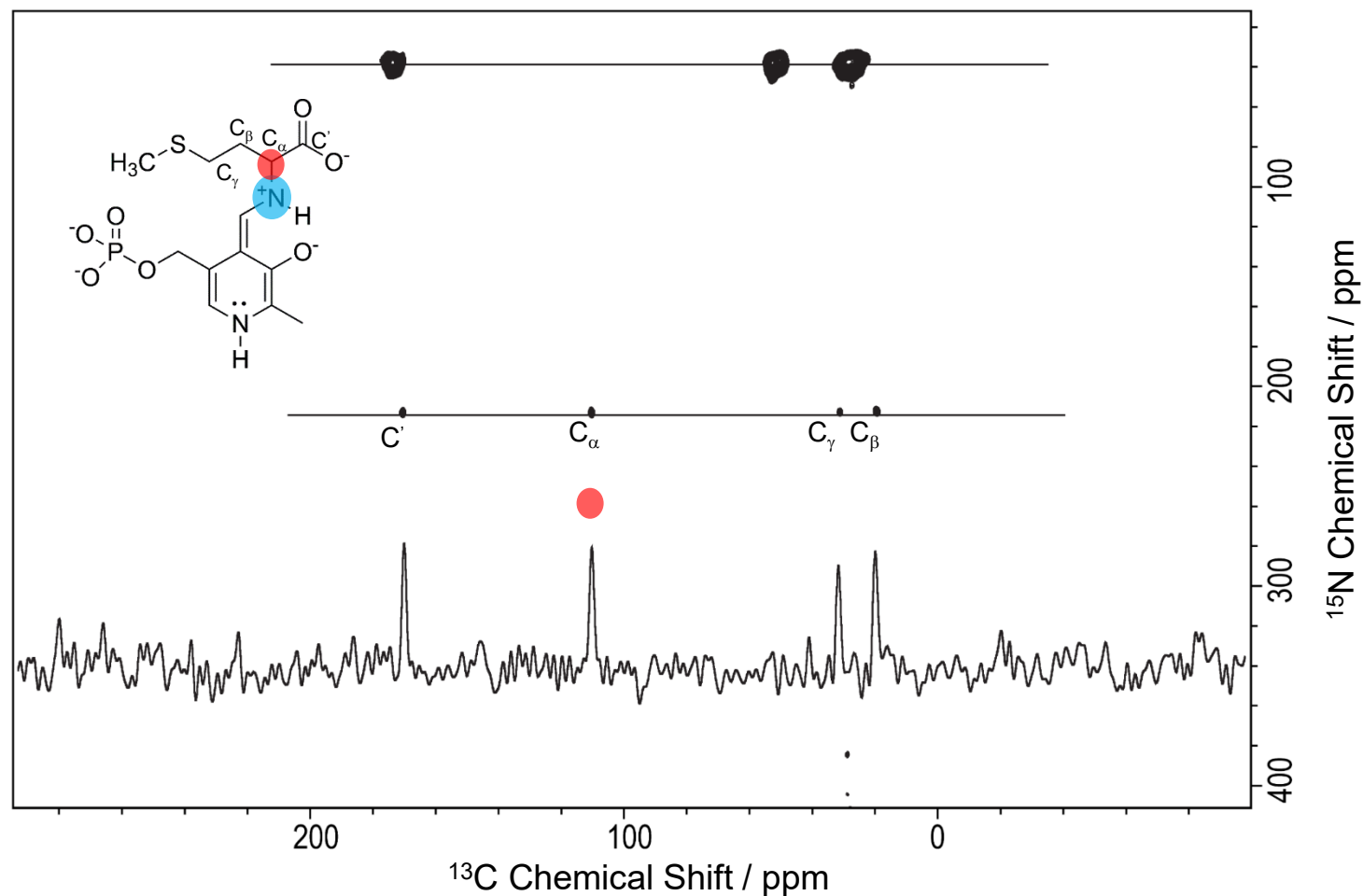


ssNMR ~ 40 hrs (~ 283 K)

^{15}N Chemical Shift / ppm



NCaCx 2D



Acknowledgements

Luiza Nogueira

Emily Peng

Mira Menon

James Collins

Faith Scott

Brooke Mangano

Adam Smith

Gwladys Riviere

Nhi Tran

Dan Downes

Bimala Lama

Lauren Schaffer



Funding

NSF, NIH

Steve Hill

Rob Schurko

Hans van Tol

Fred Mentink-Vigier

Thierry Dubroca

Wenping Mao



Jonathan Mabrey

Peter Gor'kov

Jason Kitchen



NIH R01 GM97569

Len Mueller

Jacob Holmes

Rittik Ghosh

Viktoriia Liu

Bethany Caulkins

Yangyang Wang



Melanie Rosay



DMR-1644779



P41 GM122698

S10 OD108519